Université de Montréal

THE ORPHAN NUCLEAR RECEPTOR NR5A2 REGULATES PERI-OVULATORY EVENTS AND THEIR CONSEQUENT LUTEINIZATION IN MICE

par

KALYNE BERTOLIN

Département de biomédecine vétérinaire
Faculté de médecine vétérinaire

Thèse présentée à la Faculté de médecine vétérinaire
en vue de l'obtention du grade de
philosophiae doctor (Ph.D.)
en sciences vétérinaires
option reproduction

Août, 2013

Résumé

Le récepteur nucléaire Nr5a2, également connu sous le nom de liver receptor homolog-1 (Lrh-1), est exprimé au niveau de l'ovaire chez la souris, exclusivement dans les cellules lutéales et de la granulosa. La perturbation de Nr5a2, spécifique aux cellules de la granulosa chez la souris à partir des follicules primaires dans la trajectoire du développement folliculaire a démontré que Nr5a2 est un régulateur clé de l'ovulation et de la fertilité chez la femelle. Notre hypothèse veut que Nr5a2 régule les évènements péri- et post-ovulatoires dans une séquence temporelle lors de la folliculogénèse. Afin d'étudier l'implication de Nr5a2 lors de l'ovulation et de la lutéinisation à différents stades du développement folliculaire, nous avons généré deux modèles de souris knockout spécifiques aux cellules de la granulosa pour Nr5a2: 1) $Nr5a2^{Amhr2-/-}$, avec une réduction de Nr5a2 à partir des follicules primaires et subséquents; 2) $Nr5a2^{Cyp19-/-}$, avec une réduction de Nr5a2 débutant au stade antral de développement en progressant. L'absence de Nr5a2 à partir des follicules antraux a résulté en une infertilité chez les femelles $Nr5a2^{Cyp19-/-}$, de même qu'en des structures non-fonctionnelles similaires aux structures lutéales au niveau des ovaires, en une réduction des niveaux de progestérone synthétisée ainsi qu'en un échec dans le support d'une pseudo-gestation. La synthèse de progestérone a été entravée suite à l'absence de Nr5a2 par l'entremise d'une régulation à la baisse des gènes reliés au transport du cholestérol, *Scarb1, StAR* et *Ldlr*, démontré par qPCR. Les complexes cumulus-oocytes des femelles $Nr5a2^{Cyp19-/-}$ immatures super-stimulées ont subi une expansion *in vivo*, mais l'ovulation a été perturbée, possiblement par une régulation à la baisse du gène du récepteur de la progestérone (*Pgr*). Un essai d'expansion du cumulus *in vitro* a démontré une expansion défectueuse du cumulus chez les $Nr5a2^{Amhr2-/-}$, associée à un dérèglement de la

protéine des jonctions communicantes (Gja1; Cx43). Cependant, l'expansion du cumulus chez les Nr5a2$^{Cyp19-/-}$ n'a pas été autant affectée. Des résultats obtenus par qPCR ont démontré une régulation à la baisse dans l'expression des gènes *Areg*, *Ereg*, *Btc* et *Tnfaip6* chez les deux modèles de cellules ovariennes knockout à 2h et 4h post hCG. Nous avons observé que 85% des oocytes, chez les deux génotypes mutants, peuvent subir une rupture de la vésicule germinative, confirmant leur capacité de maturation *in vivo*. La technique d'injection intra-cytoplasmique de spermatozoïdes a prouvé que les oocytes des deux génotypes mutants sont fertilisables et que 70% des embryons résultants ont poursuivi leur développement vers le stade de blastocyste, et ce, indépendamment du génotype. En conclusion, Nr5a2 régule la fertilité chez les femelles tout au long du processus du développement folliculaire. Il a été démontré que Nr5a2 est essentiel à la lutéinisation et que sa perturbation dans les cellules somatiques ovariennes ne compromet pas la capacité des oocytes à être fertilisés. En vue d'ensemble, nous avons fourni une investigation inédite et complète, utilisant de multiples modèles et techniques afin de déterminer les mécanismes par lesquels Nr5a2 régule les importants processus que sont l'expansion du cumulus, l'ovulation ainsi que la formation du corps jaune.

Mots-clés: Nr5a2, cellules de la granulosa, expansion du cumulus, lutéinisation, fertilisation, souris knockout conditionnel

Abstract

The nuclear receptor Nr5a2, also known as liver receptor homolog-1 (Lrh-1), is expressed in the mouse ovary, exclusively in granulosa and luteal cells. Granulosa-specific disruption of Nr5a2 in mice from primary follicles onward in the follicle development trajectory has shown that Nr5a2 is a key regulator of ovulation and female fertility. We hypothesized that Nr5a2 modulates peri- and post-ovulatory events in a temporal sequence during folliculogenesis. To examine the role of Nr5a2 in ovulation and luteinization at different stages of the follicular development, we generated two Nr5a2 granulosa-specific knockout mice models: 1) $Nr5a2^{Amhr2-/-}$, with Nr5a2 depletion from primary follicles forward; and 2) $Nr5a2^{Cyp19-/-}$, with Nr5a2 depletion from the antral stage of development forward. The lack of Nr5a2 beginning in antral follicles resulted in infertility in $Nr5a2^{Cyp19-/-}$ females, with ovaries displaying non-functional luteal-like structures, synthesizing reduced progesterone levels and failing in supporting pseudopregnancy. Progesterone synthesis was affected by the lack of Nr5a2 through the downregulation of the cholesterol transport-related genes, *Scarb1, StAR* and *Ldlr*, as shown by qPCR. The cumulus-oocyte complexes of superstimulated $Nr5a2^{Cyp19-/-}$ immature females underwent expansion *in vivo*, but ovulation was disrupted, likely due to the downregulation of the progesterone receptor (*Pgr*) gene. An *in vitro* cumulus expansion assay showed defective cumulus expansion in $Nr5a2^{Amhr2-/-}$ associated with a dysregulation in the gap junction alpha-1 (Gja1; Cx43). *In vitro* cumulus expansion in $Nr5a2^{Cyp19-/-}$ was less affected than in $Nr5a2^{Amhr2-/-}$ cumulus-oocyte complexes. Data from qPCR showed a downregulation in the gene expression of *Areg*, *Ereg*, *Btc* and *Tnfaip6* in both knockout ovarian cells at 2 h and 4 h post hCG. We found that 85% of the oocytes in both mutant genotypes can undergo

germinal vesicle breakdown, confirming their capability to mature *in vivo*. Intracytoplasmic sperm injection (ICSI) showed the oocytes in both mutant models to be fertilizable and 70% of the resulting embryos proceeded to a blastocyst stage, independent of the genotype. In conclusion, Nr5a2 regulates female fertility along the entire process of the follicular development. Nr5a2 is shown to be essential for luteinization and its disruption in ovarian somatic cells does not compromise oocyte fertilizability. In overview, we provided a novel and comprehensive investigation, using multiple models and techniques to determine the mechanisms by which Nr5a2 regulates the important processes of cumulus expansion, ovulation and formation of the corpus luteum.

Keywords: Nr5a2, granulosa cells, cumulus expansion, luteinization, fertilization, conditional knockout mouse

Table of contents

List of tables

List of figures

Chapter 1 – Literature review

Chapter 2 – First manuscript

Chapter 3 – Second manuscript

Chapter 5 – Appendix

List of abbreviations

AF-1	activation function-1
3Cl-AHPC	4-[3-(1-adamantyl)-4-hydroxyphenyl]-3-chlorocinnamic acid
ACTH	adrenocorticotropic hormone
Adamts-1	a disintegrin and metalloproteinase with thrombospondin motifs-1
Adamts-4	a disintegrin and metalloproteinase with thrombospondin motifs-4
AF-2	activation function-2
Amh	anti-Müllerian hormone
Amhr2	Amh type II receptor
Areg	amphiregulin
ART	assisted reproductive technology
BSA	bovine serum albumin
Btc	betacellulin
cAMP	cyclic adenosine monophosphate
CEL	carboxyl ester lipase
CETP	cholesteryl-ester-transfer protein
cKO	conditional knockout
CL	corpus luteum
COC	cumulus-oocyte-complex
CON	control group
Cx43	connexin 43
Cy3	cyanine 3
Cyp11a1	cholesterol side-chain cleavage enzyme
Cyp11b1	steroid 11β-hydroxylase
Cyp17a1	cytochrome P450 17a1
Cyp19a1	cytochrome P450 family 19 subfamily A polypeptide 1; aromatase
Cyp7a1	cholesterol 7 alpha-hydroxylase
Cyp8b1	cytochrome P450 family 8 subfamily B polypeptide 1
DAPI	4’,6-diamidino-2-phenylindole

DAX1	dosage-sensitive sex reversal adrenal hypoplasia congenital region on the X chromosome, gene 1
DBD	DNA binding domain
DLPC	dilauroyl phosphatidyl-choline
DNA	deoxyribonucleic acid
dpc	day post coitum
E2	estradiol-17β
eCG	equine chorionic gonadotropin
EGF	epidermal growth factor
EpiSCs	epiblast stem cells
ERα	estrogen receptor alpha
Ereg	epiregulin
ES	embryonic stem
floxed	flanked by *loxP*
FSH	follicle-stimulating hormone
FTF	α-fetoprotein transcription factor-1
Ftz	fushi tarazu
Ftz-F1	fushi tarazu factor 1
Gja1	gap junction alpha-1
GnRH	gonadotropin-releasing hormone
GREB1	growth regulation by estrogen in breast cancer 1
GVBD	germinal vesicle breakdown
HAS-2	hyaluronic acid synthase 2
hB1F	human B1-binding factor
hCG	human chorionic gonadotropin
HDL	high density lipoprotein
HNF4α	hepatocyte nuclear factor 4-alpha
HRP	horseradish peroxidase
Hsd3β	3 beta-hydroxysteroid dehydrogenase
ICSI	intracytoplasmic sperm injection
IgG	immunoglobulin G

iPSCs	induced pluripotent stem cells
IVF	*in vitro* fertilization
LBD	ligand binding domain
Ldlr	low-density lipoprotein receptor
LH	luteinizing hormone
LHR	luteinizing hormone receptor
LIF	leukemia inhibitory factor
Lrh-1	liver receptor homolog-1
LS	luteal-like structures
MBF-1	multiprotein bridging factor
mHTF	modified human tubal fluid
MSCs	mesenchymal stem cells
NCOR	nuclear receptor co-repressor
NLSs	nuclear localization signals
NPC	nuclear pore complex
Nr5a2	nuclear receptor subfamily 5 group A member 2
P4	progesterone
PAF	paraformaldehyde
PB	polar body
PBS	phosphate-buffered saline
PCR	polymerase chain reaction
PDX-1	pancreatic-duodenal homeobox 1
PGC-1	PPAR-g-coactivator-1
PGE2	prostaglandin E2
PGF2α	prostaglandin F2α
Pgr	progesterone receptor
PIASy	protein inhibitor of activated STAT y
PPAR	peroxisome proliferator-activated receptor
PRKO	progesterone receptor knockout
Ptgs2	prostaglandin-endoperoxide synthase 2
PVP	polyvinylpyrrolidone
RIP140	repressor interacting protein 140

RNA	ribonucleic acid
RPS18	ribosomal protein S18
RT	room temperature
Scarb1	scavenger receptor B1
SF-1	steroidogenic factor-1
SHP	short heterodimeric partner
SMRT	silencing mediator for retinoic acid and thyroid hormone receptor
SRC-1	steroid receptor co-activator-1
SREBP-2	sterol regulatory element-binding proteins
Star	steroidogenic acute regulatory protein
STAT	signal transducer and activator of transcription
SUMO	small ubiquitin-like modifier
TBST	Tris buffered saline containing 0.1% Triton-X
Tnfaip6	tumor necrosis factor-stimulated gene-6
WT	wild type

To my parents,

Ivani Moro and Henri Carlos Bertolin

Acknowledgments

First of all, I would like to gratefully acknowledge my supervisor Dr. Bruce D. Murphy. For being “Dr. Murphy”, the busy and renowned researcher who is always there for his students; for being a leader and not a boss and for all the support and confidence given to me. Above all, thank you for being “Bruce”, for the jokes, the ice creams, the ukulele shows and the Hollywood super productions. For the 5 years of partnership, mentorship and friendship. “Give a man a fish; you have fed him for today. Teach a man to fish; and you have fed him for a lifetime”. Thank you, Dr. Murphy, for not giving me that fish.

For the financial support, I thank the Canadian Institute of Health Research, Operating Grant FRN11018 for funding the original investigation from the laboratory of Dr. Bruce D. Murphy. Moreover, all my honor and gratitude to the Merit Scholarship Program for Foreign Students (PBEEE) by the Fonds québécois de la recherche sur la nature et les technologies (FQRNT).

My pleasure to thank my scientific family, the members of the BDM Laboratory. For the exchange of knowledge, culture, advice, experiences and artistic talents. For making me feel lucky to be surrounded of the nicest people and real professionals. I am particularly thankful to Vickie Roussel, for the technical help, but above all, for the lasting friendship since my first day at the lab; to Anne-Marie Bellefleur, my lab mate, office mate, lunch mate, coffee mate and great friend; to Fanny Morin, for the willing to help, sweet smile and essential laboratorial support in the last months of my thesis writing; to Sandra Ruiz, for being peaceful and lovely, unconsciously making me a better person; to Jane

Fenelon, my serene, serious and competent example of passion for research; to Arnab Banerjee, for breaking concepts and brightening the lab; and to Laurianne Gagnon, for giving me the chance to guide a student, and for being so enthusiastic as to arise my wish to be a mentor.

I devote a special thank you to Mira Dobias-Goff, for being absolutely all the good adjectives in one single person. A great professional and exceptional technician, always helpful, tireless and willing to share her wise experience. For the substantial laboratorial help and advice. Beyond all, for being an example of politeness, culture and kindness; for the 5 years of daily long conversations, making part of my personal growth. “Děkuji!”

My hearty thanks to my better half, best friend and fiancé Eduardo, for all the support, encouragement and partnership. For believing in me and for being my inspiring character, for the confidence that makes me self-confident, always having the right word in the bad times, and a smile in the good ones. I owe you my happiness, permanency and serenity during these 5 years abroad.

My friendly thanks to the Rodrigues Simard, the family that I had chosen to be mine. For a true and lasting friendship, and for proving that one can feel lonely even when surrounded by many people, but will never feel lonely if surrounded by one good friend. Thanks also to my old time friends Rosmarini dos Santos, Marcos Azevedo and Mario Binelli, for being so present in my life abroad, always sustaining the friendship flame, surpassing the physical distance.

Finally, my acknowledgment to my family, for whom I take the liberty to write in Portuguese, my maternal language. *Enfim, dedico minha mais imensa gratidão à minha família. Ao meu irmão, Thiérre, por ter me proporcionado uma das maiores alegrias*

durante a minha estadia no Canadá, com sua visita. Por muitas vezes ter que assumir dupla responsabilidade para encobrir minha ausência; por constante e diariamente me fazer sentir presente nos bons e maus momentos familiares; pela sintonia e união, e pela segurança de uma ligação inquestionavelmente sólida. E de todo o meu coração, meu muito obrigada aos meus pais, Ivani e Carlos, não só por terem me proporcionado oportunidades, mas por terem me educado para encará-las como desafio. Pelo exemplo de dignidade e honestidade, pelo incentivo à persistência, e pelos 10 anos de saudades com apoio, compreensão, e incansável espera de me ver voltar.

Introduction

Reproduction is an essential event of life, so much so that all the living organisms are the result of some form of reproductive phenomenon. In vertebrates, the natural generation of a new individual mandatorily requires the fertilization of the female gamete, or oocyte, by the male gamete, the spermatozoon. In the female reproductive system, the ovaries have a pivotal role in releasing the oocytes throughout the female reproductive life[26].

The ovaries are basically composed of ovarian follicles in different stages of development, including primary, secondary and antral follicles[90]. During the process of the follicular maturation, known as folliculogenesis, the interactions between the somatic cells of the ovary permit the growth and development of the oocyte[114]. A complex and fascinating synchrony of endocrine, biochemical and genetic events regulates the somatic cells of the ovary, including the theca, granulosa and cumulus cells[97].

The cumulus cells surround the oocyte in antral follicles, and these cells are important both prior to and after ovulation. The surge of luteinizing hormone (LH), produced by the pituitary gland, initiates the ovulatory process, stimulating the expansion of the cumulus cells in mature ovarian follicles, culminating in the release of the oocyte into the oviduct[97]. After ovulation, a series of changes remodels the follicle into the corpus luteum, comprised of reorganized theca and granulosa cells, and responsible for secreting progesterone[79]. The luteinization and cumulus expansion processes will be further detailed in the Chapters 2 and 3 of this thesis, respectively.

The physiological response induced by the reproductive endocrine and molecular events determines the phases of the female estrous cycle. The estrous cycle is comprised of proestrus, estrus, metestrus and diestrus phases. Monitoring the estrous cycle is a relevant tool for the studies in reproductive biology in the mouse, which is an important animal model in research. In the appendix section (Chapter 5) of this thesis, the mouse estrous cycle is described, including the reproductive tract changes and the methods of identification of the estrous phases.

Mutant mouse models have been widely used in research, and from knowledge obtained by the targeted disruption of genes it has become possible to identify the orphan nuclear receptor Nr5a2 as a key regulator of the ovulatory process. A conditional knockout mouse model showed that the depletion of Nr5a2 in granulosa cells of primary follicles results in female infertility in mice[25]. Because Nr5a2 is expressed in the ovary of various species, it is a potential target as the cause of and the solution to the problem of female fertility both in animals and in humans.

The information about the nuclear receptor Nr5a2 is reviewed based on a substantial ensemble of published scientific articles, acquired fewer than two decades of work since its first identification, from research in different fields. Nr5a2 is expressed in a wide variety of tissues and performs essential roles in maintaining the organism. The purpose of this investigation was to determine the role of Nr5a2 in female fertility, with focus on when Nr5a2 is essential for and how it regulates luteinization and cumulus expansion in the mouse ovary, and whether its expression is required for oocyte fertilizability.

Chapter 1

1. Literature review

The nuclear hormone receptors are a superfamily of intracellular transcription factors that regulates gene expression, directing proliferation, differentiation and apoptosis[43]. The first indications of their presence occurred in the mid-1900s, with the isolation of the estrogen receptor[8], and thereafter a number of different steroid hormone had been isolated and characterized, including progesterone and testosterone, with the subsequent cloning of their respective receptors[55]. In mammals, the nuclear receptor superfamily is composed of approximately 50 functional members, with 48 genes identified in the human genome, 49 in mice and 47 in rats[138]. This review is focused on one of these, the nuclear receptor Nr5a2, comprising the gene description, the regulation of its activity and the various biological functions, with emphasis on the events related to reproductive biology.

1.1. Nr5a2

Nr5a2 is a member of the large nuclear receptor superfamily of intracellular transcription factors. The history of the Nr5a2 nomenclature, as well as the influence of the related nuclear receptor Nr5a1 in instigating the studies about Nr5a2, will be herein characterized.

1.1.1. Nomenclature: on the way to consensus

What do the fushi tarazu factor 1 (*Ftz-F1*), the liver receptor homolog-1 (*Lrh-1*), the human B1-binding factor (*hB1F*), the Cyp7a promoter-binding factor and the α-fetoprotein transcription factor-1 (*FTF*) have in common? They are some of a long list of names given to ortholog and homolog genes of the officially named nuclear receptor subfamily 5, group A, member 2 (Nr5a2)[82]. The reason for the discrepancy in the Nr5a2 nomenclature can be assigned to at least three factors, all related to its research history.

1.1.1.1. From *Drosophila* to human

Motivated by the goal of studying the mechanisms of gene regulation, several groups independently described the same transcription factor, Nr5a2, as indicated by homology studies, but named it according to its functions in various domains of research. It was in the early 90's when the initial evidence of a gene responsible for the transcriptional activation necessary for the proper expression of the fushi tarazu (*Ftz*) was described in the *Drosophila* (*D. melanogaster*). The Ftz is a member of the pair-rule class of genes governing *Drosophila* embryo segmentation, and the purified sequence-specific deoxyribonucleic acid (DNA)-binding factor was then called Ftz-F1, containing a pattern of expression coincident to that of the Ftz[116]. Ftz-F1 is a regulator of embryogenesis and metamorphosis in this organism and it was the first Nr5a member cloned[100].

One year later, research in the mouse characterized the liver receptor homologous protein[115], the primary reference to Lrh-1. By a sequence comparison of the Ftz-F1 and the finding of an identical corresponding region of the mouse Lrh-1 (the so-called Ftz-F1 box)

it was suggested that these two genes constitute a unique subfamily of nuclear receptors[117]. Based on the sequence similarities and amino acid analysis indicating a common modular structure with the nuclear receptors, the human homolog of the Ftz-F1 was named as hB1F, for human B1-binding factor, first described in the human liver[68]. Moreover, another name, Cyp7a promoter-binding factor, is related to the known function of the gene in the liver[83], and the FTF is justified by the role of Nr5a2 in regulating the transcription of α-fetoprotein, which binds to estrogens and protects the embryos[36]. Thus, diversified and parallel research on Nr5a2 resulted in a plethora of independent synonymous.

1.1.1.2. From receptor to ligand

Another reason why Nr5a2 has different names is due to the fact that it is an orphan nuclear receptor. The nuclear receptor superfamily represents a group of gene-specific transcription factors and it is typically subdivided into seven subfamilies (N0 – N6), with three classes based on the important diversity among them[30]. Historically, endocrinology studies provided new insights by discovering new hormones through analysis of their effects on physiological or developmental processes, and the purified hormone was subsequently used to identify its partner receptor[55]. This is how the steroid receptor family (class I) was discovered, including the progesterone receptor, estrogen receptor, glucocorticoid receptor, androgen receptor and mineralocorticoid receptor; and also the thyroid/retinoid family (class II), including the thyroid receptor, vitamin D receptor, retinoic acid receptor and peroxisome proliferator-activated receptor (PPAR)[4].

Nonetheless, the concept of the orphan nuclear receptors introduced a new era in endocrinology, in which the process of ligand-receptor discovery is inverted. The orphan

receptors were cloned and than they are used to search for previously unknown ligands, what could be called "reverse endocrinology"[55]. The orphan nuclear receptors compose the third family of nuclear receptors (class III), defining a set of proteins identified as belonging to the nuclear receptor superfamily by comparative sequence analysis, but for which the cognate ligand has not yet been identified and the molecular mechanisms of their transcriptional regulation remain unclear[4]. The orphanhood of Nr5a2 explains why research groups named it according to its transcriptional functions at the moment of its discovery, and does not represent the absolute gene function.

1.1.1.3. From diversity to consensus

After almost 10 years of research on Nr5a2, the scientific community agreed to unify the nomenclature system for the nuclear receptor superfamily. A committee created in 1999 decided the current official nomenclature of nuclear receptors, justified by the frequent existence of multiple names for the same gene. The system is convenient and flexible, allowing for the inclusion of an ever-increasing number of genes and reducing the barrier to researchers outside as well as within the field for understanding both classic and newly acquired information[23]. According to the nomenclature system, each gene name starts with "NR" for nuclear receptor, followed by the Arabic number corresponding to the subfamily, then a single letter for the group and then an Arabic number again for each individual member[77]. The scheme is depicted in the phylogenetic tree of nuclear receptor classification in Figure 1.1.

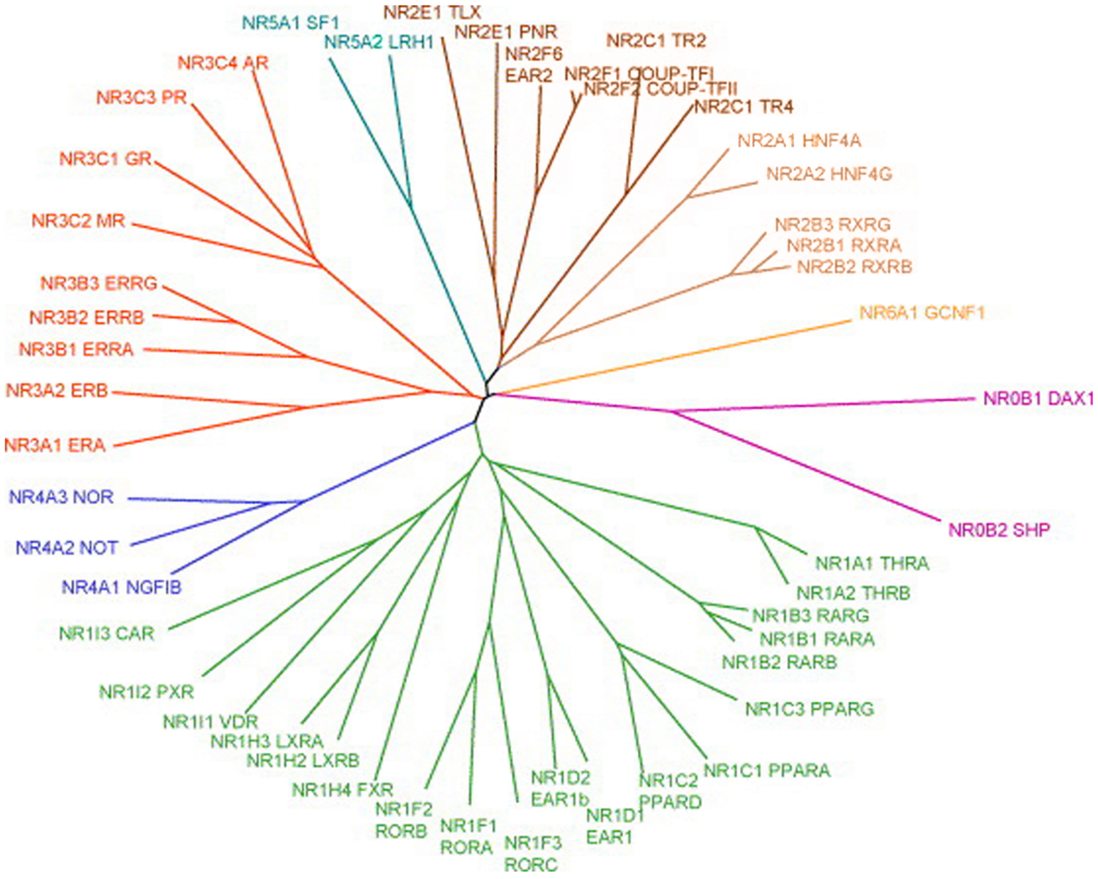

Figure 1.1 : Schematic representation of nuclear receptors classification from NR0 (pink) to NR6 (yellow). Subfamilies are represented in different colors and the unofficial name for each gene accompanies the NR nomenclature. The NR5 subfamily is colored in teal, including the two members Nr5a2 and Nr5a1. Adapted from Mooijaart et al., 2005[77].

1.1.2. The SF-1 legacy

The advances in the characterization of the Nr5a2 subfamily were undoubtedly guided by the abundance of findings on the structure and function of the steroidogenic factor-1 (SF-1). According to the unifying nomenclature system for nuclear receptors, SF-1

is the member 1 of the Nr5a subfamily (Nr5a1), and it is the closest mammalian homolog[1] to the Nr5a2[30]. Nr5a1 was first defined as a mammalian ortholog[2] of the *Drosophila* Ftz-F1[60], belonging to the nuclear receptor family, on the basis of their sequence identity[89].

As early as 1997, the literature relative to Nr5a1 was reviewed by the late Keith Parker, who defined it as a key determinant of the endocrine function within the hypothalamic-pituitary-gonadal axis at various levels, with transcripts detected in steroidogenic tissues known to express the cytochrome P450 steroid hydroxylases, regulating genes involved in steroid hormone biosynthesis, hence its name. *In vivo* data for Nr5a1 were becoming available at that time, showing its essential role in sex differentiation, by activating the expression of the anti-Müllerian hormone (Amh), and adrenal and gonadal formation[71; 89].

Nr5a1 is expressed in the hypothalamus, pituitary, adrenocortical cells, testicular Leydig cells and ovarian theca cells, with lower levels present in granulosa cells and no expression in luteal cells[30]. Data from targeted mutagenic disruption in the ovary showed aberrations in follicle development, anovulation, compromised granulosa cell proliferation and decreased expression of steroidogenic genes[8].

Numerous studies have demonstrated that both Nr5a1 and Nr5a2 are essential for the success of diverse regulatory processes in mammals, and that both are crucial for normal embryonic development[8]. They have a high degree of similarity in the amino acid sequence of their DNA binding domain (DBD, 95%), thus, both transcription factors can bind the same DNA sequences. Despite their structural conservation, they achieve a remarkable specificity both in the way they are activated and in the way they selectively

[1] Homolog : a gene related to a second gene by descent from a common ancestral DNA sequence.
[2] Ortholog : genes in different species that evolved from a common ancestral gene by speciation.

induce specific target genes and signaling pathways[30]. Nr5a1 and Nr5a2 clearly derive from separate genes and have a different pattern of distribution in the mammalian tissues[89]; they also have distinct structural ligand binding domains (LBD, 76%), and regions that recruit specific cofactors to regulate transcription. The integration of the variant domains within the receptor results in the specificity of their activities, contributing to their different biological functions[98].

Nr5a2 is mainly expressed in tissues of endodermal origin, including the liver, pancreas and intestine; high levels of Nr5a2 are also found in the ovary[30] and, at lower levels, in the endometrium[135] and the placenta, as well as in the adrenal and the testis[107]. In general, most Nr5a2 data were generated based on the discoveries about the Nr5a1; therefore Nr5a1 was the pioneer instigator of the Nr5a2 brainstorm that generated a growing mass of data contributed by studies from the highly varied areas of research.

1.2. Nr5a2 and its molecular structure

1.2.1. Nuclear receptor interactions with target sequences

Among the three classes of nuclear receptors (previously described in the section 1.1.1.3), there are subtle differences in the biochemical mechanisms by which the receptors carry out their functions. The member of the class I steroid receptor family, upon binding their hormonal ligand, translocate into the nucleus and bind as homodimers to the response elements[5]. The class II receptor proteins typically function as heterodimers. The orphan nuclear receptor Nr5a2, belonging to the class III of nuclear receptors, is known to bind as a

monomer to the target DNA[117] via the C-terminus of its DBD[30]. Figure 1.2 depicts the variation in binding systems used by the nuclear receptors.

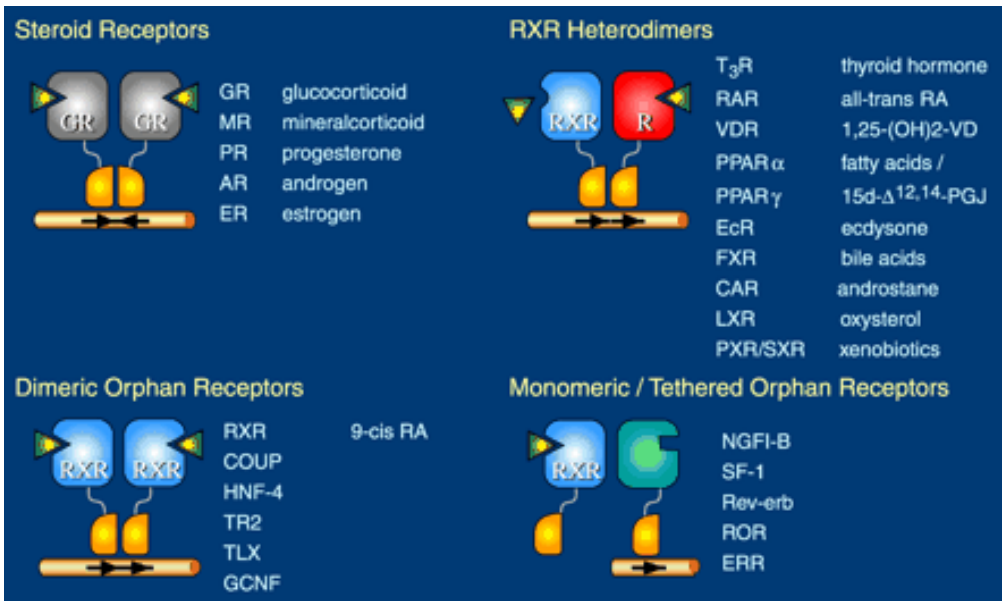

Figure 1.2 : Scheme illustrating the different dimerization of nuclear receptors. Many members of the nuclear receptor family form homo- or heterodimers[86]. As with SF-1 (Nr5a1), Nr5a2 binds to the target DNA as a monomer.

1.2.2. Nr5a2 and its modular domains

Nr5a2 was classed with the nuclear receptors because it has the typical structure of this family, albeit, with some peculiarities. As a nuclear receptor, it must be imported from the cytoplasm into the nucleus via the nuclear pore complex (NPC), and it has two functional nuclear localization signals (NLSs), responsible for mediating the location of Nr5a2 into the nucleus[129]. Nr5a2 structure is basically composed of (Figure 1.3):

- a modulatory N-terminal A/B domain; however, in contrast to other nuclear receptors, no ligand-independent activation function-1 domain (AF-1) has been identified[30];

- the highly conserved DBD (or C domain), responsible for targeting the receptor to specific DNA sequences, termed hormone response elements;

- the LBD (or E domain), which contains a conserved ligand-dependent activation function-2 (AF-2) motif that mediates co-activator interaction;

- and the D domain serving as hinge between DBD and LBD[89; 30; 129], recently showed to be more than a flexible connector, as it is required to regulate the transcriptional activity of Nr5a2 in humans[128] and important for effective *in vitro* phosphorylation of Nr5a2[64].

Members of the Nr5a subfamily contain a hallmark feature, which is an additional 30-amino acid carboxyl-terminal extension, designated Ftz-F1 box or A box[89], located adjacent to the second zinc finger motif, at the C terminus of the DBD. The Ftz-F1 box, together with the zinc finger region, are responsible for the high affinity binding of Nr5a2 to its target gene[117], dictating the specificity of Nr5a2 regulatory mechanism[61].

The human gene encoding Nr5a2 spans over 150 kb of the chromosome 1, it has eight exons and seven introns, and exons 3, 4 and 5 appear to be very important. Transcription from two polyadenylation signals results in 3.8 and 5.2 kb transcripts[136; 61], giving rise to two bands on a Northern blot. At least three Nr5a2 isoforms derived from alternative splicing are known to exist in humans[30]. Figure 1.3 represents the genomic and protein structure of human Nr5a2.

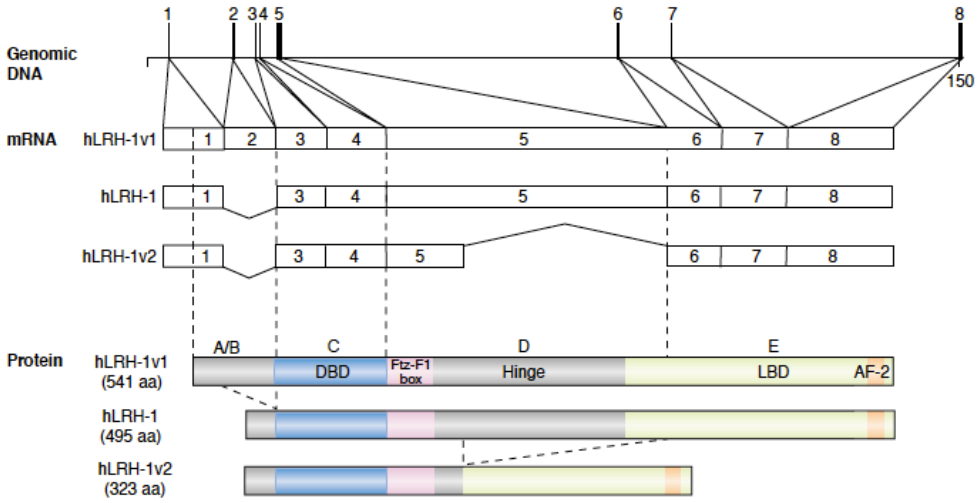

Figure 1.3 : Structure of the gene, mRNAs and protein isoforms of Nr5a2 (human liver receptor homolog-1 – hLRH-1). The human Nr5a2 genomic sequence consists of eight exons. The hLRH-1 isoform is identical to hLRH-1v1 except for a deletion in the A/B domain, due to splicing of exon 2. The hLRH-1v2 isoform contains a deletion within the D or E domain, resulting from an alternative splicing event in exon 5, in addition to the splicing of exon 2. As shown, specific exons encode particular hLRH-1 protein domains. Protein structure contains the amino acid alignment, evidencing the Ftz-F1 box between the C and D domains[30].

1.2.3. LBD in charge for the constitutive activity

Nuclear receptors have amino acid sequence similarity for the two highly conserved domains – the DBD and the LBD, and the last is responsible for binding small lipophilic ligands[108], serving as a molecular switch that recruits coregulatory proteins and activates the transcription of target genes when flipped into the active conformation by hormone binding[55]. Many of the nuclear receptors act as ligand-inducible transcription factors[43] and their activity is controlled by the binding of ligands, including hormones and metabolites[30]. Nr5a2 is constitutively expressed in the nucleus, and its crystal structure shows a large and empty hydrophobic ligand-binding pocket, suggesting that its activation is probably independent of ligands[98].

Nr5a2 has structural differences involving the Nr5a-specific N-terminal region of the LBD, which is likely to be the explanation for its capacity in constitutive activating target genes[61]. The LBD of most nuclear receptors consists of twelve α-helical regions, folded into a three-layered anti-parallel helical sandwich[61]. An extended rigid structure of helix 2 (H2) forms a structure with four layers in the helical sandwich, rather than three layers as in the other classical nuclear receptors LBDs[98]. Through the extension of H2, the active position of H12 is stabilized. H12 contains the C-terminal activation helix AF-2[30], and the folding over the AF-2 region allows the LBD to be held in an active conformation, tightly related to the ligand-independent property of Nr5a2[61].

1.3. Nr5a2 and regulation of its activity

In this section, the transactivational activity of Nr5a2 will be described, including the binding of phospholipid ligands, post-translational mechanisms and the action of transcriptional co-activators and co-repressors. Recently, it was discovered that synthetic ligands can regulate Nr5a2 activity.

1.3.1. Phospholipids

As described in the previous sections, a stable active monomeric Nr5a2 LBD can exist in the absence of ligand, coactivator peptide or homo- or heterodimeric receptor partner. Although ligands are dispensable for Nr5a2 basal activity, adding bulky side chains into its empty hydrophobic ligand-binding pocket results in full or greater activity, suggesting that Nr5a2 can accommodate potential ligands[98]. Through the crystallization of Nr5a2 LBD, independent groups have shown that small phospholipid ligands, such as

phosphatidylcholine, phosphatidylethanolamine, phosphatidylglycerol, and phosphatidylinositol-phosphates[34] can interact with Nr5a2 LBD, with consequent effect of regulating gene expression[56; 87].

Further, by molecular dynamic simulations, it was demonstrated that phospholipids cause no overall structural changes in the Nr5a2 conformation, rather ligand binding affects the interactions with cofactor peptides[14]. It is suggested that the phospholipid molecule is not an endogenous ligand for Nr5a2, and even that there might be no endogenous ligand for this receptor[137]. Therefore, it remains to be determined whether phospholipids or possibly other molecules can regulate Nr5a2 under physiological conditions *in vivo*.

1.3.2. Post-translational regulation

Nr5a2 possesses a large hinge domain that is subject to post-translational modifications[56]. Specifically, phosphorylation of the Nr5a2 regulatory hinge region, brought on by activation of the protein kinase-C pathway and the MAPK/ERK pathway, increases its transcriptional activity[64]. A second post-transcriptional modification is the conjugation of Nr5a2 to the small ubiquitin-like modifier (SUMO), at lysine residues (sumoylation)[130]. Post-translational modification by SUMO elicits a repressive effect on many transcription factors. Nr5a2 was demonstrated to be a direct substrate for the SUMO conjugation machinery and sumoylation can modulate its activity[18]. The inhibition of Nr5a2 transcriptional activity by sumoylation takes place by reduction in the binding of the receptors to their cognate DNA sequence[16], or by transport of Nr5a2 into transcriptionally inactive nuclear bodies[18; 130]. The second messenger, cyclic adenosine monophosphate

(cAMP), is believed to be an important signal for regulating the dynamics of the sumoylation pathway and Nr5a2 activity[130].

1.3.3. Co-regulators

In addition to the post-translational mechanisms controlling transactivational activity, Nr5a2 is also regulated by the interaction with positive and negative co-regulatory proteins, referred to as co-activators and co-repressors[85], and this may well be the most important mode of functional regulation of orphan nuclear receptors[61]. In general, in the absence of ligand or in the presence of ligand antagonists, the nuclear receptor typically interacts with co-repressors. Ligand binding and/or phosphorylation modulate receptor function by altering the receptor's affinity for co-regulatory proteins[94], inducing a conformational change that results in the dissociation of co-repressor complexes and recruitment of co-activator proteins by the nuclear receptors[30], and subsequent transcriptional activation. Once Nr5a2 is constitutively active, it can interact with co-repressors to modulate its activity[30].

Co-regulators can modify the chromatin structure, leading either to condensation that represses transcription, or to decondensation that facilitates the recruitment of the basal transcription machinery of nuclear receptors[12]. Ligand-activated nuclear receptors serve first as adaptors between gene regulatory regions and the chromatin modifying enzyme complexes and then as activators of ribonucleic acid (RNA) polymerase II[17], to suppress or enhance target gene expression. In general, the structure that mediates the ligand-driven exchange of co-repressors and co-activators is the helix 12 (H12), which assumes an extended position in the absence of ligand, permitting the binding of co-repressors. Binding

of agonist reorients H12 to a sequestered position that blocks the co-repressor binding site while simultaneously forming a new docking surface for co-activators[94]. As previously discussed, the long H2 twists Nr5a2 into an agonist-like conformation by affecting H12, even when Nr5a2 ligand binding pocket is empty[98].

Nr5a2 effects are modulated by the repressive actions of the Nr0 family of orphan receptors, comprising the short heterodimeric partner (SHP, Nr0b2) and dosage-sensitive sex reversal adrenal hypoplasia congenital region on the X chromosome, gene 1 (DAX1, Nr0b1). SHP and DAX1 inhibit the interaction of Nr5a2 with co-activators, thereby reducing its constitutive transcriptional effects[8]. These two receptors are unique among the nuclear receptor family in that they lack their own DBD[38], and DAX1 has neither the modulatory domain nor the hinge region[49].

Physiological feedback loops have the capacity to regulate Nr5a2 by the induction of SHP expression, which represses Nr5a2 activity by interacting with its AF-2 transactivation domain. AF-2 is a common target for co-activator interaction, so SHP not only directs transcriptional repression, but also competes with co-activators for binding to Nr5a2[65]. In contrast to other nuclear receptors, ligand binding does not effect conformational change; rather it reduces the affinity of Nr5a2 for SHP[14]. By this means, ligand binding may increase transcription by reducing inhibition. On the other hand, Nr5a2 undergoes conformational changes to accommodate the SHP docking in a potent and selective way[69].

Nr5a2 interacts through its LBD with the N-terminal LXXLL related motifs in DAX1[112], binding with high affinity to the AF-2 domain. DAX1 functions as a ligand-independent nuclear receptor and its repressive mechanism indicates that it is a competitive transcriptional co-repressor[99]. There is also evidence that DAX1 recruits co-repressors,

such as the nuclear receptor co-repressor (NCOR) and ALIEN, providing a further mechanism of inhibition of Nr5 nuclear receptor activity[49].

In addition to the DAX1 and SHP, other co-activators and co-repressors participate in regulating Nr5a2 transactivation of target genes. The repressor interacting protein 140 (RIP140) is a negative transcriptional regulator of nuclear receptor action[32]. The prospero-related homeobox transcription factor, Prox1, is another recognized co-repressor that directly interacts with both LBD and DBD of Nr5a2[95; 109]. Indirect mechanisms have also been shown to inhibit the activity of Nr5a2, such as the case of the silencing mediator for retinoic acid and thyroid hormone receptor (SMRT) that regulates but does not directly interact with Nr5a2[126].

Nonetheless, inhibition is not the sole regulatory mechanism of Nr5a2 transactivation. The multiprotein bridging factor (MBF-1) is a co-factor that enhances the transcriptional activity by interacting with the Nr5a2 Ftz-F1 box, acting as a bridging factor enabling interactions of Nr5a2 with the transcription machinery, although it does not possess histone-modifying activities, which are typical for many co-activators[12]. Steroid receptor co-activator-1 (SRC-1) interacts directly with the Nr5a2 LBD in helix 1 and AF-2, significantly potentiating its transcriptional activity[127]. The protein inhibitor of activated STAT (signal transducer and activator of transcription) y (PIASy) interacts with Nr5a2 in the AF-2 motif as well, inhibiting the binding of SRC-1 to Nr5a2, markedly repressing Nr5a2 transactivation in a competitive way[48].

The co-activator PPAR-γ-coactivator-1 (PGC-1) interacts with and enhances Nr5a2 transcriptional activity[102]. PGC-1 binds to the AF-2 domain of Nr5a2, and it has been suggested to be a key factor that promotes differentiation of granulosa cells into progesterone-producing luteal cells by regulating Nr5a2[132]. Recently, a novel isoform and

promoter region of Nr5a2 in human granulosa cells was shown to be coordinately regulated by Nr5a1 and PGC-1[52]. Blocking PGC-1 is one of the strategies used by SHP and DAX1 to repress Nr5a2 activity[61]. Nr5a2 inhibition is also possible by means of preventing the recruitment of PGC-1 by the sterol regulatory element-binding proteins (SREBP-2)[51]. In addition to this wide and growing list of co-regulators for Nr5a2, it has been shown that β-catenin is important for stable interactions with Nr5a2. The Nr5a2 surface that engages β-catenin is distinct from the known interaction surfaces of Nr5a2[10; 133]. The regulation of Nr5a2 by co-regulatory proteins is a complex and fertile field of research, as partially represented in Figure 1.4.

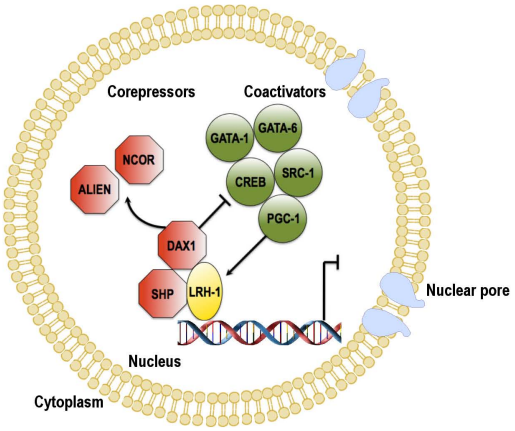

Figure 1.4 : Schematic representation of the role of co-activators and co-repressors in modulating the constitutive transcriptional activity of Nr5a2 (Lrh-1). A number of transcription factors, including those of the GATA family and CREB act in synergy with Nr5a2 to induce transcription of target genes. Co-activators such as SRC-1and PGC-1 interact directly with Nr5a2 to upregulate transcription. The orphan nuclear receptors of the NR0 family, DAX1 and SHP repress transcription by competitively inhibiting the interaction of Nr5a2 with co-activators[8].

1.3.4. Synthetic ligands

The identification of synthetic ligands for Nr5a2 provides proof of concept for ligand-dependent activation or inhibition. An early synthetic small molecule agonist for

Nr5a2 was the compound GSK8470, identified as a high-affinity ligand for Nr5a2 in liver cells[123]. Another small molecule known to activate Nr5a2 is the herbicide atrazine, but the precise mechanism leading to the increased receptor activity has not yet been defined[124]. A breakthrough into the activation of the Nr5a2 domain was the discovery of dilauroyl phosphatidyl-choline (DLPC) as an agonist ligand, by regulating Nr5a2 functions of bile acid metabolism and glucose homeostasis *in vitro*, and the administration of this lipid to diabetic mice reduces blood glucose levels[63]. This molecule ushered in the use of chemical tools to investigate the biological function of Nr5a2 *in vitro* and points to the further therapeutic utility of this nuclear receptor.

Musille et al. report that DLPC binding to Nr5a2 is a dynamic process that alters co-regulator selectivity, by simultaneously enhancing co-activator peptide recruitment and disfavoring co-repressor peptide interaction. DLPC is able to competitively displace larger phospholipids from the LBD of Nr5a2 *in vitro*. Nr5a2 undergoes profound structural changes upon DLPC binding, and functional studies have confirmed the viability of Nr5a2 as a therapeutic target for both agonist and antagonist design[81]. Both humans and mice were shown to respond to DLPC, however the *Drosophila* ortholog is incapable of DLPC binding. The use of mice as viable therapeutic models for Nr5a2-dependent diseases is a valid concept[80].

The inverse agonist is a molecule that binds to the same receptor as an agonist but induces a pharmacological response opposite to that agonist. Nr5a2 inverse agonists have been synthesized, and two probe compounds, ML179 and ML180, have been tested in transcription assays. These have been used in cell biological studies to elucidate the role of Nr5a2 *in vitro* and may also be useful in the development of repressive therapies for Nr5a2-related disease[15]. Another possibility of therapeutic method by the use of synthetic ligands

is the 4-[3-(1-adamantyl)-4-hydroxyphenyl]-3-chlorocinnamic acid (3Cl-AHPC). 3Cl-AHPC is not a direct ligand for Nr5a2, but it binds to SHP and mediates Nr5a2 repression by increasing their interaction[76].

Finally, the two first small molecules-antagonists of Nr5a2 have now been described. These ligands inhibit the transcriptional activity of Nr5a2 by affecting the transcriptional co-repressor targets SHP, cyclin E1 and G0S2 genes that are known to regulate cell growth and proliferation. Nr5a2 antagonists also diminish the expression of the receptor's target genes, and mediate the inhibition of Nr5a2-related cancer cell proliferation[6]. Figure 1.5 illustrates the difference between the action of an agonist, antagonist and inverse agonist.

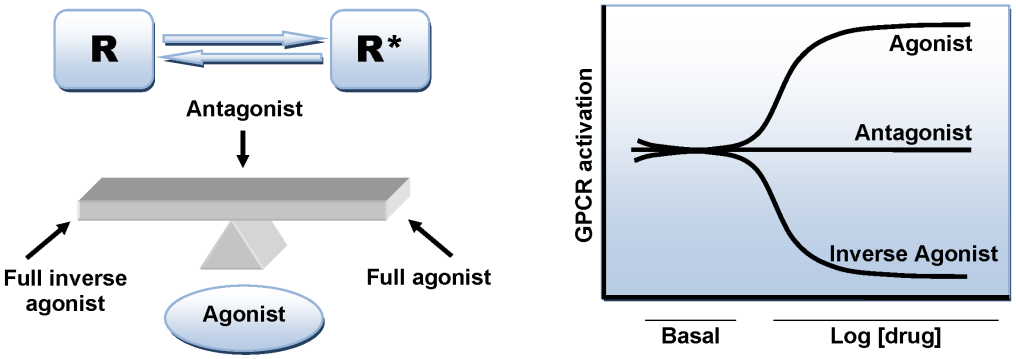

Figure 1.5 : Schematic representation comparing the action of an agonist, antagonist and inverse agonist[101]. R* and R means active and inactive state, respectively. An agonist will bind to the receptor and trigger a response; an antagonist does not provoke a biological response itself upon binding to a receptor, but blocks or dampens agonist-mediated responses; whereas an inverse agonist causes an action opposite to that of the agonist (reprinted from Saevarsottir, 2008).

1.4. Nr5a2 and its biological functions

The nuclear receptor Nr5a2 controls a wide array of biological processes, including eukaryotic development, reproduction and metabolic homeostasis[4]. Because of its versatile signaling functions and its implication in many physiological processes, Nr5a2 is a potential drug target, motivating both basic and applied biomedical researchers[30]. In this section, particular attention will be given to the functions of Nr5a2 in steroidogenesis and reproduction, to include its role in pluripotency and in human breast cancer. Table I summarizes the functions, the target genes and the localization of Nr5a2 in adult and embryonic life.

TABLE I : Nr5a2 target genes and functions (reviewed by Lazarus et al., 2012[61]).

	Target genes	Organ/tissue	Function
Embryonic	AFP-1, Prox1, HNF3β, HNF4α, HNF1α	Liver	Early enterohepatic development
	Oct4	ES cells	Early embryonic development
Adult	CYP19A1	Preadipocytes	Steroidogenesis
	APOA1, SR-B1, CETP, SHP	Liver	Cholesterol transport
	CYP7A1, CYP8B1, CEL, MRP3	Liver	Bile acid homeostasis
	ABST Cyclin D1, TCF4/β-cantenin	Intestine	Bile acid homeostasis Intestinal epithelium renewal
	CYP11A1, CYP19, HSD3B2	Ovary	Ovary steroidogenesis
	SR-BI		Cholesterol transport
	LHβ	Gonadotrope	Normal reproductive function
Disease	Cyclin E1, TCF4, β-cantenin	Intestine	Gastric cancer Intestinal inflammation Pancreatic cancer
	CYP19A1, Cyclin D1, StAR, AFP	Breast	Tumour progression and carcinogenesis
	C-Myc	Pancreas	Pancreatic cancer Pancreatic cancer

1.4.1. Nr5a2 in homeostasis, metabolism and development

Nr5a2 regulates important steps of development, endocrine homeostasis and metabolism. The pattern of expression of Nr5a2 in the liver, pancreas, intestine and also in

the adrenal has been described above. The functions of Nr5a2 in these organs will be briefly described.

1.4.1.1. Embryonic development

Nr5a2 is expressed in the morula and inner cell mass of the early embryo[39], and mice homozygous for a germline mutation in the gene encoding Nr5a2 die between embryonic (E) day E6 and E7.5, which corresponds to the gastrulation period, indicating that it plays a crucial role in the development[88]. Gastrulation is a phase early in the embryonic development, during which the single-layered blastula is reorganized into the gastrula, which contains three germ layers known as the ectoderm, mesoderm, and endoderm. The failed gastrulation is believed to be secondary to defective visceral endoderm development. The Nr5a2 homozygous embryos display growth retardation, epiblast disorganization, and impaired primitive streak morphogenesis[57].

Mouse embryonic stem (ES) cells express Nr5a2 abundantly; at day E7.5, Nr5a2 is detected in foregut endoderm, following the differentiation of the foregut into liver, intestine and pancreas, where Nr5a2 is progressively expressed. At day E17.5, Nr5a2 exhibits its adult expression profile in the liver, exocrine pancreas, intestinal crypts and stomach epithelium[30]. By day E11.5, bipotential gonads express Nr5a2; by day E13.5 testis and ovaries become anatomically distinct, and the signal for Nr5a2 declines in the developing ovary and testis at day E15.5. This signal is increased again just in the postnatal ovary on day 2, in primordial follicles in both oocyte and granulosa cells, providing evidence for a potential role for Nr5a2 in gonadal development, in initiation of folliculogenesis and regulation of estrogen biosynthesis within the ovary[47].

1.4.1.1.1. Nr5a2 and pluripotency

Transcription factors, such as the Oct4, Sox2, Foxd3 and Nanog, are pivotal in supporting the maintenance of ES cells, which are pluripotent and known for their ability to self-renew and to differentiate into cells of the embryonic germ layers[42]. Nr5a2 and Oct4 are co-localized in the inner cell mass and in the embryonic epiblast, and Nr5a2 is required to maintain Oct4 expression at the epiblast stage of embryonic development (Figure 1.6), thereby maintaining the pluripotence of ES cells[39]. The Oct4 regulation is mediated by the interaction of Nr5a2 and DAX1, which typically acts as a co-repressor, but in this case, it differently results in the transcriptional activation of Oct4[53].

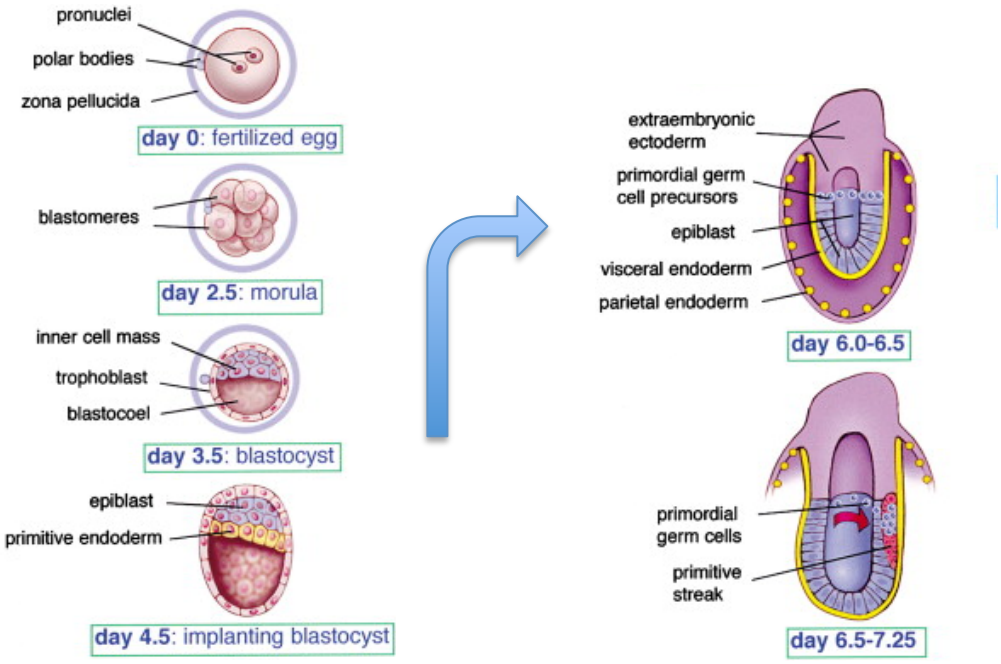

Figure 1.6 : Embryonic development from fertilization to primordial germ cell formation. The epiblast is derived from the inner cell mass of the blastocyst, and it differentiates to form the three germ layers known as ectoderm, endoderm and mesoderm in a process called gastrulation. Adapted from Zhao and Garbers, 2002[139].

The reprogramming of somatic cells into induced pluripotent stem cells (iPSCs) is possible by the introduction of factors such as Oct4, Sox2, Klf4 and c-Myc, and, among them, Oct4 is critical in inducing pluripotency due its uniqueness in being irreplaceable by other transcription factors. However, in 2009, Nr5a2 was shown to be capable of replacing Oct4 in the derivation of iPSCs from mouse somatic cells, enhancing reprogramming efficiency[41].

The factor leukemia inhibitory factor (LIF) is important to maintain pluripotency in culture, but it is dispensable for self-renewal *in viv*o. A recently identified pathway for the regulation of self renewal in ES cells is the canonical Wnt regulation of Nr5a2, by which β-catenin promotes pluripotency gene expression in an Nr5a2-dependent manner, resulting in the regulation of Tbx3, Nanog and Oct4 pluripotency factors[121]. Moreover, the epiblast stem cells (EpiSCs) are pluripotent cells derived from post-implantation mouse embryos from day E5.5 to E7.5, and they differ from ES cells because EpiSCs do not colonize host embryos when injected into the blastocyst. Nr5a2 is also an inducer of pluripotency in the EpiSCs, but in this case its activity is additional to inducing or replacing Oct4[40].

1.4.1.2. Intestine and liver

Nr5a2 was originally identified in the liver, and it is known for being involved in cholesterol and bile acid homeostasis by regulating the expression of a number of rate-limiting enzymes in the reverse cholesterol transport and bile acid synthesis pathways. Further, it has emerged as a key regulator of intestinal function[66]. The importance of Nr5a2 in homeostasis is due to its regulation of: 1) reverse cholesterol transport, by regulating the cholesteryl-ester-transfer protein (CETP) and scavenger receptor B1 (Scarb1), which are

crucial regulators of the transport of high density lipoprotein (HDL) from peripheral tissues to be excreted by the liver; 2) bile acid synthesis, which are water-soluble end products from cholesterol metabolism and essential for efficient absorption of dietary lipids, in which Nr5a2 was first showed to participate by regulating the gene transcription of the rate-limiting enzyme in bile acid biosynthesis, the cholesterol 7 alpha-hydroxylase (Cyp7a1), and the cytochrome P450 family 8 subfamily B polypeptide 1 (Cyp8b1), as showed *in vitro*; and 3) enterohepatic bile acid circulation[30].

However, by the use of targeted somatic mutagenesis in mouse hepatocytes, *in vivo* data showed that Nr5a2 regulates Cyp8b1, but not Cyp7a1[73], suggesting that Nr5a2 either is not important, or plays a minor role for Cyp7a1 expression *in vivo*, or moreover the regulation is compensated for by other factors. Recently it was discovered that the hepatocyte nuclear factor 4-alpha (HNF4α) works in concert with Nr5a2 to regulate Cyp7a1 transcription, by cooperating to maintain its basal expression[54]. Nr5a2 is also involved in the control of the inflammatory response at the hepatic level, modulating the so-called acute-phase response, which is the host reaction in response to trauma, infection, tissue damage or acute inflammation[118].

Nr5a2 controls intestinal inflammation in response to immunological stress by triggering local glucocorticoid production, which controls the activation of local intestinal immune cells[78], and it is suggested to initiate intestinal tumorigenesis both by affecting cell cycle control as well as through its role on inflammatory pathways[105]. Surprisingly, when Nr5a2 is disrupted in the intestinal epithelium *in vivo*, no evident macro or microscopic abnormalities were observed, nor there were changes in the triglyceride, free fatty acid, glucose or bile acid parameters, and plasma cholesterol was modestly decreased[66].

The cell proliferation is another role for Nr5a2, described first in the intestinal cells. It simultaneously induces G1 cyclin D1 and E1 in intestinal crypt cells, potentiated by its interaction with β-catenin, promoting cell renewal via the crosstalk with β-catenin/Tcf4 signaling pathway[10]. Combining Nr5a2 competence in proliferation and cell renewal with the role in inflammation, it is not surprising that an aberrant Nr5a2 expression can be associated with tumors, including colon and gastric cancers[24]. These tumorigenesis interactions are schematically represented in Figure 1.7.

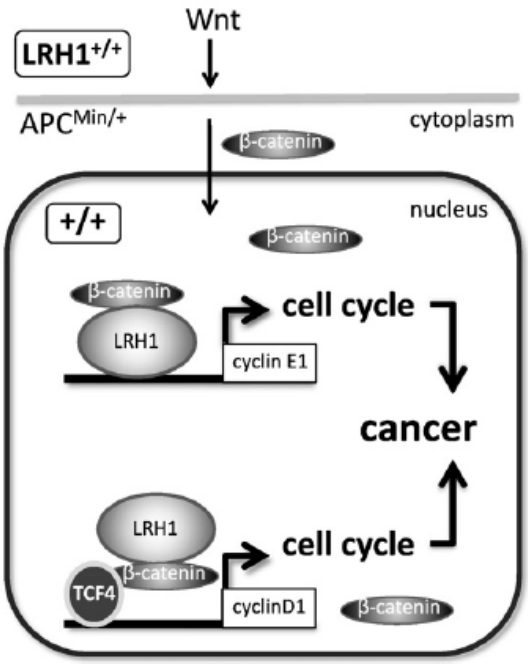

Figure 1.7 : Nr5a2 drives cell cycle progression and tumorigenesis by synergizing with the β-catenin signaling pathway, acting directly as a transcription factor (cyclin E1) and as a cofactor for Tcf-β-catenin (cyclin D1) in the gut (from Fernandez-Marcos, 2011)[33].

1.4.1.3. Pancreas

In the pancreas, Nr5a2 is co-expressed with the pancreatic-duodenal homeobox 1 (PDX-1) during embryonic development, and PDX-1 controls Nr5a2 expression in the mouse from E8.5 to E16.5[30]. Consequently, Nr5a2 participates in the regulatory cascade governing pancreatic development, differentiation and function[3]. In the adult, Nr5a2 expression becomes restricted to the murine exocrine pancreas[67], where it regulates a specific transcriptional network required for the production and secretion of pancreatic juice, for instance, the carboxyl ester lipase (CEL), which is important for the enterohepatic cholesterol homeostasis[31]. Recently, an *in vivo* study has shown that Nr5a2 is not required for the specification or development of acinar cells, but it is important for maintaining the acinar identity and reestablishing acinar fate during regeneration[120].

In 2010, Nr5a2 has been identified as a significant predisposing factor for pancreatic cancer, through a genome-wide association study[92], and its expression is found to be elevated in human pancreatic ductal adenocarcinomas[7]. The activation of Nr5a2 transcription mediates proliferation and differentiation in the pancreatic ductal, via regulation of cyclin D1, E1 and c-Myc, and moreover, it regulates cell cycle arrest in pancreatic cancer cells[61]. The possible link between Nr5a2 and pancreatic dysfunctions raised the speculations on whether Nr5a2 is related to diabetes. It has been determined that Nr5a2 plays an important role in the transcriptional activation of the adiponectin gene, which is a potential candidate for the association of obesity, diabetes and increased risk of pancreatic cancer[67].

1.4.1.4. Other tissues

The expression of Nr5a2 is not restricted to any single system, indeed, it is widely expressed throughout the mammalian organism. Nr5a2 has been shown to be expressed in murine stomach, tongue, gall bladder, alveolar type II cells of the respiratory system, transitional epithelium of the urinary system, brown adipocytes, cardiomyocytes and hypothalamus[44], but its functions in these tissues have not yet been explored in any depth.

In the rat anterior pituitary gland and in gonadotropic cell lines, Nr5a2 was shown to regulate gonadotropin gene expression, activating the follicle-stimulating hormone (FSH)β and luteinizing hormone (LH)β promoter *in vitro*[140]. On the other hand, a recent study using a mouse model with a gonadotrope specific deletion of Nr5a2 demonstrated that its expression in the pituitary is dispensable *in vivo*, since these mice had normal pituitary FSHβ and LHβ expression and intact fertility[35].

Studies in humans have shown that Nr5a2 is expressed in bone cells, modulating gene expression in osteoblasts and associated with bone mass[96]; and in the adrenal gland, possibly regulating steroidogenesis[122]. This last study was among the earliest to stimulate investigations on the role of Nr5a2 in gonadal steroid hormone production. Indeed, it is now known that Nr5a2 is expressed in the testicular Leydig cells and in ovarian follicular cells[44], and its function in reproductive related events had become an intringing and interesting area of research.

1.4.2. Nr5a2 and reproduction

The high level of ovarian and testicular Nr5a2 expression makes it likely that Nr5a2 plays an important role in the regulation of gonadal function[107], and its role in reproduction is strongly related to its steroidogenic competence. Nr5a2 is essential for female fertility[25], and this section will focus on the reproductive events regulated by Nr5a2, from the first discoveries to the state of the art.

1.4.2.1. Nr5a2 in steroidogenesis

As described previously in the section 1.1.2, Nr5a1 (or SF-1) is expressed in most steroidogenic tissues and regulates expression of several steroid-metabolizing enzymes[107], but its expression is downregulated in the ovarian corpus luteum (CL)[46]. The CL is a highly steroidogenic structure, resulting from the differentiation of theca and granulosa cells, producing progesterone. Considering that Nr5a1 and Nr5a2 are closely related, a potential role for Nr5a2 in the regulation of gonadal steroidogenesis was established for essentially two reasons: 1) Nr5a2 is expressed in the ovary, and this expression is higher in the CL compared with ovarian follicular cells[91]; and 2) the CL should have an alternative steroidogenesis regulator other than Nr5a1. Altogether, these hypotheses were the inspiration for the "*in vitro* era" of assays in human ovarian tissue and cells, in order to identify Nr5a2 steroidogenic target genes.

It is now known that, under the control of FSH[59], Nr5a2 plays a critical role in the regulation of steroidogenic proteins and enzymes by enhancing their activity, including the steroidogenic acute regulatory protein (Star), the cholesterol side-chain cleavage enzyme (Cyp11a1), the cytochrome P450 17a1 (Cyp17a1), the 3 beta-hydroxysteroid

dehydrogenase (Hsd3β) and the steroid 11β-hydroxylase (Cyp11b1)[107]. Nr5a2 also induces the promoter activity of the human and mouse Scarb1, which is involved in steroidogenesis by facilitating cholesterol transport[104]. Moreover, Nr5a2 serves as a critical factor in the transcriptional regulation of the aromatase (Cyp19a1) gene expression, hence, estrogen biosynthesis in the ovary[75]. Figure 1.8 represents steroidogenesis in ovarian follicular cells.

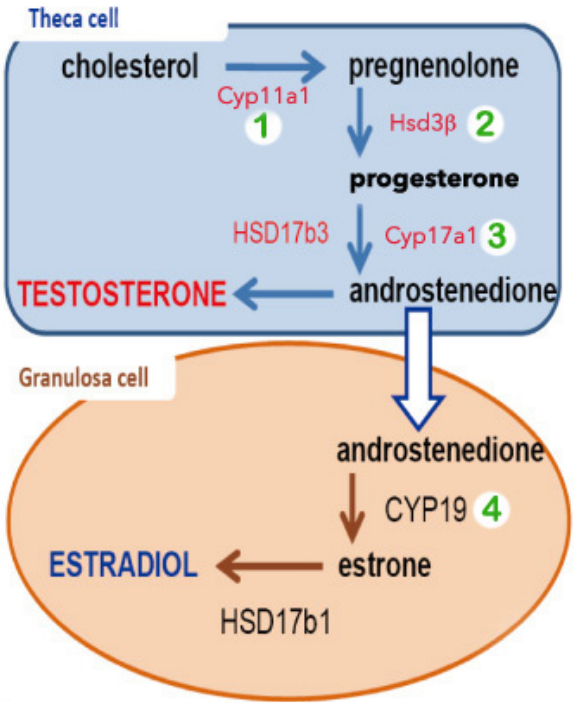

Figure 1.8 : Enzymes involved in the ovarian steroidogenesis. The precursor cholesterol is transferred within the steroidogenic cells by the Scarb1, and within the mitochondria by the enzyme Star. In the theca cells, cholesterol is converted to pregnenolone by Cyp11a1 (1). The Hsd3β (2) converts pregnenolone to progesterone, which is transformed into androgens by the Cyp17a1 (3). Androgens are the substrate for estradiol production in granulosa cells, which is catalyzed by the Cyp19a1 (4). Adapted from Oakley et al., 2011[84].

1.4.2.2. Nr5a2 in human breast

The hypothesis that Nr5a2 drives the transcription of aromatase in the breast adipose tissue came to be because of the lack of Nr5a1 expression in this tissue. Nr5a2 expression was then identified in the preadipocyte fraction of human adipose tissue, including the stromal compartment of human breast, regulating the expression of aromatase[22] by binding to the alternative promoter II and inducing local estrogen production[30]. Aromatase expression is induced 3 to 4 fold in adipose tissue of breast cancer, and it represents the source of estrogen for estrogen-dependent breast tumor growth via local conversion of circulating androgen precursors[21].

The expression of Nr5a2 in breast cancer is localized in tumor epithelial cells and intra-tumoral stroma, and evidence suggests that its expression is tightly connected with estrogen signaling pathway. It interacts with aromatase and with estrogen receptor alpha (ERα), as shown in the MCF7 breast cancer cell line[2]. The Nr5a2 promoter contains an estrogen response element, thus it not only regulates but it is also regulated by estrogen in breast cancer (Figure 1.9)[61]. Both the expression of aromatase and Nr5a2 are driven by tumor-derived factors such as prostaglandin E2 (PGE2), resulting in increased estrogen availability for tumor progression[21; 141].

Functionally, Nr5a2 is associated with invasive breast cancer, promoting estrogen-dependent cell proliferation, motility and cell invasiveness, by remodeling the actin cytoskeleton and cleaving E-cadherin[19]. One mechanism of action for Nr5a2 was recently described to be the regulation of a well characterized ER target gene, known as growth regulation by estrogen in breast cancer 1 (GREB1). Nr5a2 thus promotes cell proliferation by enhancing ER mediated transcription of target genes in a synergistically manner[20].

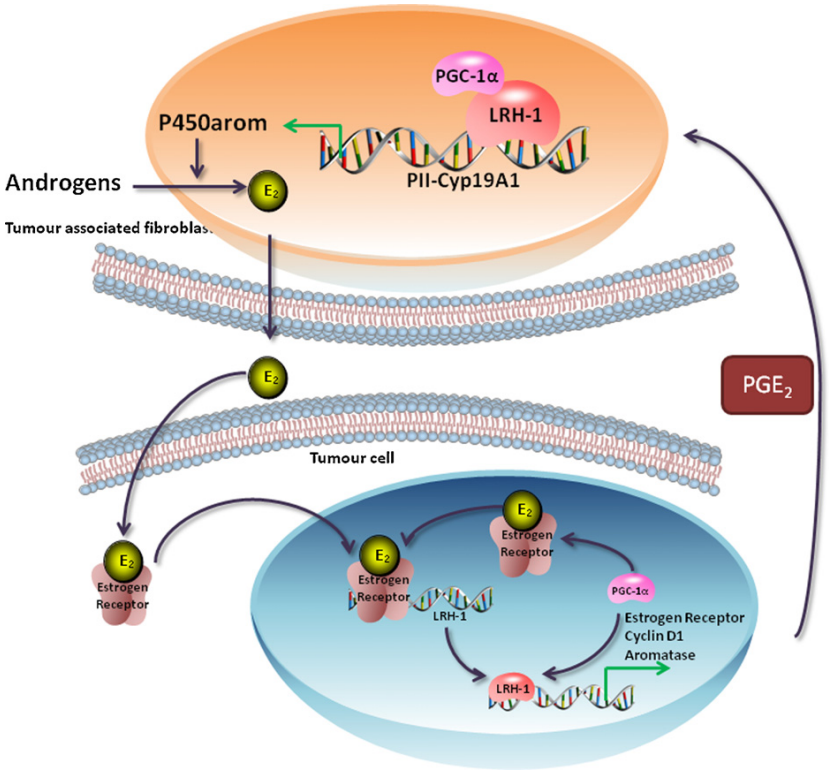

Figure 1.9 : Nr5a2 (Lrh-1) actions in the breast cancer cell. Nr5a2 activates aromatase transcription leading to increased estrogen synthesis, promoting tumor growth. The estrogen receptor (ERα) activates Nr5a2 expression in malignant epithelial cells, suggesting that the Nr5a2 is tightly linked with the estrogen signaling pathway (reviewed by Lazarus et al., 2012)[61].

Nr5a2 has been involved in invasive breast carcinomas and ductal carcinomas in situ, hence it has potential impact as a therapeutic target[61]. Aromatase inhibitors are clinically used in breast cancer treatments, but the decreased estradiol production in a global manner gives rise to side effects such as bone loss. For this reason, inhibitors or inverse agonists of Nr5a2 represent a strategy of a selective aromatase modulator for the development of breast cancer specific therapy[15].

1.4.2.3. Nr5a2 in the testis

Given the importance of Nr5a2 to induction of steroidogenic enzymes and factors[30], it is not surprising that it is highly expressed in the steroidogenic Leydig cells of the testis, as well as in pachytene spermatocytes and round spermatids. It plays an important role in the regulation of aromatase expression in Leydig cells[93], where these factors are co-expressed[106]. Nr5a2 appears not to be present in Sertoli cells, which regulate germ cell development and where Nr5a1 predominates. Mice heterozygous for Nr5a2 mutation, i.e. where only a single functional allele is present, have circulating testosterone levels that are less than half their wild type (WT) littermates[119]. Precocious expression of Nr5a2 in mice leads to precocious induction of androgen synthesis and early puberty[25].

In 2006, it was shown that Nr5a2 is involved in the differentiation of mesenchymal stem cells (MSCs) into steroid hormone-producing cells, such as testicular Leydig cells, inducing the expression of Cyp17a1. Therefore, Nr5a2 could represent a key regulator controlling the differentiation of stem cells into steroidogenic lineage, and play a pivotal role in steroid hormone production in human Leydig cells[131].

1.4.2.4. Nr5a2 in the ovary

As previously mentioned, Nr5a2 is highly expressed in the mouse ovary, specifically in the steroidogenic granulosa and luteal cells, and distinctly absent in theca cells and ovarian stroma[46]. It has also been identified in equine[9], rat[27], rabbit[1], bovine[29; 113] and human[107] ovaries. During folliculogenesis (Figure 1.10), Nr5a2 is expressed in primary follicles and at all later stages of follicular development, induced significantly in the CL during pregnancy[47]. Nr5a2 expression precedes aromatase expression during

folliculogenesis, serving as a multifunctional steroidogenic factor in ovarian physiology, regulating estradiol and progesterone production[70], although contrasting data showed no effect of Nr5a2 on the induction of estradiol *in vitro* during granulosa cell differentiation[103]. The expression of Nr5a2 is increased by FSH in granulosa cells, and by prolactin in luteal cells[27].

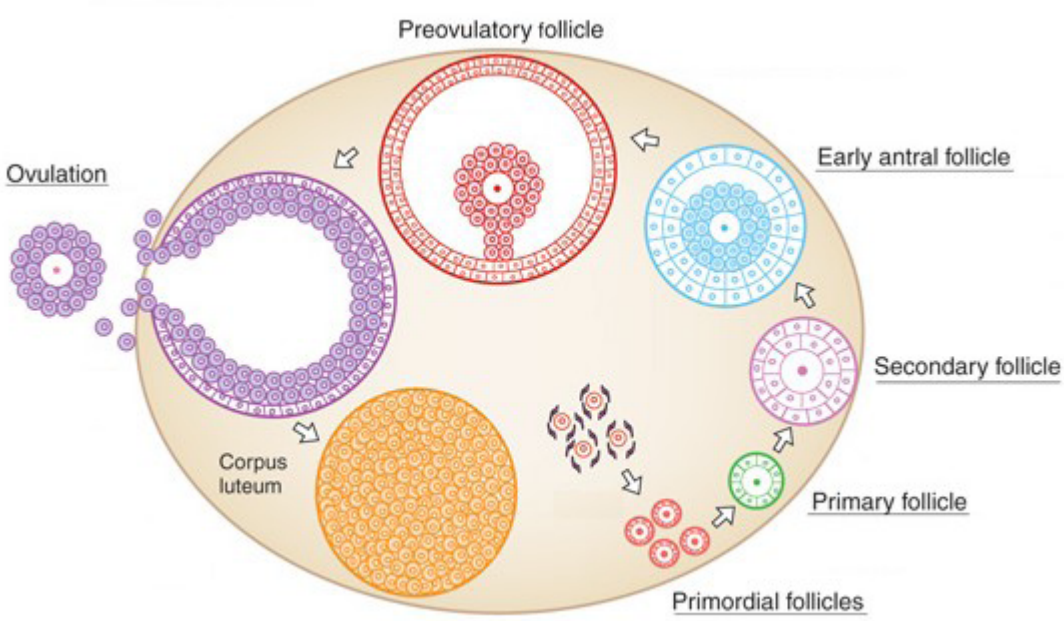

Figure 1.10 : Follicular development. A number of primordial follicles appear 1 to 2 days after birth, when flat squamous pre-granulosa cells surround oocytes. Primary follicles have one layer of granulosa cells around the oocyte, acquiring new layers during follicular development; tertiary follicles will develop to antral follicles, when granulosa cells differentiate into mural and cumulus cells. When the LH peak occurs, immediate changes happen in the follicle including cumulus expansion, ovulation and the CL formation. Adapted from Matzuk et al., 2008[74].

The ovulation process begins when FSH stimulates granulosa cells proliferation and LH receptor expression[143]. The LH surge triggers the reactivation of the oocyte from meiosis and the breakdown of the follicle wall. The peak of LH also leads the cumulus cells

to produce a hyaluronic acid matrix along which they migrate outwardly from the oocyte[26]. Ovulation is complete when the cumulus-oocyte complex (COC) is released into the oviduct[142]. Successful ovulation and fertilization are correlated with the quantity and the quality of the expanded cumulus mass[26]. Changes in gene expression and follicular structure occur with overlapping control and interdependent consequences in the theca, granulosa, cumulus and oocyte compartments of the ovarian follicle. Following ovulation, granulosa cells remaining in the postovulatory follicle undergo luteinization[144].

In 2007, the essential role of Nr5a2 in reproductive function and steroidogenesis *in vivo* was evidenced for the first time. This study employed mice heterozygous for a null mutation of Nr5a2, and the females presented a decreased fertility due to an altered luteal function[58].

A breakthrough in the role of Nr5a2 in female fertility was achieved in 2008, by the use of a conditional knockout of *Nr5a2* gene using a mouse line Cre-recombinase specific to granulosa cells of primary follicles, crossed with a mouse line with *loxP* sites flanking the third and fourth exons of the *Nr5a2* gene. The Nr5a2 granulosa-specific knockout females were infertile, and the principal cause for the sterility was the total failure in cumulus expansion and ovulation, which could not be redressed by gonadotropin stimulation[25].

The normal expression of a number of genes was disrupted in this mouse model, including the steroidogenic genes *Cyp11a1*, *Cyp19a1* and *Star*; the rate-limiting gene in prostaglandin synthesis, the prostaglandin-endoperoxide synthase 2 (*Ptgs2*); and genes associated with cholesterol transfer such as *Scarb1*[25]. Later, another transgenic mouse model was used to study the effect of transient Nr5a2 knockdown *in vivo*. The females presented a consistent reproductive phenotype if compared with the Nr5a2 granulosa-

specific knockout, but the infertility was fully reversible after the cessation of Nr5a2 knockdown, with no signs of irreversible changes due to the transient reduction of Nr5a2 expression[37].

Nr5a2 is also expressed in the mouse and human endometrium, and a recent study showed that it is necessary for the promotion of endometrial decidualization and for placenta formation[135]. This was achieved by the disruption of its expression in the ovary during luteinization, which resulted in luteal insufficiency, gestational failure, fetal growth retardation and fetal death[135]. Altogether, these data show that Nr5a2 is essential for female fertility in both gonads and the uterus (Figure 1.11), and it is considered a potential pharmaceutical target for contraception by its role in ovulation.

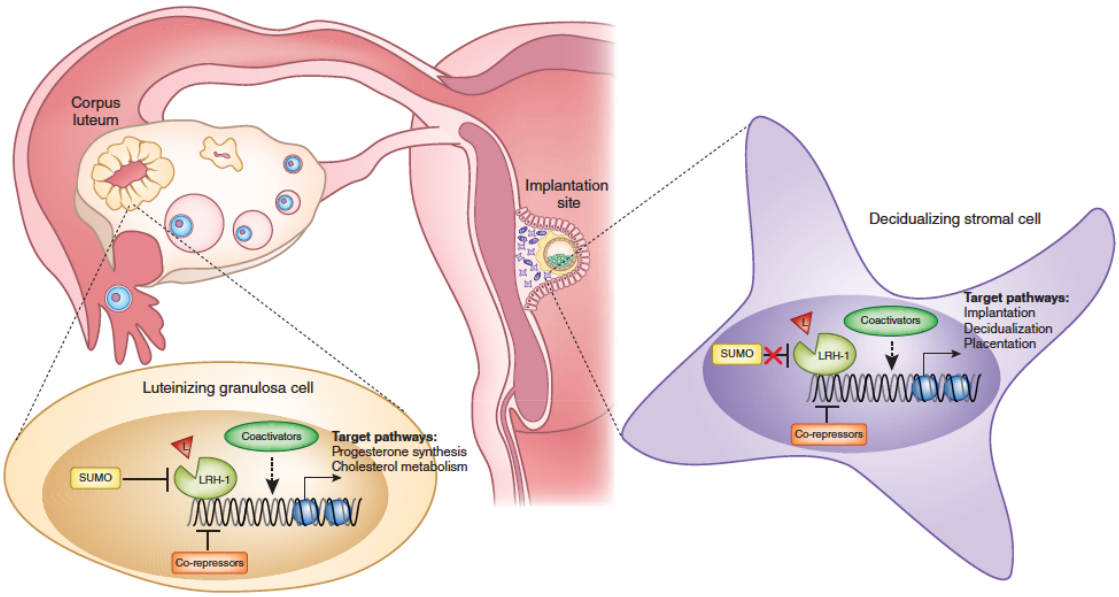

Figure 1.11 : Nr5a2 and the female reproductive system. Nr5a2 is expressed in ovarian luteal cells and it is essential for progesterone synthesis during pregnancy. In uterine cells, Nr5a2 is essential in implantation, decidualization and placentation (reviewed by Brosens et al., 2013)[13].

Hypothesis and objectives

Based on the previous published work on the expression of Nr5a2 in granulosa cells of primary ovarian follicles and its essential role in the ovulatory process, we hypothesize that Nr5a2 modulates the events leading to ovulation and their consequent luteinization in a temporal sequence.

The purpose of this investigation was to determine the role of Nr5a2 in female fertility.

Specific objectives:

1. To examine the role of Nr5a2 in ovulation and luteinization at differing stages of the follicle maturation by timed tissue specific disruption of Nr5a2 in mouse ovarian granulosa cells of primary and antral follicles. The results corresponding to this objective are described in the Chapter 2.

2. To determine when Nr5a2 is essential for and how it regulates cumulus expansion in the mouse ovary, and whether its expression is required for the developmental competence of oocytes to be fertilized. The data related to this objective are described in the Chapter 3.

Chapter 2

2. First manuscript

The orphan nuclear receptor Nr5a2 is essential for luteinization in the female mouse ovary

Kalyne Bertolin[1], Jan Gossen[2], Kristina Schoonjans[3] and Bruce D. Murphy[1,4]

Affiliations: [1]Centre de recherche en reproduction animale, Faculté de médecine vétérinaire, Université de Montréal, St-Hyacinthe, Quebec, J2S 7C6, Canada; [2]Amgen, Eindhoven, The Netherlands; [3]Laboratory of Integrative and Systems Physiology, École Polytechnique Fédérale de Lausanne, CH-1015 Lausanne, Switzerland; [4]Corresponding author

Abbreviated title: The role of Nr5a2 in luteinization

Key words: Nr5a2, granulosa cells, conditional knockout mouse, ovulation, luteinization

Status: Submitted for publication. *Endocrinology*. 2013, Aug 14th.

Author contributions: Overall, my relative contribution to this work was 90%. My contribution involved designing the experiments; protocol optimization; manipulation of animals and samples; performance of laboratory techniques; interpretation of the results; design and preparation of the figures and writing of the text. JG provided the Cyp19a1 Cre-recombinase mouse line. KS provided the Nr5a2 floxed mouse line. BDM supervised the project and contributed to the writing task.

2.1. Abstract

The corpus luteum is a temporary endocrine ovarian structure that produces progesterone. Luteal and granulosa cells express the nuclear receptor Nr5a2. Previous studies demonstrated that Nr5a2 is required for ovulation and luteal steroid synthesis. Our objectives were to analyze the temporal sequence in the regulatory effects of Nr5a2 in the ovary, with focus on luteal function. We developed a female mouse model of granulosa-specific targeted disruption from the formation of the antral follicles forward (genotype $Nr5a2^{Cyp19-/-}$). Mice lacking Nr5a2 in granulosa cells of antral follicles are infertile. Although cumulus cells undergo expansion after gonadotropin stimulation, ovulation is disrupted in those mice, at least in part, due to the downregulation of the progesterone receptor (*Pgr*) gene. The excision of Nr5a2 in antral follicles permits formation of luteal-like structures, but not functional corpora lutea as they produced reduced progesterone levels and failed to support pseudopregnancy. Progesterone synthesis is affected by depletion of Nr5a2 due to, among others, defects in the transport of cholesterol, evidenced by downregulation of *Scarb1*, *Ldlr* and *Star*. Comparison of this mouse line with that in which Nr5a2 is depleted from the primary follicle forward (genotype $Nr5a2^{Amhr2-/-}$) demonstrates that Nr5a2 differentially regulates female fertility across the trajectory of follicular development.

2.2. Introduction

Just prior to birth, the mouse ovary contains a cluster of densely packed oocytes, soon to be transformed by the process of follicle assembly[28]. The product is the primordial follicle, formed in the first two days after birth, when flat squamous pre-granulosa cells surround the oocytes. Cohorts of these follicles enter the growing pool, and the presence of cuboidal and dividing granulosa cells defines these as primary follicles[29]. The growth of the oocyte in this class of follicles correlates with the beginning of anti-Müllerian hormone (Amh) expression[26]. Amh expression is restricted to granulosa cells, first detected in the mouse ovary at day 6 after birth and it is known to regulate the number of growing follicles and their selection for ovulation[26; 12]. The expression pattern of the gene encoding the Amh type II receptor (Amhr2) overlaps with Amh in postnatal granulosa cells[20].

Primary follicles undergo the transition to secondary follicles, characterized by an additional theca layer surrounding more than one layer of granulosa cells. The first antral follicles are seen by day 13, and by day 21 after birth, follicles with multiple layers of granulosa cells containing scattered areas of interstitial fluid are present. Granulosa cells of antral follicles express aromatase, the enzyme responsible for catalyzing the conversion of androgens into estrogens. It is encoded by the cytochrome P450 family 19 subfamily A polypeptide 1 (*Cyp19a1*) gene[35]. This process is essential, as the mouse model lacking functional aromatase activity (aromatase knockout – ArKO) is infertile due to disrupted folliculogenesis and failure to ovulate[6].

During the antral stage, follicular granulosa cells differentiate into at least two populations, those in layers that surround the oocyte, known collectively as the cumulus cells, and the layers that line the follicular wall, known as mural granulosa cells. Cumulus

cells are closely connected and form a functional reciprocal communication with the oocyte[14]. The preovulatory LH surge triggers a series of events, including cumulus expansion from the oocyte in an extracellular matrix[15], a critical process for ovulation[13]. Follicular prostaglandins are mandatorily increased prior to ovulation, induced by selective induction of the prostaglandin-endoperoxide synthase-2 (*Ptgs2*) expression in granulosa cells[34]. Likewise, following the LH peak, mural granulosa cells of preovulatory follicles are induced to express the progesterone receptor (*Pgr*) gene, with the maximum *Pgr* expression at 8 hours after the LH surge, just prior to ovulation[2]. In the mouse, ovulation ensues at 12 hours after the LH peak[36]. The expression of *Pgr* regulates the proteolytic enzyme, a disintegrin and metalloproteinase with thrombospondin motifs-1 (Adamts-1)[32], whereas Adamts-4, another protease implicated in the ovulatory process, does not appear to be a major target of Pgr[31].

Following ovulation, granulosa and theca cells from the postovulatory follicle undergo cellular reorganization to form the corpus luteum (CL), a transient endocrine organ that produces progesterone, essential for endometrial cell differentiation and maintenance of pregnancy[29]. The functional remodeling of the follicle to form the CL entails a large scale increase in progesterone synthesis, requiring upregulation of cholesterol substrate availability[27]. The scavenger receptor class B type I (Scarb1) is a luteinization marker and is the receptor for high-density lipoprotein (HDL), providing much of the substrate cholesterol for ovarian steroidogenesis[21] during the luteal phase. The rate-limiting step in steroidogenesis is the expression of the steroidogenic acute regulatory protein (Star), which regulates the cholesterol transfer within the mitochondria. Cholesterol is then converted to pregnenolone by the cytochrome P450 side-chain cleavage enzyme (Cyp11a1). Another enzyme, 3-hydroxysteroid dehydrogenase (Hsd3β), converts pregnenolone to progesterone

that is secreted or can be then transformed into androgens by the 17α-hydroxylase (Cyp17a1). Androgens are the substrate for estradiol production by the aromatase activity as previously described[27].

The nuclear receptor Nr5a2, also known as liver receptor homolog-1 (Lrh-1), is highly expressed in granulosa cells of primary to preovulatory follicles[25] as well as in luteal cells[19]. Germline deletion of Nr5a2 results in early embryo lethality[22], thus, there is a need for a strategy of conditional depletion to explore its role in the ovary. By means of ovary-specific depletion, we have previously shown that Nr5a2 is required for multiple events essential for ovulation[11]. It was also reported that Nr5a2 is essential for pregnancy by regulating uterine decidualization[37]. The latter studies further indicated that Nr5a2 is required for steroidogenesis in the CL[37]. To date, these studies have focused either on the role of Nr5a2 in ovarian follicular development from primary follicles[11] or after the luteinizing stimulus[37]. The consequences of depletion at different times in the folliculogenesis suggest that there is a temporal sequence in the regulatory effects of Nr5a2. In the present study we explored the role of Nr5a2 using a mouse model with granulosa-specific knockout in antral and preovulatory follicles. This new model provides insight into the role of Nr5a2 in the later stages of follicle development.

2.3. Materials and methods

Animals and colony maintenance

All animal experiments were approved by the University of Montreal Animal Care Committee and conducted according to the guidelines of the Canadian Council on Animal

Care (CCAC). All mutant and control mice were of the C57BL/6 background. Animals were maintained under a 14:10 light:dark cycle and provided food and water ad libitum. Euthanasia was performed by anesthetizing the animals with Isoflurane (PPC, Richmond Hill, ON, Canada) in a closed container, followed by cervical dislocation. Nr5a2 floxed ($Nr5a2^{f/f}$) mice, generated by Dr. Johan Auwerx, have been described previously[5]. To generate granulosa-specific Nr5a2 mutant in antral follicles, animals expressing Cre-recombinase from Cyp19a1 ($tgCyp19a1^{Cre/+}$)[17] were crossed with $Nr5a2^{f/f}$ mice ($Nr5a2^{Cyp19-/-}$). To compare two different granulosa-specific mouse models, we employed $Nr5a2^{f/f}$ mice crossed with animals expressing Cre-recombinase from the anti-Müllerian hormone receptor-2[11] ($Amhr2^{Cre/+}$; generous gift of Dr. Richard Behringer), generating granulosa-specific Nr5a2 mutant in primary follicles ($Nr5a2^{Amhr2-/-}$). The litters were genotyped (see Supplemental Table II for primers) using DNA extracted from a biopsy of the tail. The non-mutant littermates were used as control groups, i.e., $Nr5a2^{f/f}tgCyp19^{+/+}$ and $Nr5a2^{f/f}Amhr2^{+/+}$ (respectively to the $Nr5a2^{Cyp19-/-}$ and $Nr5a2^{Amhr2-/-}$).

Estrous cycle and superstimulation protocol

For estrous cycle staging, vaginal smears were collected daily (0900) with phosphate-buffered saline (PBS) 1x; smears were placed on glass slides and cytology was evaluated under the microscope (reviewed in Chapter 5). For superstimulation, 25 to 27-day-old immature female mice, both $Nr5a2^{Cyp19-/-}$ and control were injected intraperitoneal (IP) with 5 IU of equine chorionic gonadotropin (eCG) (Folligon®, Intervet, Whitby, ON, Canada) to stimulate follicular development, followed by the injection of 5 IU of human chorionic gonadodotropin (hCG) (Chorulon®, Intervet, Whitby, ON, Canada) 44 to 48 h

post eCG, to induce ovulation. Ovaries and blood (collected by cardiac puncture) were collected at 12 h, 18 h or 24 h post hCG; ovaries were either snap frozen in liquid nitrogen and stored at -80^{o}C for RNA or fixed in paraformaldehyde (PAF) 4% (Sigma-Aldrich) and embedded in paraffin for histological examination. Ovulated cumulus-oocyte complexes were collected from oviducts at 16 h post hCG injection and counted. Pure granulosa and cumulus cells were collected from Nr5a2$^{Cyp19-/-}$ and control at 12 h post hCG for the detection of *Nr5a2* by qPCR and immunoblotting; these cells were isolated by puncturing both ovaries with 25G5/8" needles in PBS 1x, treating with hyaluronidase (from bovine testes, Sigma) and filtered (BD Falcon, Cell Strainer, 40 μm Nylon, Mexico) to remove the oocyte. At 4 h post hCG, pure granulosa and cumulus cells were isolated from Nr5a2$^{Cyp19-/-}$ and Nr5a2$^{Amhr2-/-}$ and their respective control females for RNA analysis.

Breeding trials

For breeding assays, 8-week-old Nr5a2$^{Cyp19-/-}$ and control females were housed with reproductively proven C57BL/6 males for 6 months. Cages were inspected daily, and parturition dates and litter sizes were recorded. Another group of 8-week-old Nr5a2$^{Cyp19-/-}$ females was housed with C57BL/6 males, while control females were housed with vasectomized males for 40 days to establish the frequency of mating. The occurrence of copulatory plugs was verified by visual examination at 9:00 a.m. each day. For vasectomies, male mice were anesthetised by injection of Ketamine (100 mg/kg; Bioniche Animal Health, Belleville, ON, Canada) and Xylazine (10 mg/kg; Bayer Inc., Toronto, ON, Canada) then an incision of 1 cm through the skin along the midline of the lower abdomen was made, and 1 cm of vas deferens on each side was removed. Two weeks later, the

sterility of the vasectomized males was confirmed by housing with fertile females and subsequent observation of the absence of pregnancy for 60 days. For analysis of progesterone, adult (> 60 days of age) $Nr5a2^{Cyp19-/-}$ and control females were bred to males of proven fertility. Animals were examined daily at 9:00 a.m. for copulatory plugs, and the day that a plug was found was designated day 1 post coitum (dpc). Animals were terminated at 5.5 dpc for morphological analysis of the uterus and ovaries, and blood was collected for progesterone radioimmunoassay.

RNA isolation and real time polymerase chain reaction (qPCR)

Total RNA from ovary, liver and granulosa/cumulus cells was extracted with RNeasy® Mini Kit (Qiagen) as per manufacturer's instructions; adipose tissue total RNA was extracted by using the RNeasy® Lipid Tissue Midi Kit (Qiagen). Reverse transcription was performed with the SuperScript® II First Reverse Transcriptase (Invitrogen) and random hexamer primers. Real-time quantitative PCR (qPCR) was performed using Power SYBR® Green PCR Master Mix (Applied Biosystems, Warrington, UK), with the 7300 real-time PCR system (Applied Biosystems, Foster City, CA, USA). A common thermal cycling parameter (2 min at 50°C, 10 min at 95°C, then 40 cycles of 15 s at 95°C and 60 s at 60°C) was used to amplify each transcript. Melting curve analyses were performed to verify product identity, adding a dissociation step to the PCR run (15 s at 95°C, 60 min at 60°C, 15 s at 95°C, and 15 s at 60°C). The sequences of the primers used are listed in Supplemental Table II, each was used in a final concentration of 3000 nM. Primers were validated by standard curves. Samples were run in triplicate and results were expressed relative to the ribosomal protein S18 (RPS18) levels. Data were then normalized to a

calibrator sample using ΔΔCt method, as described by Pfaffl[18], with correction for amplification efficiency by LinRegPCR 11.0 software (Academic Medical Center, Amsterdam, the Netherlands).

Immunoblotting

Total protein was extracted with 25μg lysis buffer from granulosa/cumulus cells, separated on 10% SDS-PAGE, and subsequently transferred to a PVDF membrane. The membrane was blocked using 0.5% non-fat milk in Tris buffered saline containing 0.1% Triton-X (TBST) for 1 h at room temperature, incubated with rabbit polyclonal Nr5a2 (Abcam, ab18293), diluted 1:500 in blocking solution overnight at 4°C, and then incubated in horseradish peroxidase (HRP)-conjugated goat anti-rabbit immunoglobulin G (IgG; Santa Cruz Biotechnology) diluted 1:50,000 in TBST for 1 h at room temperature. Proteins were visualized by chemiluminescence (Immobilon Western, Millipore Corporation, Billerica, MA). Subsequently, membranes were washed in TBST, blocked as above, and incubated with HRP conjugated anti-mouse-β-actin (Santa Cruz Biotechnology), diluted 1:80,000 in blocking solution for 20 minutes at room temperature. The optical density of bands detected at the expected molecular weight for Nr5a2 and β-actin was quantified by the Image Processing and Analysis in Java (ImageJ) software. The ratio of Nr5a2 and β-actin densities was calculated for each sample.

Immunofluorescence

For histological examination, ovaries were fixed in PAF 4% overnight, then washed

in PBS 1x and paraffin embedded. Ovarian cell-specific localization of Nr5a2 and Scarb1 was verified by fluorescence immunohistochemistry. Briefly, paraffin sections of ovaries were rehydrated, boiled in 10 mM sodium citrate (pH 6) for 30 minutes, and cooled to room temperature (RT). Sections were blocked overnight with 5% bovine serum albumin (BSA; IgG-Free, Protease-Free; Jackson Immunoresearch Lab., Inc.) at 4^{o}C. Samples were then incubated with Nr5a2 (Abcam, ab18293) or rabbit polyclonal anti-mouse Scarb1 (Novus Biologicals), both diluted 1:50 in PBS 1x with 5% BSA overnight at 4^{o}C. As a negative control, some sections were incubated with 5% BSA only. Sections were washed and incubated with cyanine 3 (Cy3)-conjugated goat anti-rabbit IgG (Jackson Immunoresearch Lab., Inc.), diluted 1:400 in PBS 1x for 1 h at RT. Slides were then washed, and sections were counterstained with 4',6-diamidino-2-phenylindole (DAPI, Sigma, MO), diluted 1:1,000 in PBS 1x, for 5 min. Slides were mounted in Permafluor (Thermo Fisher Scientific). Ovarian distribution of Nr5a2 and Scarb1 was observed by Axio imager M1, Zeiss Microscopy.

Hormone assays

Radioimmunoassay for progesterone (serum) and estradiol-17β (serum and follicular fluid) concentrations were evaluated in single assays according to a protocol previously described[11]. The intra-assay coefficients of variation were calculated between duplicates ranged from 4 to 9%.

Statistical analyses

All data were analysed using JMP (Version 5.0.1a. SAS Institute Inc.) statistical

software. Differences between mutant and control mice for a single data point were determined by Student's *t*-test. For data obtained at multiple time points or multiple genotypes, two-way analysis of variance and differences between individual means were determined by the JMP LSMeans Contrast test. All numerical data are represented as mean ± SEM. Significant difference was recognized at $p < 0.05$.

2.4. Results

The reproductive performance of female Nr5a2 conditional knockout mice in granulosa cells of antral follicles

The conditional knockout (cKO; $Nr5a2^{Cyp19-/-}$) mouse model generated by crossing Nr5a2-floxed mice with mice expressing the Cre-recombinase driven by the aromatase promoter, i.e., the transgenic line $tgCyp19a1^{Cre/+;}$ [17], presented an efficient and tissue-specific disruption of the *Nr5a2* target gene as indicated by dramatically reduced mRNA abundance in ovarian granulosa cells from antral follicles, but not in the other organs expressing Nr5a2 (Figure 2.1A-C). Protein levels of Nr5a2 were also reduced in granulosa cells of the $Nr5a2^{Cyp19-/-}$ ovaries, as shown by immunoblotting (Figure 2.1D-E) and by immunofluorescence (Figure 2.1F-L). The temporal specificity of Nr5a2 downregulation in the $Nr5a2^{Cyp19-/-}$ ovarian sections was evident by depletion in granulosa cells of antral follicles (Figure 2.1I) but not in preantral follicles (Figure 2.1G), as expected. After a 6-month breeding trial with reproductively proven males, the control group composed of intact littermates ($Nr5a2^{f/f}$ $tgCyp19a1^{+/+}$) generated the expected frequency of litters per female and litter size, while no litters were born from the $Nr5a2^{Cyp19-/-}$ females (Figure

2.2A). Daily consecutive evaluation of the vaginal epithelium evidenced a normal pattern of estrous cyclicity of 4 to 5 days in Nr5a2$^{Cyp19-/-}$ females compared to the control group (Figure 2.2B), with no abnormally prolonged intervals, indicating that the inability of the Nr5a2 conditional knockout mouse model to produce pups is not due to an irregular estrous cycle.

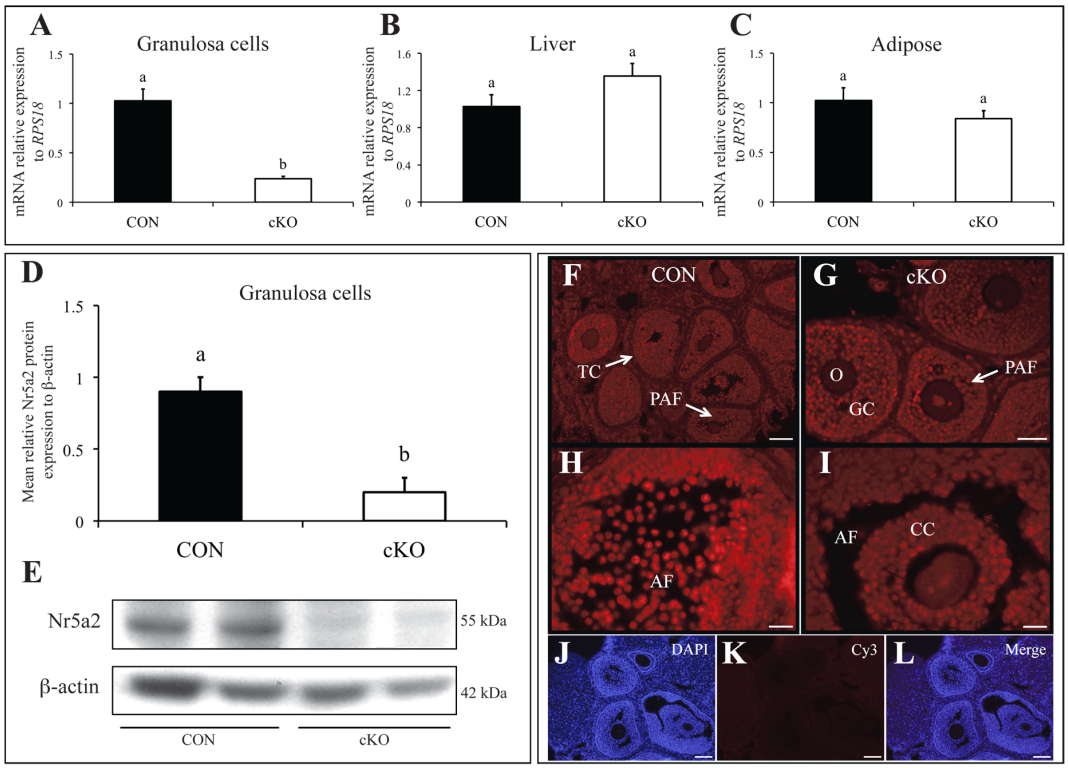

Figure 2.1 : Characterization of the granulosa-specific knockout mouse Nr5a2$^{Cyp19-/-}$. (**A**) Relative abundance of *Nr5a2* mRNA in granulosa cells of superstimulated immature females isolated by ovarian puncture (n = 4 per genotype) ($p < 0.001$). Relative abundance of *Nr5a2* mRNA in the liver (**B**) and adipose tissue (**C**) of adult females (n = 5 per genotype) ($p > 0.1$). (**D**) Relative abundance of Nr5a2 protein in granulosa cells of superstimulated immature females by immunoblotting ($p < 0.05$). (**E**) Representative immunoblot. Immunofluorescence demonstrating the depletion of Nr5a2 protein in granulosa cells of the conditional knockout ovary exclusively in the antral follicle (**I**), but not in preantral follicles (**G**). (**F**, **H**) Positive control for fluorescent immunohistochemistry staining. (**J**) DAPI staining the nuclei; (**K**) negative control using BSA 5%; and (**L**) merged DAPI and Cy3. Bars = **F**, **J**, **K, L** (60 μm); **G** (40 μm); **H**, **I** (20 μm). TC, theca cells; PAF, preantral follicle; GC, granulosa cells; O, oocyte; AF, antral follicle; CC, cumulus cells. CON = control; solid bars (Nr5a2$^{f/f}$tgCyp19$^{+/+}$); cKO = conditional knockout, open bars (Nr5a2$^{Cyp19-/-}$).

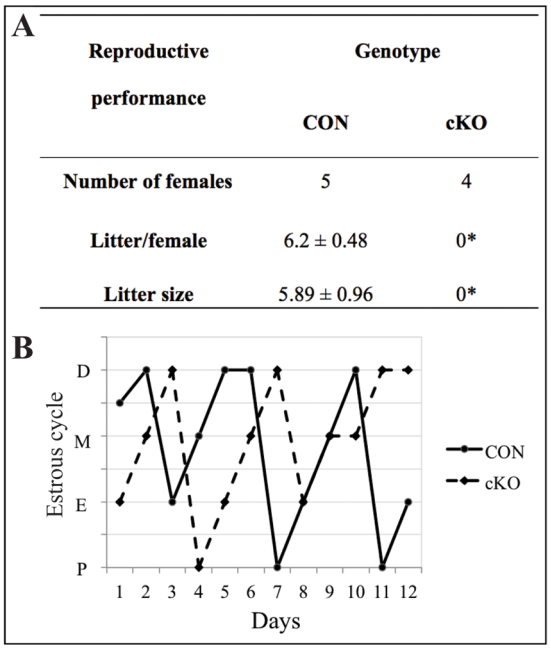

Figure 2.2 : Reproductive performance of granulosa specific Nr5a2$^{Cyp19-/-}$ female mice. (**A**) Six month breeding trial employing CON (n = 5) and cKO (n = 4) adult females housed with reproductively proven C57BL/6 males; (*) $p < 0.001$. (**B**) Representative vaginal smear profiles from CON (solid line) and cKO (dotted line) female mice showing a normal 4 to 5 day estrous cycle length for both genotypes. P, proestrus; E, estrus; M, metestrus; D, diestrus.

Antral follicles lacking Nr5a2 in granulosa cells are anovulatory

Although preantral and antral follicle formation was observed in Nr5a2$^{Cyp19-/-}$ ovaries (Supplemental Figure 2.1A-B), and cumulus expansion was stimulated by gonadotropin administration as seen at 12 h post hCG (Figure 2.3A-C), almost no cumulus-oocyte complexes (COCs) were retrieved from the Nr5a2$^{Cyp19-/-}$ oviduct 16 h after hCG injection, unlike the superovulation induced in the control group (Figure 2.3D-F).

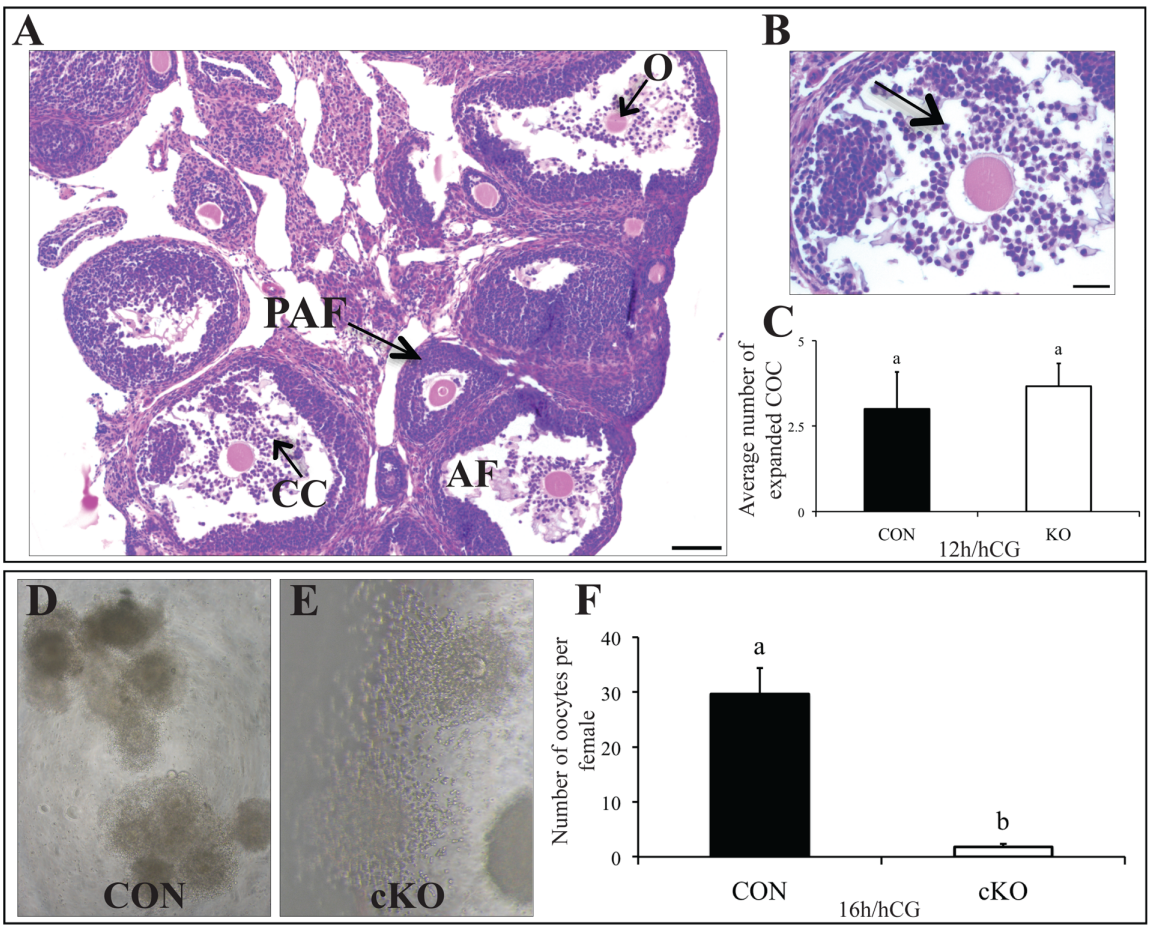

Figure 2.3 : Ovarian superstimulation promotes cumulus expansion but not ovulation in granulosa-specific knockout female mice. (**A**) Bright field microscopy images of hematoxylin-eosin stained sections of ovaries from immature cKO mice superstimulated with eCG and hCG and collected at 12 h post hCG. Bar = 100 μm. PAF, preantral follicle; AF, antral follicle; CC, cumulus cells; O, oocyte. (**B**) Arrow indicates expanded cumulus cells at 12 h post hCG in cKO follicle. Bar = 40 μm. (**C**) Quantification of cumulus expansion by averaging the number of follicles containing expanded cumulus-oocyte complexes (COC) in CON and cKO ovarian sections at 12 h post hCG (n = 6 sections – from the middle of the ovary – per genotype) ($p > 0.1$). Ovulation rate (number of oocytes in the oviduct at 16 h post hCG) of CON (**D**; 10x magnification) and cKO (**E**; 40x magnification) immature female mice in response to superstimulation. (**F**) Mean number of oocytes in the oviduct in CON vs cKO mice. Different superscripts indicate significant differences at $p < 0.001$.

Analysis of ovarian granulosa and cumulus cells comparing our $Nr5a2^{Cyp19-/-}$ with the previously described $Nr5a2^{Amhr2-/-}$ mouse revealed that the pattern of gene expression differed between the two knockout models at 4 h post hCG (Figure 2.4A-F).

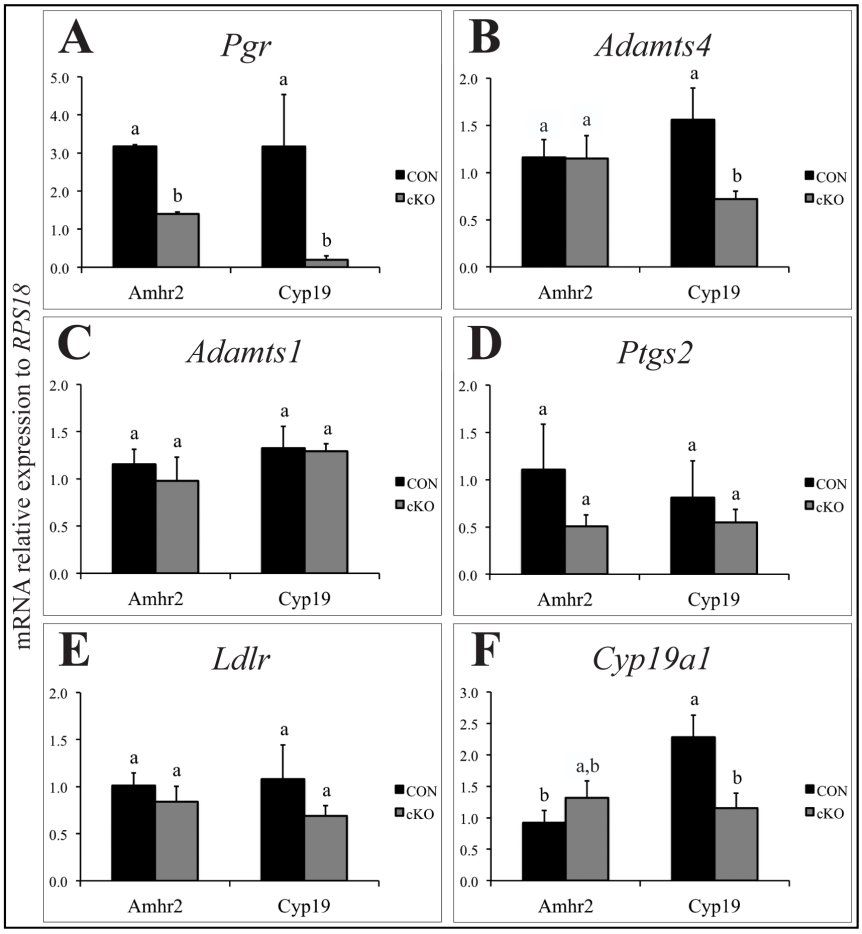

Figure 2.4 : Abundance of mRNA as determined by qPCR for *Pgr* (**A**), *Adamts4* (**B**), *Adamts1* (**C**), *Ptgs2* (**D**), *Ldlr* (**E**) and *Cyp19a1* (**F**) relative to *RPS18* comparing two granulosa-specific knockout mouse lines distinguished by the timing of *Nr5a2* depletion during the follicular development. Superstimulated ovaries from immature females were collected at 4 h post hCG (n = 5 per group) and granulosa cells were isolated by ovarian puncture. Amhr2 (Cre-recombinase) = left bars, mutation in primary follicles, genotype $Nr5a2^{Amhr2-/-}$; Cyp19 (Cre-recombinase) = right bars, mutation in antral follicles, genotype $Nr5a2^{Cyp19-/-}$. CON = control; black bars ($Nr5a2^{f/f}$ $tgCyp19^{+/+}$; or $Nr5a2^{f/f}$ $Amhr2^{+/+}$); cKO = conditional knockout, gray bars ($Nr5a2^{Cyp19-/-}$ / or $Nr5a2^{Amhr2-/-}$) respectively. Differing superscripts indicated differences at $p < 0.05$.

The *Pgr*, which is essential for ovulation, showed decreased mRNA levels in both models (Figure 2.4A), whereas *Adamts4* was downregulated in the Nr5a2$^{Cyp19-/-}$ model, but not in Nr5a2$^{Amhr2-/-}$ ovary (Figure 2.4B). For *Adamts1*, no difference in gene expression was seen between both conditional knockout models relative to their respective controls (Figure 2.4C). Although there was no statistically significant difference for mRNA levels of the *Ptgs2* (Figure 2.4D) and the low-density lipoprotein receptor (*Ldlr*) (Figure 2.4E), a tendency towards downregulation was observed in the granulosa cells of both Nr5a2$^{Cyp19-/-}$ and Nr5a2$^{Amhr2-/-}$. Further, at 4 h post hCG, *Cyp19a1* presented a tendency towards upregulation in the Nr5a2$^{Amh2-/-}$, whereas it was downregulated in Nr5a2$^{Cyp19-/-}$ (Figure 2.4F). These data indicate that Nr5a2 expression in granulosa cells of antral and preovulatory follicles is not essential for cumulus expansion but it is essential for ovulation.

Antral expression of Nr5a2 is required for the formation of a functional corpus luteum

We then investigated the role of Nr5a2 in luteinization using standard hormonal superstimulation in immature mice and analyzing the ovaries at later time points following the ovulatory stimulus (Figure 2.5A-E). At 12 h, 18 h and 24 h post hCG, when corpora lutea are normally abundant in the control ovary (Figure 2.5A-B), we identified the formation of luteal-like structures (LS) in Nr5a2$^{Cyp19-/-}$ ovarian sections. These structures appeared to be comprised of theca cells invading the follicles, and the follicles often contained a trapped oocyte (Figure 2.5C-D). The number of luteal-like structures in Nr5a2$^{Cyp19-/-}$ ovaries was significantly lower than the number of corpora lutea found in the control ovarian sections (n = 16 sections analyzed per group) (Figure 2.5E) at 12 h, 18 h or

24 h post hCG. We then asked whether the luteal-like structures were functional. During a 40-day breeding trial, adult Nr5a2$^{Cyp19-/-}$ females were mated with reproductively proven males, and control females were mated with vasectomized males to establish the frequency of mating by examining copulatory plugs. The Nr5a2$^{Cyp19-/-}$ females showed frequent and irregular mating (mean interval, 3.67±0.21 days) compared to the control group (10.38±0.51 days), indicating the absence of a persistent pseudopregnant CL in Nr5a2$^{Cyp19-/-}$ females compared to the control mice. To determine whether the Nr5a2$^{Cyp19-/-}$ luteal-like structures could promote normal circulating levels of progesterone, adult Nr5a2$^{Cyp19-/-}$ and control females were bred to fertile males, examined for copulatory plugs and euthanized 5.5 dpc (Figure 2.5G-J). By this time of expected early post-implantation gestation, we found shorter uterine horns in Nr5a2$^{Cyp19-/-}$ (Fig. 2.5H), in contrast to the elongated pregnant control uterus (Figure 2.5G). Although luteal-like structures were observed in the Nr5a2$^{Cyp19-/-}$ ovaries (Figure 2.5J), they were fewer than the normal number of corpora lutea in the control ovaries (Figure 2.5I) and extremely low progesterone concentrations were detected in Nr5a2$^{Cyp19-/-}$ serum at 5.5 dpc (Figure 2.5K), whereas equivalent levels of serum and intra-follicular estradiol-17β were identified in Nr5a2$^{Cyp19-/-}$ females compared to the control levels (Supplemental Figure 2.1C-D). Insufficiency of the Nr5a2$^{Cyp19-/-}$ luteal-like structures was confirmed by reduced circulating concentrations of progesterone in the Nr5a2$^{Cyp19-/-}$ serum relative to control mice at 12 h, 18 h or 24 h post hCG (Figure 2.5L).

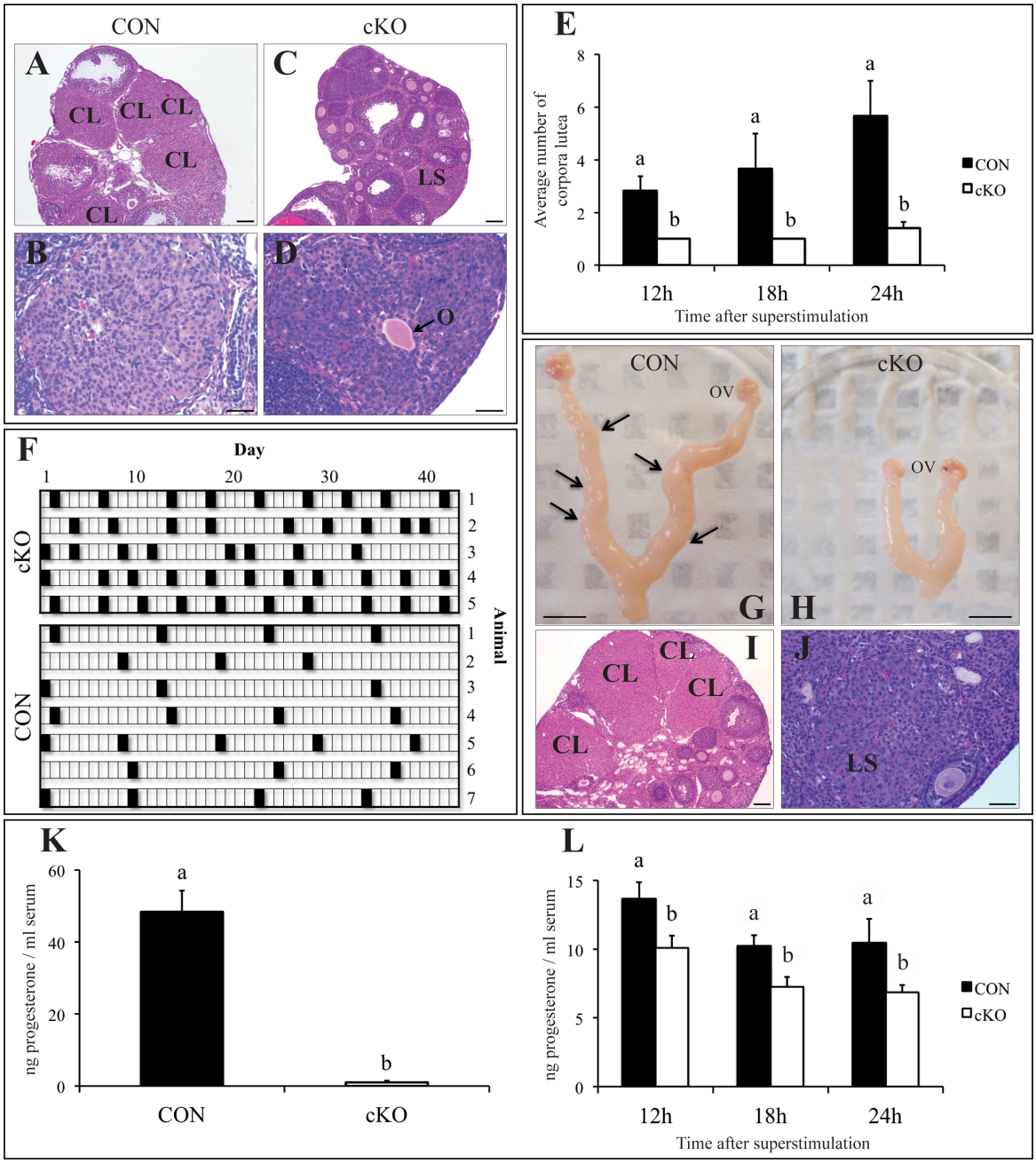

Figure 2.5 : Nr5a2 is important for the formation of a normal corpus luteum. (**A-D**) Bright field microscopy images of hematoxylin-eosin stained sections of ovaries from immature control and Nr5a2$^{Cyp19-/-}$ mice superstimulated with eCG / hCG and collected at 18 h post hCG. (**A**) Overview of the control ovary containing several corpora lutea. Bar = 100 µm. (**B**) A single corpus luteum (CL) from a control ovarian section. Bar = 40 µm. (**C**) General overview of the Nr5a2$^{Cyp19-/-}$ ovary containing one luteal-like structure (LS). Bar = 100 µm. (**D**) Nr5a2$^{Cyp19-/-}$ luteal-like structure showing an entrapped oocyte (O) indicated by the arrow. Bar = 40 µm. (**E**) Quantification of luteinization by averaging the frequency of luteal formation in control and Nr5a2$^{Cyp19-/-}$ ovarian sections at 12 h, 18 h and 24 h post hCG (n = 5 sections per genotype) ($p < 0.001$). (**F**) Mating frequency comparing adult control and Nr5a2$^{Cyp19-/-}$ females during a 40-day breeding

trial. Control females were housed with vasectomized C57BL/6 males and Nr5a2$^{Cyp19-/-}$ females were housed with reproductively proven C57BL/6 males. Black squares indicate the observation of a copulatory plug, with short and irregular intervals between plugs for Nr5a2$^{Cyp19-/-}$ females, whereas the control group averaged 10 to 13 days interval between plugs; $p < 0.0001$. Ovaries (OV) and uteri of control (**G**) and Nr5a2$^{Cyp19-/-}$ (**H**) adult females housed with a reproductively proven C57BL/6 male and collected at day 5.5 post coitum. (**G**) Elongated uterine horns containing implantation sites (indicated by the arrows) and the presence of several corpora lutea (CL) in the hematoxylin-eosin stained ovary (**I**) represents the control female reproductive system under the influence of the progesterone. A few luteal-like structures (LS) are found in the hematoxylin-eosin stained sections of the Nr5a2$^{Cyp19-/-}$ ovaries (**J**). Bars = **G, H** (4 mm); **I, J** (40 μm). Plasma progesterone concentrations in control and Nr5a2$^{Cyp19-/-}$ adult female mice at 5.5 dpc (**K**) and in immature superstimulated female mice at 12 h, 18 h and 24 h post hCG ($p < 0.001$).

Based on the progesterone levels found after superstimulation, we then combined the eCG / hCG protocol with the 5.5 dpc scheme to check whether superstimulation would promote appropriate synthesis of progesterone in adult females after mating. Whilst control females were pregnant at 5.5 dpc (Supplemental Figure 2.2A), no implantation sites were observed in the Nr5a2$^{Cyp19-/-}$ uterine horns (Supplemental Figure 2.2B) and progesterone was consistently low in Nr5a2$^{Cyp19-/-}$ serum compared to progesterone concentrations in control females (Supplemental Figure 2.2C). We conclude that depletion of Nr5a2 in granulosa cells from the antral follicle stage results in luteal-like structures that are insufficient to promote normal serum levels of progesterone.

The expression pattern of luteinization-related genes driven by Nr5a2 in preovulatory follicles

To explore the abundance of transcripts of genes essential for cholesterol supply and progesterone synthesis in granulosa cells in response to LH stimulation, immature females were treated with eCG / hCG and whole ovaries were collected at 12 h, 18 h or 24 h post

hCG (Figure 2.6A-F). The relative abundance of *Scarb1* mRNA was markedly reduced beginning at 18 h and continuing through 24 h post hCG in the Nr5a2$^{Cyp19-/-}$ group compared to the controls (Figure 2.6A). The abundance of *Ldlr*, *Star* and *Cyp11a1* was lower in Nr5a2$^{Cyp19-/-}$ ovaries at 18 h post hCG, while at 12 h and 24 h there was a tendency of downregulation for these genes (Figure 2.6B-D). This notwithstanding, the strength of the mRNA signal for *Hsd3β* and *Cyp19a1* showed increased expression in control mice over 12 h post hCG, but the expression was not altered by the depletion of Nr5a2 in granulosa cells of antral follicles at 18 h and 24 h (Figure 2.6E-F). We then examined the expression of Scarb1 in ovarian sections by immunofluorescence to determine whether the luteal-like cells were indeed luteinized granulosa cells (Figure 2.6G-H). In Nr5a2$^{Cyp19-/-}$ ovaries, luteal-like structures have an apparent higher signal of Scarb1 than granulosa cells in the same sections (Figure 2.6H), but the protein expression appears substantially lower than in the normal corpus luteum of control animals (Figure 2.6G). These data demonstrate that the deficient luteinization resulting from the absence of Nr5a2 in preovulatory follicles is related to the compromised expression of certain genes, mainly those involved in cholesterol transport.

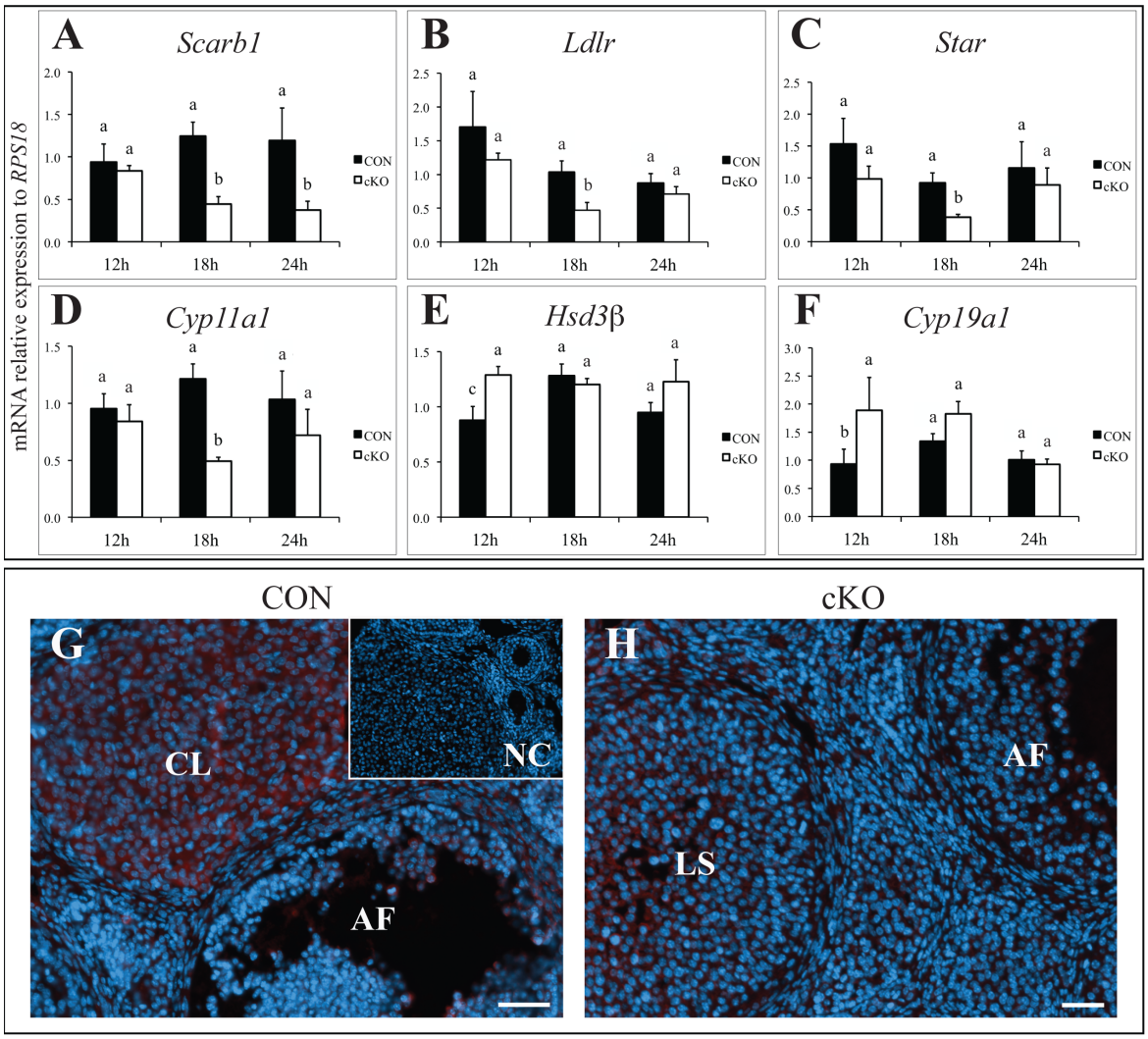

Figure 2.6 : Pattern of expression as determined by qPCR for genes related to steroidogenesis at intervals around the time of and after expected ovulation. Relative abundance of mRNA of *Scarb1* (**A**), *Ldlr* (**B**), *Star* (**C**), *Cyp11a1* (**D**), *Hsd3β* (**E**) and *Cyp19a1* (**F**) in whole ovaries of superstimulated immature females collected at 12 h, 18 h or 24 h post hCG (n = 5 per group) comparing control and Nr5a2$^{Cyp19-/-}$ ($p < 0.05$) groups. Merged microscopy images of fluorescent immunohistochemistry of Scarb1 in ovarian sections of control (**G**) and Nr5a2$^{Cyp19-/-}$ (**H**) adult females. CL, corpus luteum; AF, antral follicle; LS, luteal-like structure. Bar = 50 µm. Panel G insert: negative control with 5% BSA using DAPI to stain the nuclei.

2.5. Discussion

From the time of its discovery in *Drosophila*[23; 7] to our present state of knowledge, the orphan nuclear receptor Nr5a2 has not only been designated by multiple names – liver receptor homolog-1, LRH-1, α-fetoprotein transcription factor, FTZ-F1-related factor and CYP7A1 promoter binding factor, among others – but it has been recognized to have an immense range of functions in both vertebrate and invertebrate models. Nr5a2 is expressed in steroidogenic tissues[9], and its strong granulosa-specific expression has led to investigation of its role in reproduction, especially in the ovary[4; 33; 19]. More recently, it has been shown to be an important regulator in the mouse endometrium, to be essential for successful gestation[37], and it appears to be upstream to regulation of gonadotropin secretion in the hypothalamus[3].

Nr5a2 is necessary for proper embryonic primitive streak formation, thus preventing early embryo survival in the mouse[22], precluding study of its germline mutation in postnatal animals. Employing a mouse line with *loxP* sites flanking the third and fourth exons of *Nr5a2* gene, and taking advantage of the Cre-*loxP* system has allowed in depth exploration of Nr5a2 in the ovary in recent years. By the use of a Cre-recombinase mouse line guided by Amhr2 ($Nr5a2^{Amhr2-/-}$), it was shown that Nr5a2 is essential for cumulus expansion, ovulation and female fertility[11]. A later study on the role of Nr5a2 in reproduction applied the Cre-recombinase mouse line guided by the Pgr ($Nr5a2^{Pgr-/-}$), which was responsible for depleting Nr5a2 during the late peri-ovulatory period in follicles and in the uterus, resulting in successful ovulation, formation of small but functional corpora lutea and infertility due to compromised endometrial decidualization[37].

In the present study we employed a third model with a different temporal pattern of depletion of Nr5a2. Mating with the Cyp19a1 Cre-recombinase mouse line ($Nr5a2^{Cyp19-/-}$) resulted in excision of Nr5a2 from the antral follicle forward in the follicle development trajectory[17]. Females were infertile with an ovarian phenotype distinct from the two previous models, demonstrating another variant reproductive profile for conditional knockout mice lines in these studies. Our $Nr5a2^{Cyp19-/-}$ mouse model confirms that Nr5a2 is essential for ovulation with COCs almost completely absent in $Nr5a2^{Cyp19-/-}$ female oviducts following treatment with an ovulation induction protocol. This indicates that expression of Nr5a2 in antral follicles is required to provide the necessary ovulatory signals. The $Nr5a2^{Pgr-/-}$ mouse model demonstrates that ovulation is independent of Nr5a2 after approximately 4 h following the ovulatory stimulus, as these animals showed normal ovulatory rates[37].

Although the non-ovulatory phenotype is present in both the $Nr5a2^{Cyp19-/-}$ and the $Nr5a2^{Amhr2-/-}$ mouse models, one interesting difference between them is that cumulus expansion is absent when Nr5a2 is depleted in primary follicles in the $Nr5a2^{Amhr2-/-}$ mouse[11], whereas the presence of Nr5a2 in preantral follicles is able to promote cumulus expansion in the $Nr5a2^{Cyp19-/-}$ females. This phenotype of cumulus expansion without ovulation is similar to that found in the progesterone receptor knockout (PRKO) mouse. Granulosa cells from preovulatory follicles of mice in the PRKO are responsive to the LH surge, demonstrated by the presence of expanded cumulus cells[24], but Pgr is essential for LH-induced follicular rupture leading to ovulation[2]. In the present investigation, Nr5a2 depletion in either the $Nr5a2^{Cyp19-/-}$ model or the $Nr5a2^{Amhr2-/-}$ is accompanied by significant downregulation of *Pgr*. This suggests that Nr5a2 is upstream of the *Pgr* gene, and regulates ovulation as a transcription factor to activate the critical progesterone receptor pathway.

The progesterone receptor, in turn, is an important regulator of the transcription of other genes linked to ovulatory success, including *Adamts1*[16]. At 4 h post hCG the *Adamts1* levels are normal for both Nr5a2$^{Amhr2-/-}$ and Nr5a2$^{Cyp19-/-}$ ovaries. However, at 12h post hCG a downregulation of *Adamts1* occurs in Nr5a2$^{Cyp19-/-}$ (data not shown), while in the Nr5a2$^{Amhr2-/-}$ ovaries normal levels are still observed[11]. While this could be related to the different cumulus expansion profiles in these two mouse models, other pathways may also be involved. The pattern of abundance of the *Adamts4* transcript also differs between the two granulosa-specific knockout models; while it is downregulated in Nr5a2$^{Cyp19-/-}$ ovaries, it is normally expressed at 4 h post hCG in the Nr5a2$^{Amhr2-/-}$ ovaries. While Adamts4 is closely related to Adamts1, with some distinct and overlapping functions, it does not appear to be a target for the progesterone receptor[30].

Although the progesterone pathway seems to be regulated by Nr5a2, the expression of *Ptgs2*, a marker of follicular commitment to ovulation following the LH peak[34], appears to be normal in the PRKO mice[32], whereas *Ptgs2* tends to be downregulated in both Nr5a2$^{Cyp19-/-}$ and Nr5a2$^{Amhr2-/-}$ models. Thus the complex phenotypes resulting from depletion of Nr5a2 in granulosa cells at different stages of follicular maturation strongly indicate that Nr5a2 regulates multiple pathways of female fertility. Further evidence that Nr5a2 regulates multiple pathways can be found in the observation that, despite the failure to ovulate, luteinization proceeds normally in the PRKO mice[32], but not in our models lacking Nr5a2 in granulosa cells.

In our previous studies using Nr5a2$^{Amhr2-/-}$ and Nr5a2$^{Pgr-/-}$ models, although they suggested that Nr5a2 has a role in ovarian luteinization[11; 37], the time of depletion of the gene was either very early in the follicular development or after the LH peak. In the Nr5a2$^{Amhr2-/-}$ model, the lack of Nr5a2 in granulosa cells in primary follicles prevents

corpus luteum formation[11]. In the Nr5a2$^{Pgr-/-}$ model, albeit at reduced size, corpora lutea were formed in the Nr5a2$^{Pgr-/-}$ ovaries[37], and this formation is probably due to the persistence of Nr5a2 expression in luteal cells for at least 4 h post hCG, when Cre-recombinase resumes Nr5a2 depletion in this model. The compromised corpus luteum in the Nr5a2$^{Pgr-/-}$ ovaries indicates the importance of Nr5a2 up to later stages of the luteinization, but this model does not provide information on the role of Nr5a2 in early period of luteinization, due to persistence of Nr5a2[37]. Our Nr5a2$^{Cyp19-/-}$ model is probably the best currently available to allow insight into the early luteal regulation of Nr5a2.

Therefore, with the Nr5a2$^{Cyp19-/-}$ model we provide valuable information on the role of Nr5a2 in corpus luteum formation, as the time of Nr5a2 excision in granulosa cells of antral follicles is guided by the Cyp19a1 expression, which appears before the LH peak in the ovary[17]. Yet, our granulosa-specific Nr5a2$^{Cyp19-/-}$ knockout mice present a luteal-like formation in the ovaries, which is apparently comprised of luteinized theca cells surrounding granulosa cells. These structures were present in adult and immature superstimulated females. Although the number of these structures is reduced if compared to the normal number of corpora lutea in the control group, they appear able to generate some circulating levels of progesterone after hormonal superstimulation, but this secretion did not persist in adult females to 5.5 dpc. During a 40-day breeding trial, control females became pseudopregnant following a sterile mating. In the mouse pseudopregnancy, the surge of prolactin and the progesterone producing by the corpora lutea prevent the LH peak; with increased secretion of prostaglandin (PGF2α) in the absence of embryos, progesterone starts to reduce and females resume the estrous cycle[10], making an expected interval of 10 to 13 days between copulations. The frequent and irregular interval between copulations in

the Nr5a2$^{Cyp19-/-}$, indicating the return to estrus, confirms the non-functionality of the luteal-like structures to produce the necessary progesterone amount to promote pseudopregnancy.

At the molecular level, luteinization in Nr5a2$^{Cyp19-/-}$ mice appears to be impaired by disruptions in the cholesterol supply and transport of proteins. Of importance is the downregulation of Scarb1. This factor is responsible for mediating the selective uptake of cholesterol from HDL, the principal source of cholesterol supply in the mouse ovary[21]. We have shown that ablation of Scarb1 results in defective intake of the precursor cholesterol into the granulosa-derived luteal cells[1]. *Ldlr* is also downregulated in the Nr5a2$^{Cyp19-/-}$ ovaries. The expression of other genes known to be necessary for steroidogenesis was also disrupted, including *Star*, the protein that governs the transport of cholesterol from the outer to inner mitochondrial membrane[8] and *CYP11a1*, which is involved in the conversion of cholesterol to pregnenolone. The transcript for the next enzyme in the synthetic pathway, the *Hsd3β*, is upregulated earlier after ovulation, perhaps to compensate for the downregulation of the previous steroidogenic steps.

In conclusion, our findings demonstrate that Nr5a2 regulates ovulation and female fertility differently but consistently in granulosa cells across the trajectory of follicular development (Figure 2.7). The progesterone receptor pathway seems to be the immediate downstream target for Nr5a2 activity in ovulation. The inadequate luteal function can be attributed, at least in part, to the disruption of the cholesterol transport pathways, although other pathways are also affected.

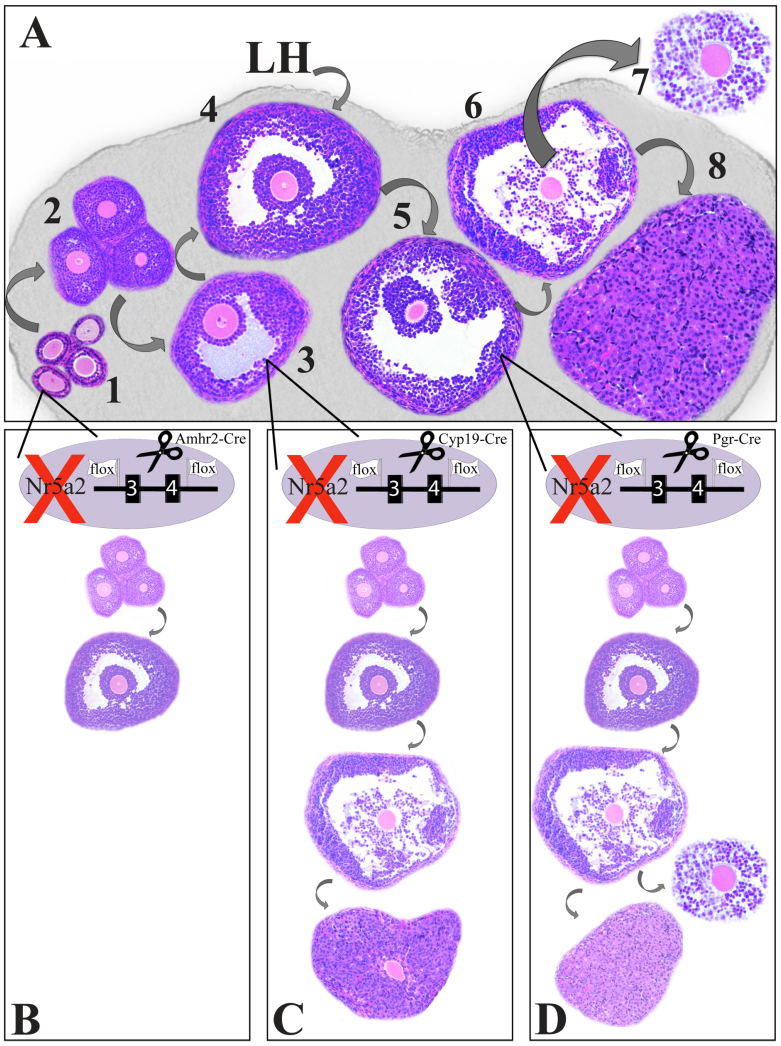

Figure 2.7 : Summary of the Nr5a2 functions in the ovary: lessons from the three different conditional knockout mouse models. (**A**) Diagram of normal follicular maturation in the mouse ovary. Primary follicles (**1**) have one layer of granulosa cells around the oocyte, acquiring new layers during follicular development; secondary follicles (**2**) will develop to antral follicles (**3**), when granulosa cells differentiate into mural and cumulus cells. When the LH peak occurs (**4**), immediate changes happen in the follicle (**5**) including cumulus expansion (**6**), ovulation (**7**) and luteinization (**8**). (**B**) By the *Cre-loxP* system, flanking the 3rd and 4th Nr5a2 exons and using the Amhr2-Cre recombinase, Nr5a2 is excised at the primary follicle stage, which does not affect folliculogenesis; on the other hand cumulus expansion, ovulation and luteinization are absent. (**C**) Excising Nr5a2 at the antral follicle stage before the LH peak, by the use of the Cyp19-Cre recombinase, both folliculogenesis and cumulus expansion are observed, but ovulation is impaired; luteinization is abnormal and oocytes are trapped in the luteal-like formations. (**D**) Excising Nr5a2 at the antral follicle stage after the LH peak, by the use of the Pgr-Cre recombinase, the aberrant ovarian phenotype is restricted to the formation of reduced size corpora lutea, but folliculogenesis, cumulus expansion and ovulation occur normally.

2.6. Supplemental material

TABLE II : List of primers used in these studies for both genotyping and qPCR. All primers are 5’ to 3’.

Primer	Forward	Reverse
Genotyping		
Nr5a2-flox	GCTATAGGGAGTCAGGATACCATGG	GTTCGTACCACTTTCATCTCCTCACG
Cyp19a1-Cre	ACTTGGTCAAAGTCAGTGCG	CCTGGTGCAAGCTGAACAAC
Amhr2-Cre	GAACCTGATGGACATGTTCAGG	AGTGCGTTCGAACGCTAGAGCCTGT
qPCR		
RPS18	GTGGTGTTGAGGAAAGCAGACA	TGATCACACGTTCCACCTCATC
Adamts1	TAAGTGTGGCGTTTGTGGAG	CCCTTTGATTCCGATGTTTC
Adamts4	TCAACACCCCTAACGACTCA	TGCATGGCTTGGAGTTATCA
Cyp11a1	CTGCCTCCAGACTTCTTTCG	TTCTTGAAGGGCAGCTTGTT
Cyp19a1	ATGTTCTTGGAAATGCTGAACCC	AGGACCTGGTATTGAAGACGAGC
Hsd3β	GGTTTTTGGGGCAGAGGATCA	GGTACTGGGTGTCAAGAATGTCT
Ldlr	AATGGTGGTTGCCAGTACCT	CCCTGGGTGGTCAGTACAGT
Nr5a2	TCATGCTGCCCAAAGTGGAGA	TGGTTTTGGACAGTTCGCTT
Ptgs2	ATCCTGAGTGGGGTGATGAG	AAGTGGTAACCGCTCAGGTG
Pgr	AGGTCTACCCGCCATACCTT	CAGGTAAGCACGCCATAGTG
Scarb1	TTGGCCTGTTTGTTGGGATG	GGATTCGGGTGTCATGAAGG
Star	TTGGGCATACTCAACAACCA	GCGGTCCACAAGTTCTTCAT

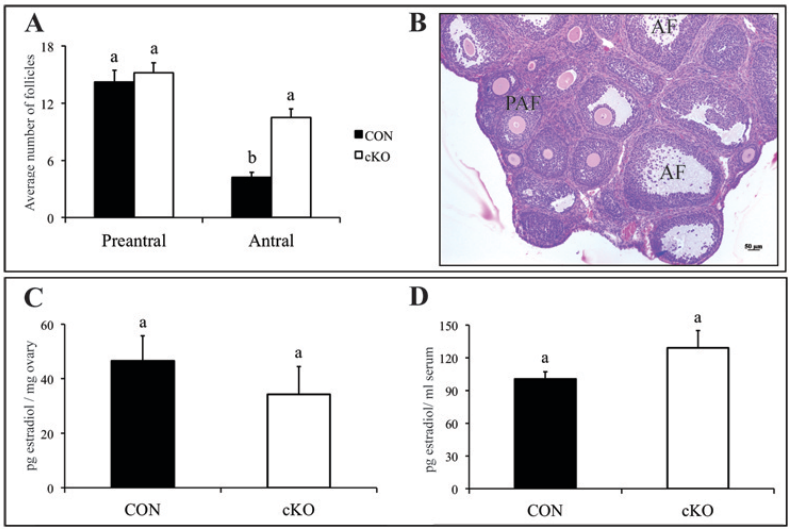

Supplemental Figure 2.1 : Follicle classes and estradiol-17β levels in Nr5a2$^{Cyp19-/-}$ mice. (**A**) Quantification of folliculogenesis by averaging the number of preantral and antral follicles in control and Nr5a2$^{Cyp19-/-}$ ovarian sections at 12 h post hCG (n = 5 sections per genotype) ($p < 0.5$). (**B**) Bright field microscopy image of hematoxylin-eosin stained ovarian section from immature Nr5a2$^{Cyp19-/-}$ mice superstimulated with eCG / hCG and collected at 12 h post hCG, showing the formation of preantral (PAF) and antral (AF) follicles. Bar = 50 µm. Estradiol-17β concentrations in the follicular fluid (**C**) and serum (**D**) of control and Nr5a2$^{Cyp19-/-}$ adult females at 5.5 dpc ($p > 0.1$).

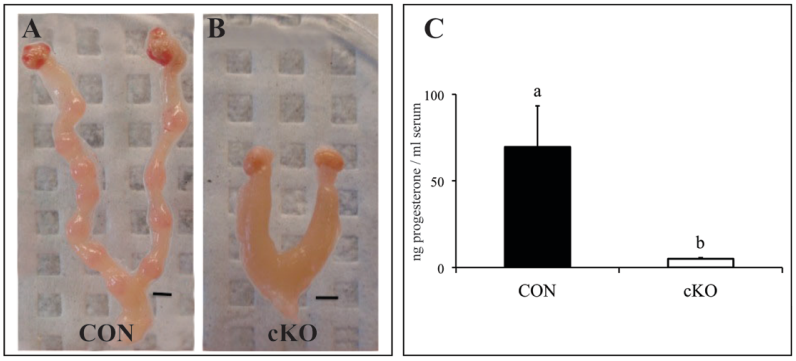

Supplemental Figure 2.2 : Breeding trial combining superstimulation and mating using Nr5a2 granulosa specific knockout female mice. At 5.5 dpc, control superstimulated females showed implantation sites confirming pregnancy, represented by the ovaries and elongated uterine horns (**A**), while their absence in Nr5a2$^{Cyp19-/-}$ (**B**) females confirms their infertility and short uterine horns phenotypically representing the low levels of progesterone. Bars = 2 mm. (**C**) Plasma progesterone concentrations from control and Nr5a2$^{Cyp19-/-}$ adult superstimulated female mice at 5.5 dpc.

Acknowledgements

The authors thank Mira Dobias Goff and Anne-Marie Bellefleur for valuable scientific discussions; Mira Dobias Goff, Vickie Roussel and Fanny Morin for technical assistance; Dr. Jane Fenelon for carefully reading this manuscript; and Dr. Richard Behringer for the Amhr2$^{Cre/+}$ mouse line. This study was funded by an operating grant from the Canadian Institutes of Health Research (FRN11018) to BDM. Kalyne Bertolin was supported by the Fonds québécois de la recherche sur la nature et les technologies (FQRNT) – Merit Scholarship Program for Foreign Students (PBEEE).

References

1. Acton S, Rigotti A, Landschulz KT *et al.* (1996) Identification of scavenger receptor SR-BI as a high density lipoprotein receptor. *Science* **271**, 518-520.

2. Akison LK & Robker RL (2012) The critical roles of progesterone receptor (PGR) in ovulation, oocyte developmental competence and oviductal transport in mammalian reproduction. *Reprod Domest Anim* **47 Suppl 4**, 288-296.

3. Atkin SD, Owen BM, Bookout AL *et al.* (2013) Nuclear receptor LRH-1 induces the reproductive neuropeptide kisspeptin in the hypothalamus. *Mol Endocrinol* **27**, 598-605.

4. Boerboom D, Pilon N, Behdjani R *et al.* (2000) Expression and regulation of transcripts encoding two members of the NR5A nuclear receptor subfamily of orphan

nuclear receptors, steroidogenic factor-1 and NR5A2, in equine ovarian cells during the ovulatory process. *Endocrinology* **141**, 4647-4656.

5. Botrugno OA, Fayard E, Annicotte JS *et al.* (2004) Synergy between LRH-1 and beta-catenin induces G1 cyclin-mediated cell proliferation. *Mol Cell* **15**, 499-509.

6. Britt KL, Drummond AE, Dyson M *et al.* (2001) The ovarian phenotype of the aromatase knockout (ArKO) mouse. *J Steroid Biochem Mol Biol* **79**, 181-185.

7. Broadus J, McCabe JR, Endrizzi B *et al.* (1999) The Drosophila beta FTZ-F1 orphan nuclear receptor provides competence for stage-specific responses to the steroid hormone ecdysone. *Mol Cell* **3**, 143-149.

8. Christenson LK & Devoto L (2003) Cholesterol transport and steroidogenesis by the corpus luteum. *Reprod Biol Endocrinol* **1**, 90.

9. Clyne CD, Speed CJ, Zhou J *et al.* (2002) Liver receptor homologue-1 (LRH-1) regulates expression of aromatase in preadipocytes. *J Biol Chem* **277**, 20591-20597.

10. Dewar AD (1959) Observations on pseudopregnancy in the mouse. *J Endocrinol* **18**, 186-190.

11. Duggavathi R, Volle DH, Mataki C *et al.* (2008) Liver receptor homolog 1 is essential for ovulation. *Genes & Development* **22**, 1871-1876.

12. Durlinger AL, Visser JA & Themmen AP (2002) Regulation of ovarian function: the role of anti-Mullerian hormone. *Reproduction* **124**, 601-609.

13. Elvin JA, Clark AT, Wang P *et al.* (1999) Paracrine actions of growth differentiation factor-9 in the mammalian ovary. *Mol Endocrinol* **13**, 1035-1048.

14. Eppig JJ (1991) Intercommunication between mammalian oocytes and companion somatic cells. *Bioessays* **13**, 569-574.

15. Espey LL & Richards JS (2006) Ovulation. *Knobil and Neilsl's - Physiology of Reproduction* **1**, 425-474.

16. Espey LL, Yoshioka S, Russell DL *et al.* (2000) Ovarian expression of a disintegrin and metalloproteinase with thrombospondin motifs during ovulation in the gonadotropin-primed immature rat. *Biol Reprod* **62**, 1090-1095.

17. Fan HY, Shimada M, Liu Z *et al.* (2008) Selective expression of KrasG12D in granulosa cells of the mouse ovary causes defects in follicle development and ovulation. *Development* **135**, 2127-2137.

18. Hellemans J, Mortier G, De Paepe A *et al.* (2007) qBase relative quantification framework and software for management and automated analysis of real-time quantitative PCR data. *Genome Biol* **8**, R19.

19. Hinshelwood MM, Repa JJ, Shelton JM *et al.* (2003) Expression of LRH-1 and SF-1 in the mouse ovary: localization in different cell types correlates with differing function *Molecular and Cellular Endocrinology* **207**.

20. Jamin SP, Arango NA, Mishina Y *et al.* (2003) Genetic studies of the AMH/MIS signaling pathway for Müllerian duct regression. *Molecular and Cellular Endocrinology* **211**, 15-19.

21. Jimenez LM, Binelli M, Bertolin K *et al.* (2010) Scavenger receptor-B1 and luteal function in mice. *J Lipid Res* **51**, 2362-2371.

22. Labelle-Dumais C, Jacob-Wagner M, Pare JF *et al.* (2006) Nuclear receptor NR5A2 is required for proper primitive streak morphogenesis. *Dev Dyn* **235**, 3359-3369.

23. Lavorgna G, Ueda H, Clos J *et al.* (1991) FTZ-F1, a steroid hormone receptor-like protein implicated in the activation of fushi tarazu. *Science* **252**, 848-851.

24. Lydon JP, DeMayo FJ, Funk CR *et al.* (1995) Mice lacking progesterone receptor exhibit pleiotropic reproductive abnormalities. *Genes Dev* **9**, 2266-2278.

25. Mendelson CR & Kamat A (2007) Mechanisms in the regulation of aromatase in developing ovary and placenta. *J Steroid Biochem Mol Biol* **106**, 62-70.

26. Munsterberg A & Lovell-Badge R (1991) Expression of the mouse anti-mullerian hormone gene suggests a role in both male and female sexual differentiation. *Development* **113**, 613-624.

27. Murphy BD (2000) Models of luteinization. *Biol Reprod* **63**, 2-11.

28. Peters H (1969) The development of the mouse ovary from birth to maturity. *Acta Endocrinol (Copenh)* **62**, 98-116.

29. Rajkovic A, Pangas SA & Matzuk MM (2006) Follicular Development: Mouse, Sheep, and Human Models. *Knobil and Neill's - Physiology of Reproduction* **1**, 383-423.

30. Richards JS (2005) Ovulation: New factors that prepare the oocyte for fertilization. *Molecular and Cellular Endocrinology* **234**, 75-79.

31. Richards JS, Hernandez-Gonzalez I, Gonzalez-Robayna I *et al.* (2005) Regulated expression of ADAMTS family members in follicles and cumulus oocyte complexes: evidence for specific and redundant patterns during ovulation. *Biol Reprod* **72**, 1241-1255.

32. Robker RL, Russell DL, Espey LL *et al.* (2000) Progesterone-regulated genes in the ovulation process: ADAMTS-1 and cathepsin L proteases. *Proc Natl Acad Sci U S A* **97**, 4689-4694.

33. Sirianni R, Seely JB, Attia G *et al.* (2002) Liver receptor homologue-1 is expressed in human steroidogenic tissues and activates transcription of genes encoding steroidogenic enzymes. *J Endocrinol* **174**, R13-17.

34. Sirois J, Sayasith K, Brown KA *et al.* (2004) Cyclooxygenase-2 and its role in ovulation: a 2004 account. *Hum Reprod Update* **10**, 373-385.

35. Stocco C (2008) Aromatase expression in the ovary: hormonal and molecular regulation. *Steroids* **73**, 473-487.

36. Tullet JM, Pocock V, Steel JH *et al.* (2005) Multiple signaling defects in the absence of RIP140 impair both cumulus expansion and follicle rupture. *Endocrinology* **146**, 4127-4137.

37. Zhang C, Large MJ, Duggavathi R *et al.* (2013) Liver receptor homolog-1 is essential for pregnancy. *Nat Med* **19**, 1061-1066.

Chapter 3

3. Second manuscript

The orphan nuclear receptor Nr5a2 regulates cumulus expansion in the female mouse ovary without affecting oocyte fertilizability

Kalyne Bertolin[1], João Suzuki[2], Anne-Marie Bellefleur[1] and Bruce D. Murphy[1,3]

Affiliations: [1]Centre de recherche en reproduction animale, Faculté de médecine vétérinaire, Université de Montréal, St-Hyacinthe, Quebec, J2S 7C6, Canada; [2]Dept. Obstetrics and Gynecology, McGill University, Montreal, Quebec, Canada; [3]Corresponding author

Abbreviated title: The role of Nr5a2 in cumulus expansion

Key words: Nr5a2, granulosa cells, conditional knockout mouse, cumulus expansion, fertilization

Status: Work in progress. To be submitted to the journal *Biology of Reproduction*.

Author contributions: Overall, my relative contribution to this work was 85%. My contribution involved designing the experiments; protocol optimization; manipulation of animals and samples; performance of laboratory techniques; interpretation of the results; design and preparation of the figures and writing of the text. JS performed the micromanipulation of the mice oocytes for the intracytoplasmic sperm injection. AMB collaborated on designing the experiments and on protocol optimization. BDM supervised the project and contributed to the writing task.

3.1. Abstract

The orphan nuclear receptor Nr5a2, a.k.a. liver receptor homolog-1, is expressed in granulosa, cumulus and luteal cells of the mouse ovary, and it is a key modulator of female fertility. Conditional knockout mice with depletion of Nr5a2 in ovarian granulosa cells from primary follicles onward exhibited disrupted cumulus expansion. In contrast, mice with depletion of Nr5a2 in granulosa cells from antral follicles onward undergo cumulus expansion after hormonal superstimulation. We hypothesized that Nr5a2 modulates cumulus expansion in a spatiotemporal manner. We employed the two previously described granulosa-specific knockout mouse models genotyped as: 1) $Nr5a2^{Amhr2-/-}$, bearing Nr5a2 depletion from preantral follicles; and 2) $Nr5a2^{Cyp19-/-}$, bearing Nr5a2 depletion from antral follicles. Cumulus expansion occurred spontaneously in $Nr5a2^{Cyp19-/-}$ females at approximately 12 h after the endogenous LH peak. Nr5a2 is depleted in mural granulosa cells of the $Nr5a2^{Cyp19-/-}$ ovaries, but its expression is detected in their cumulus cells. To establish a comparison between the two mutant models for their cumulus expansion capability, an *in vitro* cumulus expansion assay was performed. Both $Nr5a2^{Amhr2-/-}$ and $Nr5a2^{Cyp19-/-}$ cumulus-oocyte complexes underwent expansion *in vitro*, but the degree of expansion was reduced relative to that observed in the controls at 12 h of culture. We evaluated the cumulus expansion-related genes regulated by Nr5a2 in both mutant strains *in vivo* and found downregulation of *Areg*, *Ereg*, *Btc* and *Tnfaip6* gene expression at 2 h and 4 h post hCG ($p < 0.05$). Protein expression of connexin 43 (Cx43; Gja1) was evaluated by immunofluorescence in the $Nr5a2^{Amhr2-/-}$ ovarian sections, and the intensity for Gja1 in granulosa and cumulus cells of the $Nr5a2^{Amhr2-/-}$ mutant follicles was lower at 0 h and maximum at 8 h post hCG, as opposed from the pattern of Gja1 protein expression

observed in control ovaries. The oocytes in both mutant genotypes can undergo germinal vesicle breakdown, confirming their capability to mature *in vivo*. To establish whether the oocytes are fertilizable, adult females $Nr5a2^{Amhr2-/-}$, $Nr5a2^{Cyp19-/-}$ and control groups were hormonally synchronized and the oocytes presenting polar bodies were fertilized by ICSI. Subsequent observation indicated that approximately 70% of the resulting embryos were capable of proceeding to the blastocyst stage *in vitro*, independent of the genotype. We conclude that the cumulus cells of $Nr5a2^{Cyp19-/-}$ mice are able to expand more efficiently that the $Nr5a2^{Amhr2-/-}$ both *in vivo* and *in vitro*. Moreover, cumulus expansion-related gene expression is equally disrupted in both mutant models. The disruption of the Nr5a2 gene expression that occurs in the somatic cells of the follicle does not affect the capability of the oocytes to be fertilized.

3.2. Introduction

Within the ovary, follicular granulosa cells differentiate into mural granulosa cells and cumulus cells, working in reciprocal communication with the oocyte, the female germ cell[17]. Mural granulosa cells express aromatase, which is encoded by the cytochrome P450 family 19 subfamily A polypeptide 1 (Cyp19a1)[34] gene. Under the control of follicle-stimulating hormone (FSH), aromatase converts the theca-derived androgens into estrogens, whereas estradiol-17β (E2) is the predominant aromatized estrogen. Estradiol-17β regulates the proliferation of granulosa cells[29], inducing the expression of LH receptors (LHR) and causing granulosa cells to become responsive to LH[6].

Cumulus granulosa cells within the preovulatory follicle are closely connected to the oocyte[27]. An acute peak of LH triggers the occurrence of important reproductive events

in the female, including the migration of the cumulus cells outwardly from the oocyte[19], in a process known as cumulus expansion, critical for normal oocyte development, ovulation, and fertilization[15]. The LH stimulus induces a transient and sequential expression of the epidermal growth factor (EGF)-related factors, including epiregulin (Ereg), amphiregulin (Areg) and betacellulin (Btc) that have been recently identified as essential for oocyte maturation and cumulus expansion[26].

The peak of LH also induces the expression of other genes with a pivotal role in cumulus expansion, such as the hyaluronic acid synthase 2 (HAS-2)[5], involved in the deposition of a hyaluronic acid matrix between the cumulus cells[9]. The entire ovulatory process involves inflammatory-like ovarian changes[29], implying the importance of the prostaglandin-endoperoxide synthase-2 (PTGS2)[32] and the tumor necrosis factor-stimulated gene-6 (Tnfaip6)[18]. Cumulus expansion is further complex, involving the regulation and modification of gap-junctional proteins[12], such as the connexin 43 (gap junction alpha-1; GJA1)[36]. Several gene products of the follicular cells are required for successful and optimal ovulation, in a combined endocrine and paracrine intra-follicular communication[31].

Recently, it has been shown that the orphan nuclear receptor, Nr5a2, is essential for ovulation. A conditional knockout mouse model bearing a depletion of Nr5a2 in granulosa cells from primary follicles presented impaired cumulus expansion that could not be rescued by hormonal superstimulation[14]. On the other hand, another study of the role of Nr5a2 in later stages of the follicular development showed that granulosa-specific knockout females underwent cumulus expansion after a protocol of hormonal injection[2]. The lack of ovulation was consistent in both mutant models, but there is no evidence on whether the oocytes are affected by the disruption of Nr5a2 in somatic cells[2; 14]. Our objectives were to compare the cumulus expansion process using the two previously described Nr5a2

granulosa-specific knockout mice models, and to determine whether the expression of Nr5a2 in granulosa cells is essential for the oocytes to be fertilized. We hypothesize that the inconsistent pattern of cumulus expansion in both mice models is due to a distinct spatiotemporal depletion of Nr5a2.

3.3. Materials and methods

Animals and colony maintenance

All animal experiments were approved by the University of Montreal Animal Care Committee and conducted according to the guidelines of the Canadian Council on Animal Care (CCAC) – Guide to the Care and Use of Experimental Animals. All mutant and control mice were of the C57BL/6 background. Animals were maintained under a 14:10 light:dark cycle, provided food and water ad libitum. All euthanasia was performed by anesthetizing the animals with Isoflurane (PPC, Richmond Hill, ON, Canada) in a closed container, followed by cervical dislocation. Nr5a2 floxed ($Nr5a2^{f/f}$) mice, generated by Dr. Johan Auwerx, have been described previously[3]. To generate granulosa-specific Nr5a2 mutant in antral follicles, animals expressing Cre-recombinase from the cytochrome P450 family 19 subfamily A polypeptide 1 (Cyp19a1 a.k.a. aromatase[20]) designated $Cyp19a1^{Cre/+}$ were crossed with $Nr5a2^{f/f}$ mice; conditional knockout (cKO) genotype: $Nr5a2^{Cyp19-/-}$. To generate granulosa-specific Nr5a2 mutant in primary follicles, we employed the previously described $Nr5a2^{f/f}$ mice crossed with animals expressing Cre-recombinase from the anti-Müllerian hormone receptor-2[14] ($Amhr2^{Cre/+}$; generous gift of Dr. Richard Behringer); cKO genotype: $Nr5a2^{Amhr2-/-}$. The litters were genotyped (see Table III for primers) using DNA

extracted from a biopsy of the tail. The non-mutant littermates were used as control groups, i.e., $Nr5a2^{f/f}tgCyp19^{+/+}$ and $Nr5a2^{f/f}Amhr2^{+/+}$, respectively for the $Nr5a2^{Cyp19-/-}$ and $Nr5a2^{Amhr2-/-}$.

Superstimulation protocol

For hormonal superstimulation, female mice both $Nr5a2^{Cyp19-/-}$, $Nr5a2^{Amhr2-/-}$ and their respective controls were injected intraperitoneally (IP) with 5 IU of equine chorionic gonadotropin (eCG) (Folligon® – Intervet, Whitby, ON, Canada) to stimulate follicular development, followed by the injection of 5 IU of human chorionic gonadodotropin (hCG) (Chorulon® – Intervet, Whitby, ON, Canada) 44 to 48 h post eCG, to induce ovulation. Ovaries were collected at the moment of the euthanasia in different time-points varying for each experiment; ovaries were either snap frozen in liquid nitrogen and stored at -80°C for RNA or fixed in paraformaldehyde (PAF 4%) (Sigma-Aldrich) and embedded in paraffin for histological examination.

Estrous cycle and natural cumulus expansion

Experimental design for the detection of natural cumulus expansion was made based on the mouse estrous cycle (as reviewed in the Chapter 5 of this thesis). For estrous cycle staging, vaginal smears were collected daily (at 09 00) with phosphate-buffered saline (PBS) 1x from adult 8-wk-old $Nr5a2^{Cyp19-/-}$ and control females; smears were placed on glass slides and cytology was evaluated under the microscope. The day when proestrus was detected, the female was moved to a cage with one C57BL/6 wild type (WT) male. The occurrence of the LH peak was confirmed by the presence of a copulatory plug verified by

visual examination in the morning of the next day (at 04 00), and euthanasia was performed at this time. The ovaries were fixed in PAF 4% and embedded in paraffin for histological examination by hematoxylin and eosin staining.

Cumulus expansion assay

Immature female mice $Nr5a2^{Cyp19-/-}$, $Nr5a2^{Amhr2-/-}$ and the controls were hormonally superstimulated with eCG and the cumulus-oocyte complexes (COCs) were collected by ovarian puncture at 40 h post eCG as previously described[13]. COCs were then cultured in 25 µl drops of MEM-α (Invitrogen) supplemented with penicillin/streptomycin sulfate (Invitrogen), bovine serum albumen (BSA) 0.3% and bovine FSH (National hormone and peptide program, CA) at a density of 1 COC/µl and kept at 37°C incubation chamber 5% CO_2 in humidified air. The expansion of the cumulus cells was evaluated at 0 h, 4 h, 8 h, 12 h and 24 h of treatment in culture and the images were recorded by the Axio imager M1, Zeiss Microscopy. For co-culture experiments, 50 fully-grown denuded oocytes from WT females primed with eCG and collected at 44 h – 48 h post eCG were added to the drops containing the COCs as detailed above. Cumulus expansion was graded from 0 (no expansion) to 4 (full expansion) and the rates of expansion potential were calculated at 12 h of FSH treatment.

RNA isolation and real time polymerase chain reaction (qPCR)

Populations of granulosa and cumulus cells were collected from 25 to 27-day-old immature female mice $Nr5a2^{Cyp19-/-}$, $Nr5a2^{Amhr2-/-}$ and their respective controls at 2 h or 4 h post hCG (as previously described hormonal superstimulation) for RNA analysis. The cells

were isolated by puncturing both ovaries with 25G 5/8" needles in PBS 1x, oocytes were separated from cumulus cells by up-and-down pipetting and removed from the final samples by filtering (BD Falcon, Cell Strainer, 40 μm Nylon, Mexico). Total RNA from granulosa/cumulus cells was extracted with RNeasy® Mini Kits (Qiagen) as per manufacturer's instructions. Reverse transcription into cDNA was performed with the SuperScript® II First Reverse Transcriptase (Invitrogen) and random hexamer primers. Real-time qPCR was performed using Power SYBR® Green PCR Master Mix (Applied Biosystems, Warrington, UK), with the 7300 real-time PCR system (Applied Biosystems, Foster City, CA, USA). General PCR conditions (2 min at 50°C, 10 min at 95°C, then 40 cycles of 15 s at 95°C and 60 s at 60°C) were used to amplify the product. Melting curve analyses were performed to verify product identity, adding a dissociation step to the PCR run (15 s at 95°C, 60 min at 60°C, 15 s at 95°C, and 15 s at 60°C). The sequences of the primers sets used are listed in Table III, each used in a final concentration of 3000 nM. Primers were validated by standard curves. Samples were run in triplicates and results were expressed relative to the ribosomal protein S18 (RPS18) levels. Data were then normalized to a calibrator sample using ΔΔCt method, as described by Pfaffl[28], with correction for amplification efficiency by LinRegPCR 11.0 software (Academic Medical Center, Amsterdam, the Netherlands).

Immunofluorescence

For histological examination, ovaries were fixed in PAF 4% overnight, then washed in PBS 1x and paraffin embedded. Ovarian cell-specific localization of Nr5a2 and Gja1 was verified by fluorescence immunohistochemistry. Briefly, paraffin sections of ovaries were

rehydrated, boiled in 10 mM sodium citrate (pH 6) for 30 min, and cooled to room temperature (RT). Sections were blocked overnight with 5% bovine serum albumin (BSA) immunoglobulin G (IgG)-Free, protease-Free (Jackson Immunoresearch Lab., Inc.) at 4°C. Samples were then incubated with Nr5a2 (Abcam, ab18293) diluted 1:50 and rabbit polyclonal IgG connexin 43 (Gja1; Santa Cruz Biotechnology) diluted 1:100 both in PBS with 5% BSA overnight at 4°C. As negative control, some sections were incubated with 5% BSA only in place of the first antibody. Sections were washed, incubated with cyanine 3 (Cy3)-conjugated goat anti-rabbit IgG (Jackson Immunoresearch Lab., Inc.), diluted 1:400 in PBS 1x for 1 h at RT. Slides were then washed, and sections were counterstained with 4',6-diamidino-2-phenylindole (DAPI, Sigma, St. Louis, MO), diluted 1:1000 in PBS, for 5 min. Slides were mounted in Permafluor (Thermo Fisher Scientific, UK). Ovarian distribution of Nr5a2 and Gja1 was observed by Axio imager M1 (Zeiss Microscopy).

Intracytoplasmic sperm injection (ICSI)

Adult (8-wk-old) female mice $Nr5a2^{Cyp19-/-}$, $Nr5a2^{Amhr2-/-}$ and controls were hormonally superstimulated and euthanasia was performed as previously described. COCs were collected from 5 females per genotype by ovarian puncture with 25G 5/8" needles at 11 h post hCG. Cumulus cells were dispersed by incubating the COCs for 1 minute with 80 units/ml of hyaluronidase (from bovine testes, Sigma), and the cells were removed pipetting gently. Oocytes were evaluated for the presence of a polar body (PB), indicating metaphase II maturation, and pooled together according to the genotype. For sperm collection, two WT male mice were euthanized and the sperm were collected from the cauda region of each excised epididymis. Sperm were incubated in one drop of modified

human tubal fluid (mHTF) containing 0.9% BSA for 90 min at 37°C in 5% CO_2 in humidified air to induce capacitation. ICSI was conducted as previously described[37]. Briefly, 5 µl of sperm suspension were mixed with 5 µl of 12% polyvinylpyrrolidone (PVP) solution under oil. Oocytes were transferred from the mHTF medium to Hepes buffered mHTF medium under oil. By the means of a Nikon microscope (Eclipse) equipped with Narishige micromanipulators and a Piezo system (Prime Tech, Japan), the head of a morphologically normal and highly motile sperm was separated from the tail and injected into the oocyte (n = 25 injected oocytes per genotype). After injection, the oocytes were transferred into a 50 µl drop of embryo maintenance medium under oil and cultured at 5% CO_2 in humidified air. Fertilization rate was assessed by cleavage of the survived oocytes 24 h after ICSI, and embryonic development to morula stage was observed 96 h after ICSI. Blastocyst development was visualized at 120 h after ICSI. The rate of cleavage (2-cell) was based on the number of MII injected oocytes, and the rate of blastocyst development was based on the number of cleaved oocytes after ICSI.

Statistical analyses

All data were analysed using JMP (Version 5.0.1a. SAS Institute Inc.) statistical software. Differences between mutant and control mice for data obtained at multiple time points or multiple genotypes were determined by two-way analysis of variance followed by JMP LSMeans Contrast post hoc test to determine the differences between individual means. All numerical data are represented as mean ± SEM. Significant difference was recognized at $p < 0.05$.

3.4. Results

Characterization of the cumulus cells profile in the Nr5a2$^{Cyp19-/-}$ ovaries

The granulosa-specific knockout (cKO; Nr5a2$^{Cyp19-/-}$) mouse model generated by crossing Nr5a2-floxed mice with the transgenic line tgCyp19a1$^{Cre/+}$, expressing the Cre-recombinase driven by the aromatase promoter, was evaluated for the occurrence of natural cumulus expansion in adults *in vivo* without ovarian superstimulation. Control and cKO Nr5a2$^{Cyp19-/-}$ females in proestrus were housed with a reproductively proven WT male, and the natural LH peak was confirmed by the visualization of a vaginal copulatory plug. At approximately 12 h after the assumed LH peak, ovarian histology showed the expected cumulus expansion in control females (Figure 3.1A), and that in adult Nr5a2$^{Cyp19-/-}$ ovaries (Figure 3.1B) cumulus expansion also happens naturally. To study the spatial depletion of Nr5a2 driven by aromatase, immature Nr5a2$^{Cyp19-/-}$ and control females were superstimulated and the ovaries were collected at 12 h post hCG (Figure 3.1C-F). Immunofluorescence showed that the protein levels of Nr5a2 were reduced in mural granulosa cells of Nr5a2$^{Cyp19-/-}$ ovarian follicles when compared to the control ovaries (Figure 3.1C), whereas the expression in cumulus cells is not depleted in the cKO (Figure 3.1E,F). Thus, the depletion of Nr5a2 is more efficient in mural granulosa cells than in cumulus cells when the aromatase promoter drives Nr5a2-flox Cre-recombination.

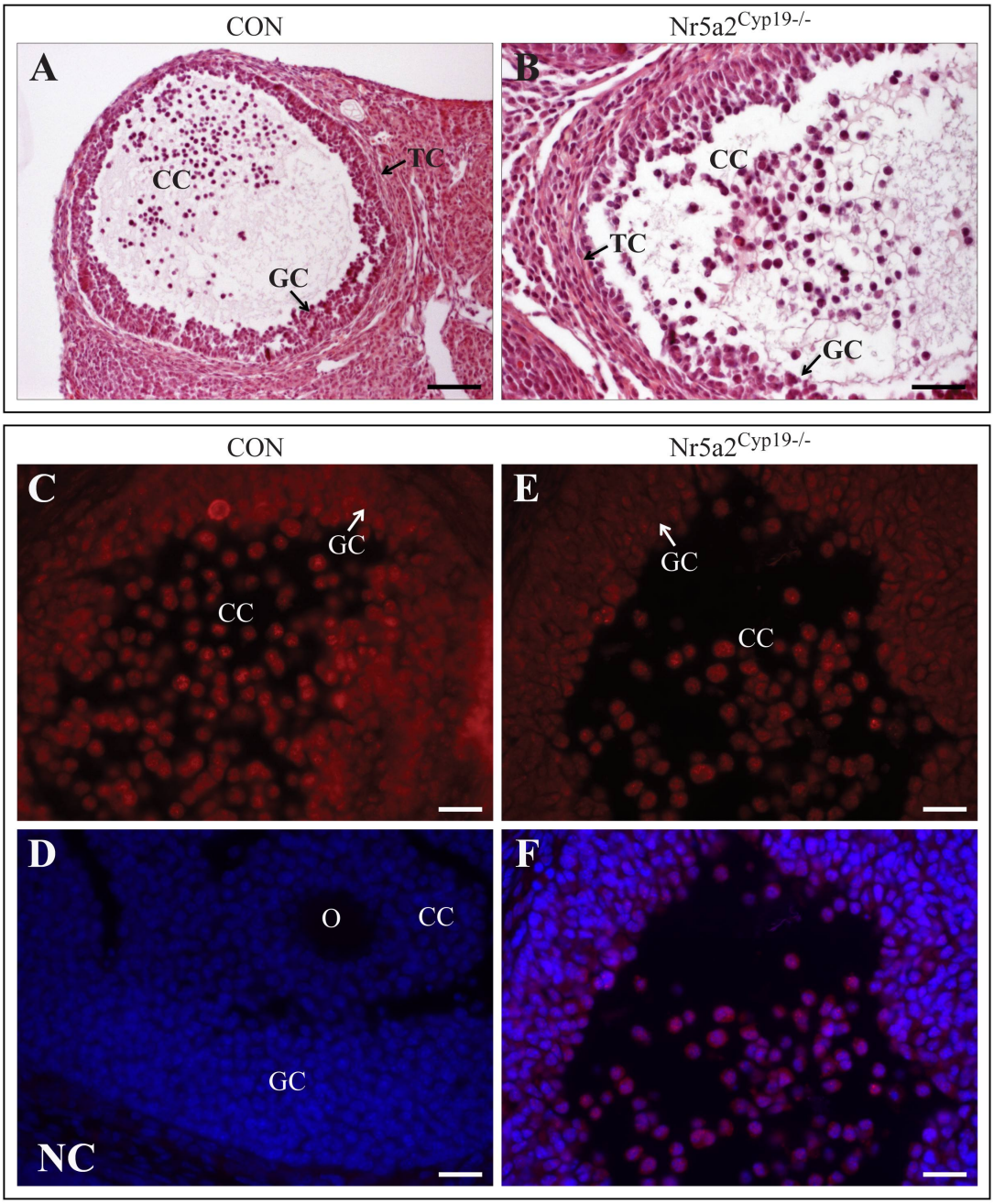

Figure 3.1 : Characterization of cumulus cells in the granulosa-specific knockout mouse $Nr5a2^{Cyp19-/-}$. Bright field microscopy images of hematoxylin-eosin stained sections of ovaries from adult CON (A) and $Nr5a2^{Cyp19-/-}$ (B) mice in estrus showing cumulus expansion. (C-F) Microscopic images of Nr5a2 immunofluorescence in ovarian sections. (C) Positive control for staining of granulosa and cumulus cells; (D) negative control using BSA 5%; (E) depletion of Nr5a2 protein in granulosa cells of the conditional knockout ovary exclusively in granulosa cells but not in cumulus cells; and (F) DAPI and Cy3 merged. CC, cumulus cells; TC, theca cells; GC, granulosa cells; O, oocyte. Bars = A (80 μm); B (40 μm); C-F (20 μm). CON = control ($Nr5a2^{f/f}tgCyp19^{+/+}$); $Nr5a2^{Cyp19-/-}$ = conditional knockout.

***In vitro* potential of cumulus expansion in two Nr5a2 granulosa-specific knockout mice models**

Females Nr5a2$^{Cyp19-/-}$, Nr5a2$^{Amhr2-/-}$ and controls (n = 10 per group) were superstimulated and the COCs were collected at 40 h post eCG to evaluate their capacity of expansion *in vitro*. COCs were treated with FSH during 24 h in culture. Based on the negative control (Figure 3.2B) incubated in medium without FSH, the degree 0 (minimum) of expansion was determined. The maximum expansion for the control group (Figure 3.2A) occurred at 12 h of treatment, and it was rated as degree 4 of expansion. Based on the evaluation of the recorded images taken at 12 h of treatment for all the COCs, the expansion of the Nr5a2$^{Amhr2-/-}$ group (Figure 3.2C) was shown to be less efficient than in the control group. The expansion of the Nr5a2$^{Cyp19-/-}$ (Figure 3.2D) group was also compromised *in vitro*. Co-culture of the COCs showed that the expansion of the two mutant models Nr5a2$^{Amhr2-/-}$ (Figure 3.2E) and Nr5a2$^{Cyp19-/-}$ (Figure 3.2F) was not rescued by the presence of the WT oocytes. Quantification of the cumulus expansion resulted in an average of maximum expansion in the control group, and a compromised expansion in the two Nr5a2 knockout models, with the Nr5a2$^{Amhr2-/-}$ females presented the lower degree of cumulus expansion *in vitro* (Figure 3.2G).

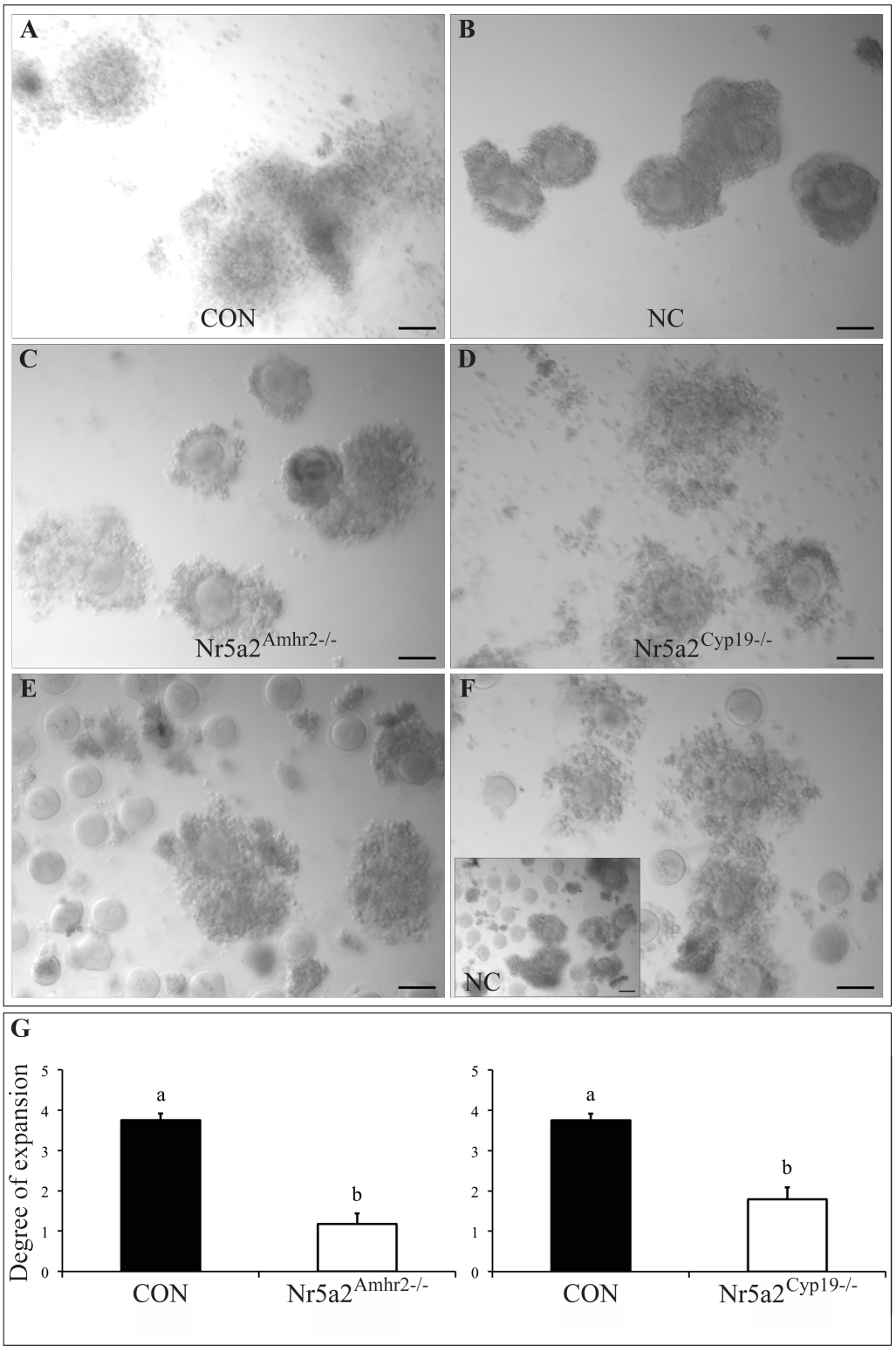

Figure 3.2 : Expansion potential of cumulus-oocyte complexes from two granulosa-specific knockout mouse lines distinguished by temporal and spatial depletion of Nr5a2 during the follicular development. (A) Control (CON) females and (B) negative control without FSH (NC). (C) Cumulus-oocyte complexes of cKO Nr5a2$^{Amhr2-/-}$; and (D) cKO Nr5a2$^{Cyp19-/-}$ at 12 h of *in vitro* incubation with FSH. (E-F) Co-

culture of Nr5a2 granulosa-specific knockout cumulus-oocyte complexes with wild type oocytes; (E) cKO Nr5a2$^{Amhr2-/-}$ and (F) cKO Nr5a2$^{Cyp19-/-}$. Panel F insert: negative control (NC) without FSH. Bar = 50 μm. (G) Quantification of cumulus expansion potential of control (CON), cKO Nr5a2$^{Cyp19-/-}$ and Nr5a2$^{Amhr2-/-}$; (*) $p < 0.05$.

The expression pattern of cumulus expansion-related genes driven by Nr5a2 in preantral and preovulatory follicles

Analysis of ovarian granulosa and cumulus cells of Nr5a2$^{Cyp19-/-}$ and Nr5a2$^{Amhr2-/-}$ mice revealed that the expression of cumulus expansion-related genes is compromised in both granulosa-specific knockout mouse models (Figure 3.3A-D). The pattern of gene expression at 2 h or 4 h post hCG showed a consistent downregulation in both time-points and for both mutant genotypes for the EGF-related factors *Areg* (Figure 3.3A), *Ereg* (Figure 3.3B) and *Btc* (Figure 3.3C). The *Tnfaip6* (Figure 3.3D) also shows the same pattern of expression in all the groups. In contrast, histological analysis of hematoxylin and eosin stained ovaries indicated that the Nr5a2$^{Cyp19-/-}$ COCs (Figure 3.3F) revealed no apparent difference if compared to those found in the control group (Figure 3.3E) at 4 h post hCG. We conclude that Nr5a2 expression in granulosa cells of preantral or antral follicles modulates cumulus expansion by regulating important genes necessary for this event.

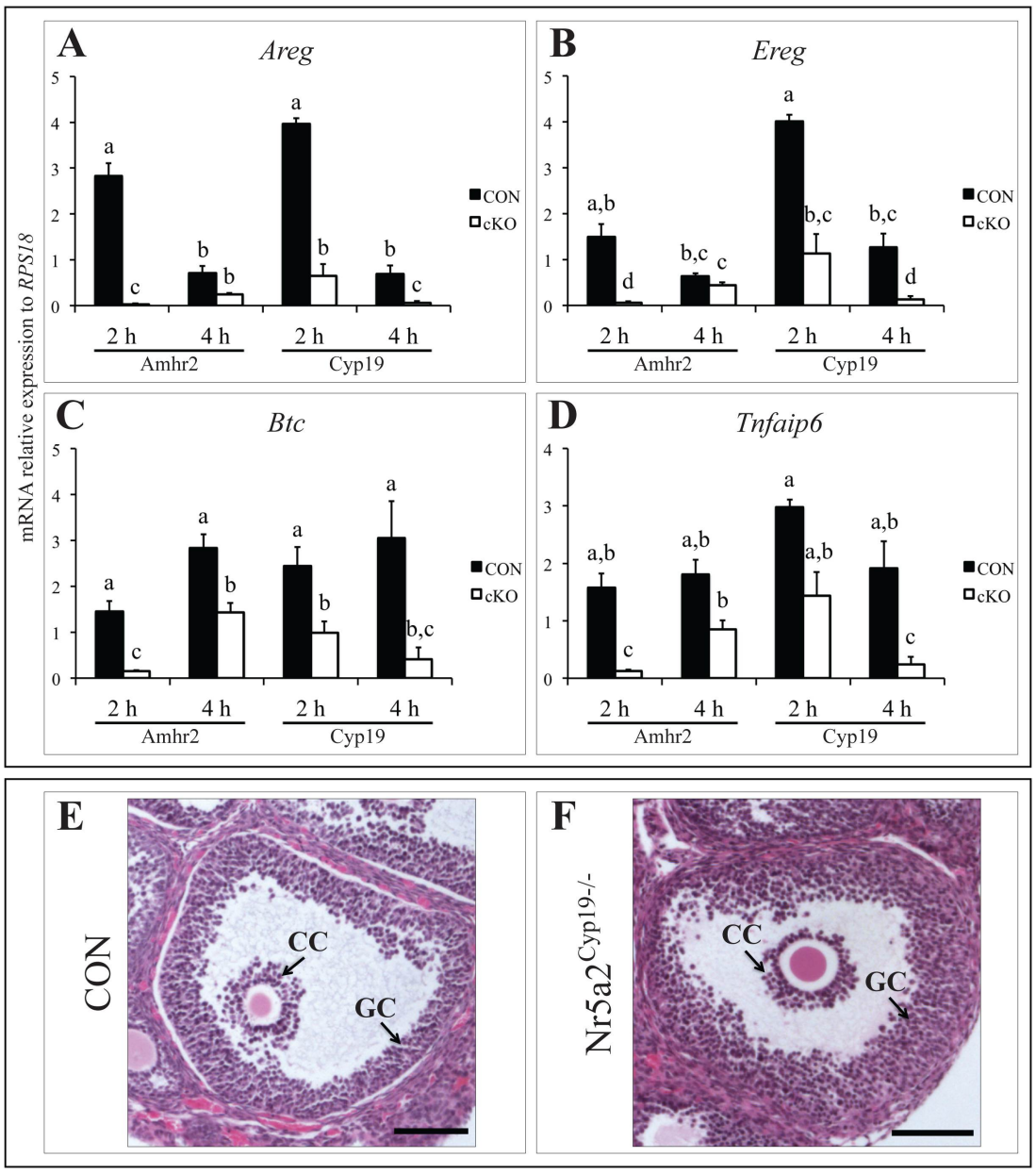

Figure 3.3 : Abundance of mRNA as determined by qPCR for (A) *Areg*, (B) *Ereg*, (C) *Btc* and (D) *Tnfaip6* relative to *RPS18* comparing two granulosa-specific knockout mouse models distinguished by the timing of *Nr5a2* depletion during the follicular development; superstimulated ovaries from immature females were collected at 2 h or 4 h post hCG (n = 5 per group) and granulosa cells were isolated by ovarian puncture. Amhr2 (Cre-recombinase) = left bars, mutation in primary follicles. Cyp19 (Cre-recombinase) = right bars, mutation in antral follicles. CON = control, black bars ($Nr5a2^{f/f}$ $tgCyp19^{+/+}$; or $Nr5a2^{f/f}$ $Amhr2^{+/+}$); cKO = conditional knockout, white bars ($Nr5a2^{Cyp19-/-}$ / or $Nr5a2^{Amhr2-/-}$) respectively. Differing superscripts indicated differences at $p < 0.05$. (E-F) Bright field microscopy images of hematoxylin-eosin stained sections of ovaries from (E) immature control (CON) and (F) cKO $Nr5a2^{Cyp19-/-}$ mice superstimulated with eCG and hCG and collected at 4 h post hCG. Bar = 100 μm. CC, cumulus cells; GC, granulosa cells.

Gja1 expression is dysregulated in Nr5a2$^{Amhr2-/-}$ ovarian granulosa and cumulus cells

We examined the expression of the Gja1 in Nr5a2$^{Amhr2-/-}$ ovarian sections (Figure 3.4A-H) by immunofluorescence to determine whether the more severe impairment in their cumulus expansion is related to a problem in cell-to-cell communication. In immature superstimulated Nr5a2$^{Amhr2-/-}$ ovaries at 0 h post hCG (Figure 3.4B,D), qualitative analysis of the Gja1 protein expression shows an apparent downregulation in granulosa and cumulus cells compared to the control group (Figure 3.4A,C). This pattern of protein downregulation is reversed in the cKO ovaries at 8 h post hCG (Figure 3.4 F,H), when a lower expression of Gja1 is expected to be normal in the control group (Figure 3.4E-G). Overall, Gja1 expression appears to decrease as follicles develop from 0 h to 8 h post hCG in the control ovaries, however in the cKO cells, the staining appear more intense at 8 h than at 0 h post hCG, suggesting that the communication between granulosa and cumulus cells is dysregulated in Nr5a2$^{Amhr2-/-}$ ovaries.

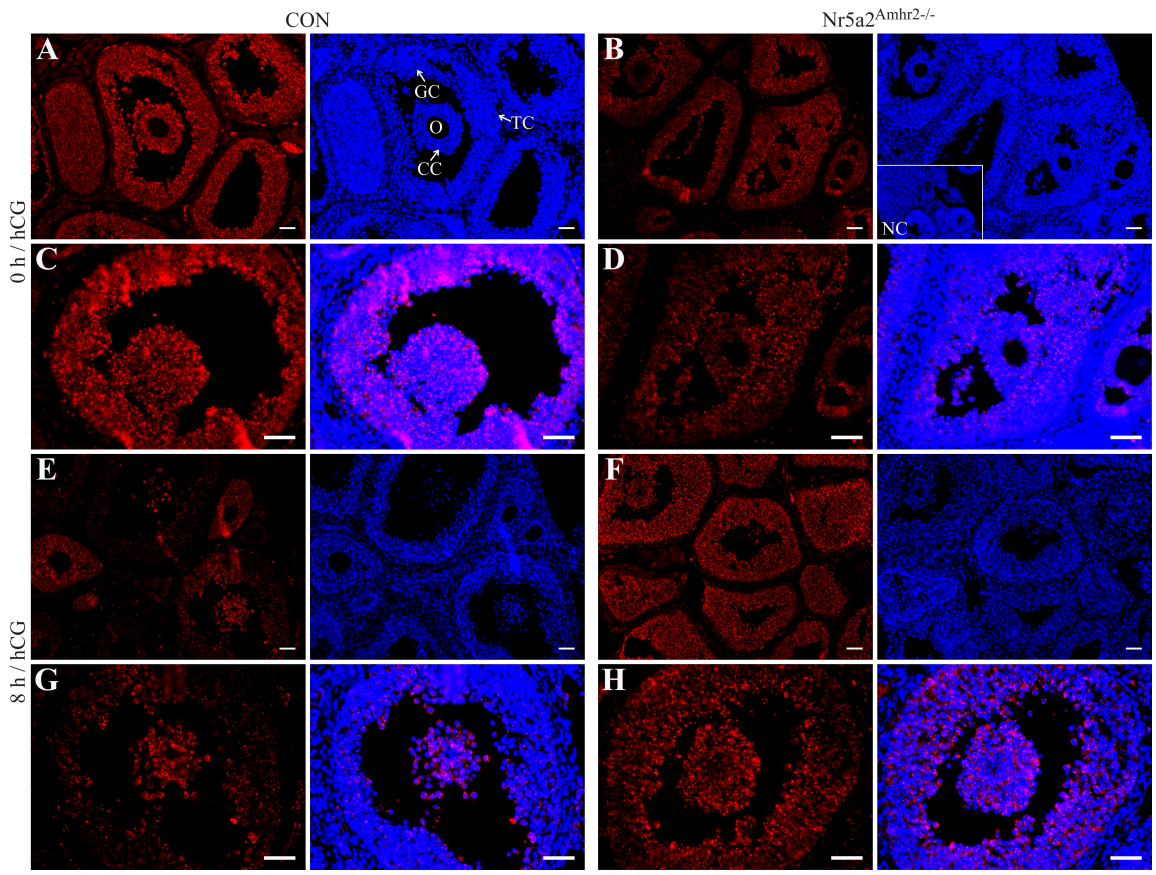

Figure 3.4 : Microscopic images of fluorescent immunohistochemistry of Gja1 (connexin 43; red; Cy3) in ovarian sections of CON and Nr5a2$^{Amhr2-/-}$ immature female mice superstimulated with eCG and hCG and collected at 0 h (A-D) or 8 h (E-H) post hCG, using DAPI to stain the nuclei (blue). CC, cumulus cells; TC, theca cells; GC, granulosa cells; O, oocyte. Bar = 40 μm. Panel B insert: negative control (NC) with 5% BSA.

The disruption of Nr5a2 in granulosa cells of preantral or antral follicles does not affect the oocyte fertilizability

We found that 85% of the oocytes from both $Nr5a2^{Cyp19-/-}$ and $Nr5a2^{Amhr2-/-}$ cKO (n = 5 per group) exhibited polar body formation after 12 h post hCG injection (Figure 3.5A), in concordance with the results obtained in the control groups (data not shown). To establish whether the oocytes were fertilizable, adult females $Nr5a2^{Cyp19-/-}$ and $Nr5a2^{Amhr2-/-}$ cKO and control groups (n = 5 per group) were hormonally synchronized. At 12 h post hCG, oocytes presenting a polar body were fertilized by ICSI. Subsequent observation of the oocytes at 24 h post ICSI indicated that approximately 70% of the oocytes were fertilized and cleaved into 2-cell embryonic stage, independent of the genotype (Figure 3.5B). Morula formation was observed at 96 h post ICSI in all the genotypes (Figure 3.5C), and the resulting embryos were capable of proceeding to the blastocyst stage (Figure 3.5D) *in vitro* in a rate of approximately 70% (Figure 3.5E) for both $Nr5a2^{Cyp19-/-}$ and $Nr5a2^{Amhr2-/-}$ cKO and the control groups. These data indicate that the expression of Nr5a2 in ovarian somatic cells is not essential for the ability of the oocyte to be fertilizable.

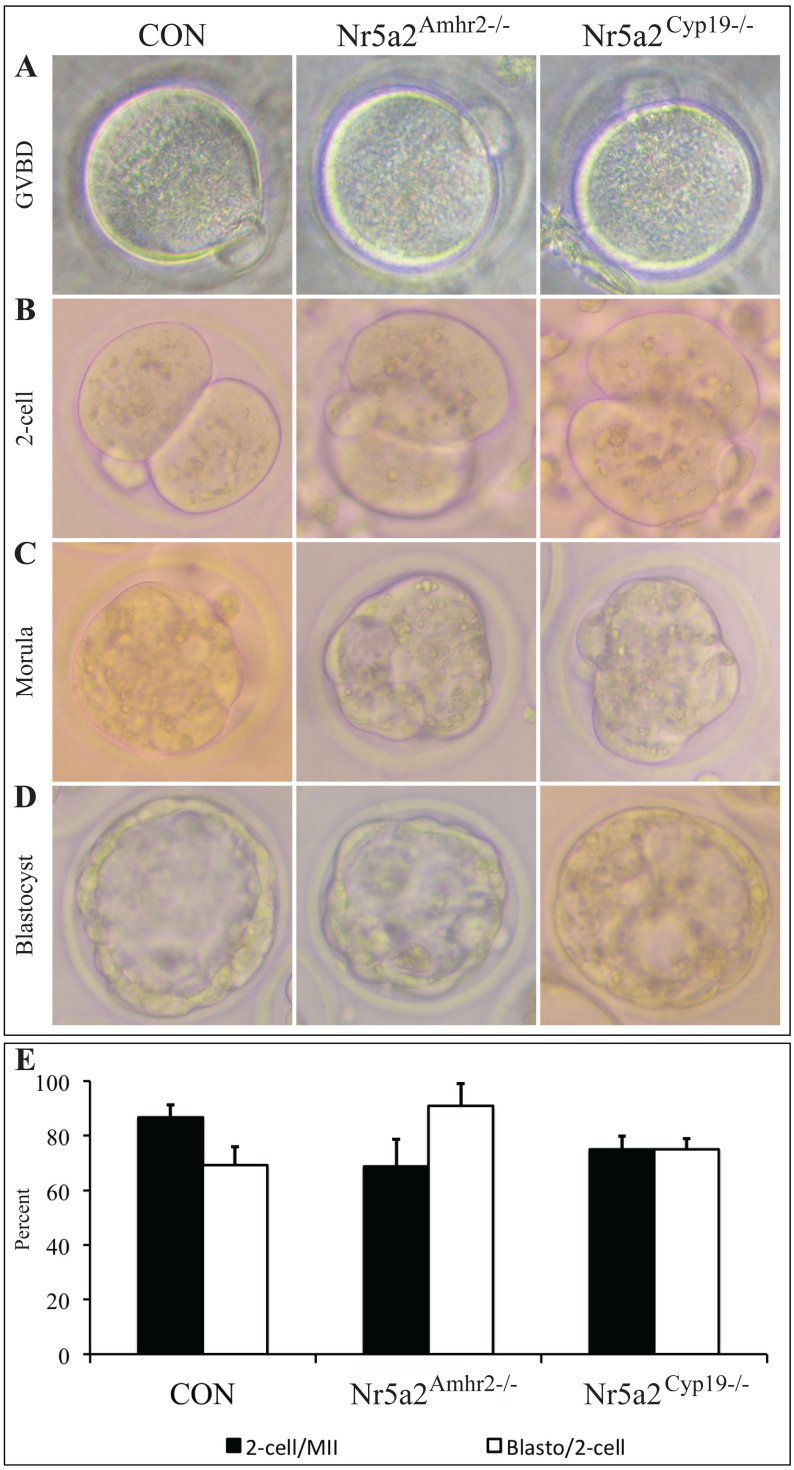

Figure 3.5 : The lack of Nr5a2 in granulosa cells does not compromise oocyte fertilizability. Microscopy image of (A) oocytes representing germinal vesicle breakdown (GVBD); (B) 2-cell embryo; (C) morula and (D) blastocyst of CON (control), conditional knockout Nr5a2$^{Amhr2-/-}$ and Nr5a2$^{Cyp19-/-}$ female mice. (E) Fertilization rate of CON, conditional knockout Nr5a2$^{Amhr2-/-}$ and Nr5a2$^{Cyp19-/-}$. Black bars = percentage of mature oocytes (MII) reaching the 2-cell embryonic stage for each genotype; white bars = percentage of 2-cell embryos reaching the blastocyst stage for each genotype ($p > 0.1$).

3.5. Discussion

The cumulus oophorus undergoes dramatic changes in morphology in response to gonadotropins, as it becomes expanded by the deposition of a hyaluronic acid matrix between the cumulus cells, culminating in ovulation[9]. Cumulus expansion is an essential process in ovulation, and in its absence, ovulation is impaired[6]. Previous work using mouse somatic targeted mutagenesis showed that the nuclear receptor Nr5a2 is a key regulator of the ovulatory process. The disruption of Nr5a2 in granulosa cells from primary follicles onward ($Nr5a2^{Amhr2-/-}$) resulted in lack of cumulus expansion[8]. Recently, a complementary study applied the disruption of Nr5a2 from antral follicles onward ($Nr5a2^{Cyp19-/-}$). This second mouse model also presented an anovulatory phenotype, but surprisingly showed that cumulus expansion was occurring after hormonal superstimulation[2].

Aiming to elucidate the role of Nr5a2 in peri-ovulatory events, we employed these two previously described mouse models in parallel, determining a comparative study about the role of nuclear receptor Nr5a2 in a time line sequence of follicular development. In this particular study, we focused on the role of Nr5a2 in cumulus oophorus cells.

Hormonal protocols of ovarian superovulation are widely used in research with the mouse model. The protocol consists of one injection of eCG, inducing FSH activity[14], followed by one injection of hCG, mimicking the LH peak[10]. This protocol is used to synchronize and superovulate female mice, and also to bypass potential pituitary deficiency in FSH and LH secretion. This artificial hormonal superstimulation was applied in the previous studies showing cumulus expansion in the $Nr5a2^{Cyp19-/-}$ model[2]. Therefore, it was deemed important to determine whether these females can spontaneously undergo cumulus expansion *in vivo*.

Based on multiple previous studies it was possible to approximate the occurrence of the natural LH peak by following the consistent mouse estrous cyclicity (Chapter 5). Taking into account the timeline of the cycle, ovulation takes place between 2330 and 0430 of the estrus day[16], at 12 to 14 hours after the surge of LH. A vaginal copulatory plug confirmed the female estrus phase, and by collecting the ovaries at 0400 we expected to visualize spontaneous cumulus expansion in ovarian histologic sections. Our estimative protocol was shown to be precise, since all of the control group presented cumulus expansion at that time. Our data demonstrated that $Nr5a2^{Cyp19-/-}$ females undergo cumulus expansion in nature, and that the LH peak is also occurring.

Following confirmation that the $Nr5a2^{Cyp19-/-}$ model undergoes cumulus expansion and knowing that the $Nr5a2^{Amhr2-/-}$ does not, we hypothesized that the excision of Nr5a2 in these two models was not only temporally different, but also spatially different. We employed the Cre-*loxP* system to generate our two mouse models. In this system, Cre-recombinase protein causes recombination of specific sequences of DNA with high fidelity[13]. It efficiently catalyzes site-specific DNA recombination between two loci of crossover (*x*) in P1 (*loxP*), inserted around a functionally essential part of the gene of interest, and a single recombinase splices together the two halves of the target DNA, resulting in the inactivation of the gene[18]. The transgenic mouse line expressing the Cre-recombinase is guided by a promoter with a desired temporal and/or spatial pattern[18]. In rodents, aromatase enzyme expression, encoded by the *Cyp19a1* gene, is restricted to the gonads and the brain. In the ovaries of sexually mature animals, aromatase expression is limited only to mural granulosa cells of healthy large antral follicles, preovulatory follicles and luteal cells[17]. Nr5a2 is expressed in the cumulus cells, whereas Cyp19a1 is not[12]. Cyp19a1 is the promoter guiding the excision of Nr5a2 in our $Nr5a2^{Cyp19-/-}$ model. The

absent expression of Cyp19a1 in cumulus cells results in unrecombined target gene, remaining intact and functional in the cells where the recombinase is not expressed[13].

We then performed an *in vitro* cumulus expansion assay to better understand the cumulus behavior of each mutant model. Because cumulus oophorus cells do not respond to LH *in vitro*[9], we used FSH treatment to induce a regular cumulus expansion in our control group. Surprisingly, some degree of expansion was observed in the $Nr5a2^{Amhr2-/-}$, an event that was not detected *in vivo*[8]. For the $Nr5a2^{Cyp19-/-}$ COCs, expansion was occurring but not in a normal degree. We conclude that the lack of Nr5a2 in mural granulosa cells of the $Nr5a2^{Amhr2-/-}$ ovaries is affecting cumulus expansion *in vivo*. The persistent expression of Nr5a2 in cumulus cells of the $Nr5a2^{Cyp19-/-}$ ovaries is not sufficient to promote full expansion, indicating that the expression of Nr5a2 in mural granulosa cells of antral follicles is essential for the cumulus cells to acquire the competence to expand.

Taking into account that the two mouse models have a different pattern of cumulus expansion *in vivo*, and that both underwent a morphologically deficient expansion *in vitro*, we performed analysis to determine the cumulus expansion-related genes that are disrupted by depletion of Nr5a2. The EGF-like factors, *Areg*, *Ereg* and *Btc* are shown for the first time to be disrupted following deletion of Nr5a2 in granulosa cells of preantral and antral follicles. These genes are also disrupted in the progesterone receptor knockout (PRKO) mouse, which presents a phenotype of cumulus expansion without ovulation[15]. The expression of *Tnaifp6*, involved in the prostaglandin pathway, is also downregulated in both mutants. The regulation of these genes by Nr5a2 may impact the functional aspects of cumulus expansion that lead to ovulation.

Before an ovulatory stimulus, i.e., an endogenous LH surge or hCG administration, an extensive gap junction network links the cumulus cells to one another and to the

developing oocyte[3]. Connexin 43 (Gja1) is suggested to be involved in follicle development and oocyte growth, and the amount of Gja1 in the large antral follicles is relatively elevated in a stage of high serum concentrations of FSH or eCG[11]. The preovulatory surge of LH interrupts cell-to-cell communication in the follicle, and consequently a decline in the level of *Gja1* may suggest a specific function of Gja1 for ovulation as well as for the early luteal phase in processes of angiogenesis and luteal cell differentiation[1]. A preliminary unpublished (Duggavathi, 2008) electron microscopy study revealed that the mural granulosa cells of preovulatory follicles in $Nr5a2^{Amhr2-/-}$ knockout mice display an apparent reduction in normal cell-cell contacts.

In our study, Gja1 expression in ovarian granulosa cells of the $Nr5a2^{Amhr2-/-}$ knockout group was downregulated at 0 h post hCG. After exposure to circulating ovulatory gonadotropins, the majority of the gap junctions are endocytosed, the oocyte resumes meiosis, and components of the extracellular matrix are deposited between the cumulus cells[5], resulting in cumulus expansion. At 8 h post hCG, Gja1 was shown to remain upregulated in granulosa cells of $Nr5a2^{Amhr2-/-}$, which could be an effect of impaired post-translational modification. The LH-induced reinitiation of meiosis involves the breakdown of communication between the oocyte and the somatic-cell compartment[7], and the high levels of Gja1 by the time of ovulation found in our study may be an explanation for the lack of cumulus expansion in the $Nr5a2^{Amhr2-/-}$ mice.

Cumulus cells create a microenvironment conducive to oocyte growth and development and that is necessary for ovulation and fertilization[3]. Successful fertilization is correlated with the quantity and the quality of the expanded cumulus mass. Optimal expansion of the cumulus mass appears to be essential for oocyte cytoplasmic maturation[4]. Interestingly, although granulosa and cumulus cells present a deficient morphological and

functional pattern in your Nr5a2$^{Amhr2-/-}$ and Nr5a2$^{Cyp19-/-}$ mice, the oocytes were fertilizable for both mutant models. Another indication that the oocytes are not involved in the infertility phenotype of these females is that co-culture of WT oocytes with the mutant COCs was unable to rescue cumulus expansion.

We conclude that Nr5a2 regulates cumulus expansion in a temporal and spatial manner in ovarian follicles, and that the disruption of this gene in granulosa cells does not affect the fertilizability of the germ cells.

3.6. Supplemental material

TABLE III : List of primers used in these studies for both genotyping and qPCR. All primers are 5' to 3'.

Primer	Forward	Reverse
Genotyping		
Nr5a2-flox	GCTATAGGGAGTCAGGATACCATGG	GTTCGTACCACTTTCATCTCCTCACG
Cyp19a1-Cre	ACTTGGTCAAAGTCAGTGCG	CCTGGTGCAAGCTGAACAAC
Amhr2-Cre	GAACCTGATGGACATGTTCAGG	AGTGCGTTCGAACGCTAGAGCCTGT
qPCR		
RPS18	GTGGTGTTGAGGAAAGCAGACA	TGATCACACGTTCCACCTCATC
Areg	CATCGGCATCGTTATCACAG	TGTCGAAGCCTCCTTCTTTC
Ereg	CCATCATGCATCCCAGGAGAA	TAGCCGTCCATGTCAGAACTACACT
Btc	AACTGCACAGGTACCACCCCTAGA	ACAGATGCAGGAGGGAGTTTGC
Tnfaip6	TGAAGGTGGTCGTCTCGCAACC	TCCACAGTTGGGCCCAGGTTTCA

Acknowledgements

The authors thank Mira Dobias Goff, Fanny Morin and Vickie Roussel for technical assistance. Dr. Jane Fenelon and Sandra Ruiz for aid with the ICSI performance; and Dr. Richard Behringer for the Amhr2$^{Cre/+}$ mouse line. This study was funded by an operating

grant from the Canadian Institutes of Health Research (FRN11018) to BDM. Kalyne Bertolin was supported by the Fonds québécois de la recherche sur la nature et les technologies (FQRNT) – Merit Scholarship Program for Foreign Students (PBEEE).

References

1. Berisha B, Bridger P, Toth A *et al.* (2009) Expression and localization of gap junctional connexins 26 and 43 in bovine periovulatory follicles and in corpus luteum during different functional stages of oestrous cycle and pregnancy. *Reprod Domest Anim* **44**, 295-302.

2. Bertolin K, Gossen J, Schoonjans K *et al.* The orphan nuclear receptor Nr5a2 in essential for luteinization in the female mouse ovary.

3. Botrugno OA, Fayard E, Annicotte JS *et al.* (2004) Synergy between LRH-1 and beta-catenin induces G1 cyclin-mediated cell proliferation. *Mol Cell* **15**, 499-509.

4. Brower PT & Schultz RM (1982) Intercellular communication between granulosa cells and mouse oocytes: existence and possible nutritional role during oocyte growth. *Dev Biol* **90**, 144-153.

5. Camaioni A, Hascall VC, Yanagishita M *et al.* (1993) Effects of exogenous hyaluronic acid and serum on matrix organization and stability in the mouse cumulus cell-oocyte complex. *J Biol Chem* **268**, 20473-20481.

6. Channing CP, Schaerf FW, Anderson LD *et al.* (1980) Ovarian follicular and luteal physiology. *Int Rev Physiol* **22**, 117-201.

7. Chen L, Russell PT & Larsen WJ (1993) Functional significance of cumulus expansion in the mouse: roles for the preovulatory synthesis of hyaluronic acid within the cumulus mass. *Mol Reprod Dev* **34**, 87-93.

8. Chen L, Russell PT & Larsen WJ (1994) Sequential effects of follicle-stimulating hormone and luteinizing hormone on mouse cumulus expansion in vitro. *Biol Reprod* **51**, 290-295.

9. Chen L, Wert SE, Hendrix EM *et al.* (1990) Hyaluronic acid synthesis and gap junction endocytosis are necessary for normal expansion of the cumulus mass. *Mol Reprod Dev* **26**, 236-247.

10. Davis BJ, Lennard DE, Lee CA *et al.* (1999) Anovulation in cyclooxygenase-2-deficient mice is restored by prostaglandin E2 and interleukin-1beta. *Endocrinology* **140**, 2685-2695.

11. Dekel N, Lawrence TS, Gilula NB *et al.* (1981) Modulation of cell-to-cell communication in the cumulus-oocyte complex and the regulation of oocyte maturation by LH. *Dev Biol* **86**, 356-362.

12. Dell'Aquila ME, Caillaud M, Maritato F *et al.* (2004) Cumulus expansion, nuclear maturation and connexin 43, cyclooxygenase-2 and FSH receptor mRNA expression in equine cumulus-oocyte complexes cultured in vitro in the presence of FSH and precursors for hyaluronic acid synthesis. *Reprod Biol Endocrinol* **2**, 44.

13. Diaz FJ, O'Brien MJ, Wigglesworth K *et al.* (2006) The preantral granulosa cell to cumulus cell transition in the mouse ovary: development of competence to undergo expansion. *Dev Biol* **299**, 91-104.

14. Duggavathi R, Volle DH, Mataki C *et al.* (2008) Liver receptor homolog 1 is essential for ovulation. *Genes & Development* **22**, 1871-1876.

15. Elvin JA, Clark AT, Wang P *et al.* (1999) Paracrine actions of growth differentiation factor-9 in the mammalian ovary. *Mol Endocrinol* **13**, 1035-1048.

16. Eppig JJ (1980) Regulation of Cumulus Oophorus Expansion by Gonadotropins in vivo and in vitro. *Biology of Reproduction* **23**, 545-552.

17. Eppig JJ (1991) Intercommunication between mammalian oocytes and companion somatic cells. *Bioessays* **13**, 569-574.

18. Espey LL & Richards JS (2002) Temporal and spatial patterns of ovarian gene transcription following an ovulatory dose of gonadotropin in the rat. *Biol Reprod* **67**, 1662-1670.

19. Espey LL & Richards JS (2006) Ovulation. *Knobil and Neilsl's - Physiology of Reproduction* **1**, 425-474.

20. Fan HY, Shimada M, Liu Z *et al.* (2008) Selective expression of KrasG12D in granulosa cells of the mouse ovary causes defects in follicle development and ovulation. *Development* **135**, 2127-2137.

21. Fowler RE & Edwards RG (1957) Induction of superovulation and pregnancy in mature mice by gonadotrophins. *J Endocrinol* **15**, 374-384.

22. Granot I & Dekel N (1997) Developmental expression and regulation of the gap junction protein and transcript in rat ovaries. *Mol Reprod Dev* **47**, 231-239.

23. Hinshelwood MM, Repa JJ, Shelton JM *et al.* (2003) Expression of LRH-1 and SF-1 in the mouse ovary: localization in different cell types correlates with differing function *Molecular and Cellular Endocrinology* **207**.

24. Jorgez CJ, Lin Y-N & Matzuk MM (2005) Genetic manipulations to study reproduction. *Molecular and Cellular Endocrinology* **234**, 127-135.

25. Murphy BD (2012) Equine chorionic gonadotropin: an enigmatic but essential tool *Anim Reprod* **9**, 223-230.

26. Park JY, Su YQ, Ariga M *et al.* (2004) EGF-like growth factors as mediators of LH action in the ovulatory follicle. *Science* **303**, 682-684.

27. Pedersen T & Peters H (1968) Proposal for a classification of oocytes and follicles in the mouse ovary. *J Reprod Fertil* **17**, 555-557.

28. Pfaffl MW (2001) A new mathematical model for relative quantification in real-time RT-PCR. *Nucleic Acids Res* **29**, e45.

29. Richards JS (1980) Maturation of ovarian follicles: actions and interactions of pituitary and ovarian hormones on follicular cell differentiation. *Physiol Rev* **60**, 51-89.

30. Robker RL, Russell DL, Espey LL *et al.* (2000) Progesterone-regulated genes in the ovulation process: ADAMTS-1 and cathepsin L proteases. *Proc Natl Acad Sci U S A* **97**, 4689-4694.

31. Russell DL & Robker RL (2007) Molecular mechanisms of ovulation: co-ordination through the cumulus complex. *Human Reproduction Update* **13**, 289-312.

32. Sirois J, Sayasith K, Brown KA *et al.* (2004) Cyclooxygenase-2 and its role in ovulation: a 2004 account. *Hum Reprod Update* **10**, 373-385.

33. Snell GD, Fekete E, Hummel KP *et al.* The relation of mating, ovulation and the estrous smear in the house mouse to time of day. *The Anatomical Record* **76**.

34. Stocco C (2008) Aromatase expression in the ovary: hormonal and molecular regulation. *Steroids* **73**, 473-487.

35. Sun Q-Y, Liu K & Kikuchi K (2008) Oocyte-Specific Knockout: A Novel In Vivo Approach for Studying Gene Functions During Folliculogenesis, Oocyte Maturation, Fertilization, and Embryogenesis. *Biology of Reproduction* **79**, 1014-1020.

36. Teilmann SC (2005) Differential expression and localisation of connexin-37 and connexin-43 in follicles of different stages in the 4-week-old mouse ovary. *Mol Cell Endocrinol* **234**, 27-35.

37. Yan J, Suzuki J, Yu XM *et al.* (2011) Effects of duration of cryo-storage of mouse oocytes on cryo-survival, fertilization and embryonic development following vitrification. *J Assist Reprod Genet* **28**, 643-649.

Chapter 4

4. Discussion

Infertility in humans is a major health issue, with significant medical, physiological and economic aspects. According to the World Health Organization (WHO), infertility is defined as a failure to achieve a clinical pregnancy after 1 year or more of regular unprotected sexual intercourse by women of reproductive age[134]. Female factor is the main source of infertility, accounting for at least 37% of the cases in which a couple does not succeed in procreating. Among the causes of female infertility, ovulatory disorders lead the ranking (25% of the cases) while the most common female factors are endometriosis (15%), pelvic adhesions (12%), tubal abnormalities (22%) and hyperprolactinemia (7%)[125].

In 2010, demographic and reproductive surveys available worldwide estimated the infertility prevalence and trends from 1990 and 2010. Interestingly, despite the medical advances that are ever improving, infertility rates have hardly changed over the past 20 years[72]. It was in 2008 when the nuclear receptor Nr5a2 has become known as the key regulator of ovulation and female fertility[25]. Our investigation is part of a basic research project toward increasing fundamental knowledge about the role of Nr5a2 in the ovary, aiming to provide the basis for understanding the female infertility associated with the ovulatory process.

Nr5a2 was first described in the *Drosophila* (named Ftz-F1)[116], next related to the mouse (Lrh-1)[117] and human livers (hB1F)[68], and also shown to be involved in the regulation of a fetoprotein (FTF)[36]. In Chapter 1 of this thesis, the basis of different nomenclature for the nuclear receptor Nr5a2 was chronicled and shown to be due to its multifunctional distribution in the organisms of different species. Further, it is classified as

an orphan nuclear receptor and the unifying nomenclature, officially naming it Nr5a2, occurred 10 years after its discovery[23].

The truth is that in combination with these factors implicated in the plethora of names, the access to public information was more restricted in the 90's[45]. The integrative computer and web-based compiling of data became an essential tool for scientific communication. One well-known available scientific data bank is the National Center for Biotechnology Information (NCBI), launching the digital archive PubMed Central in 2001, providing access to biomedical and genomic information to accelerate the exchange of knowledge. By adopting the official gene name Nr5a2 in this thesis, we supported the idea of unifying the nomenclature to make this information approachable for other research outside as well as within the field.

The motivation for studying the role of Nr5a2, in most of the cases, was a consequence of the available knowledge for its homolog nuclear receptor, Nr5a1. In 1997, Nr5a1 was already known to be a key determinant of the endocrine function, supported by *in vivo* data[89]. Indeed, Nr5a2 was commonly expected to be important in the steroidogenic-related events in which Nr5a1 was absent or inactive. These hypotheses were true for the role of Nr5a2 in the breast adipose tissue in regulating aromatase[22], and for its role in regulating gonadal steroidogenesis[91], for instance. Nr5a2 deficiency in the ovary is not compensated by the expression of Nr5a1, ensuring the key function of Nr5a2 in ovulation and ovarian steroidogenesis[25].

In general, *in vitro* studies are a conventional system to originate new insights in experimental biology. They permit a detailed and convenient analysis, substantially faster and with fewer ethical concerns than the *in vivo* studies. *In vitro* experiments are regularly

chosen as the first step for unexplored fields. However, the *in vivo* verification is necessary to confirm the translation of the *in vitro* data. For Nr5a2, *in vitro* data showed the importance of its transcriptional regulation of Cyp7a1 in bile acid biosynthesis[30]. Even more, Cyp7a promoter-binding factor is one of the first names given to Nr5a2[83]. Surprisingly, by the use of targeted somatic mutagenesis, *in vivo* data showed that Nr5a2 might not be important or plays a minor role for Cyp7a1 expression[73]. Another example of a discrepancy between the *in vitro* and *in vivo* data is the regulation of LHβ and FSHβ transcription by Nr5a2 in gonadotrope-like cells *in vitro*. In this matter, Nr5a2 was recently shown to be dispensable for gonadotropin synthesis and fertility *in vivo*[35].

Supporting the importance of an *in vivo* extrapolation of the *in vitro* acquired knowledge, we employed our $Nr5a2^{Cyp19\text{-}/\text{-}}$ mouse model to study the role of Nr5a2 in luteinization. It was previously shown that Nr5a2 enhances the activity of Star, Cyp11a1, Cyp17a1, Hsd3β[107], Scarb1[104] and Cyp19a1[75] *in vitro*. Our data, as shown in the Chapter 2, corroborate the *in vitro* information and demonstrate that the nuclear receptor Nr5a2 is essential for the formation of a morphologically and functionally normal corpus luteum.

The transgenic mouse model used in our study takes advantage of the well-established Cre-*loxP* system. This system overcomes the problem encountered in the transgenic null-mice when the gene in evidence is important for development, causing embryonic lethality, well known to occur following germline deletion of Nr5a2[88]. Through insertion of *loxP* sites into a gene of interest and by targeting the Cre-recombinase expression to a specific cell type using a tissue-specific promoter, it is possible to delete a specific portion of DNA in a specific location, such as a tissue or a cell type[62]. The transgenic mouse line expressing the Cre-recombinase is guided by a promoter with a

desired temporal and/or spatial pattern[111]. After intercrossing to produce double transgenic offspring, the recombinase may delete or modify the conditional allele in expressing cells, while the unrecombined target gene remains intact and functional in the cells of other tissues where the recombinase is not expressed[50]. In our studies, we took advantage of the unrecombined target gene, by the absence of the Cre-recombinase verified by genotyping, to compose our control group.

Our two granulosa-specific knockout models presented a short window of difference between those carrying the Amhr2-Cre (expressed in granulosa cells of primary and growing ovarian follicles)[28] and the Cyp19-Cre (limited only to mural granulosa cells of healthy large antral follicles, preovulatory follicles and luteal cells)[110]. Our data provides the first insight into the role of Nr5a2 in the ovarian function in a time line manner. We compared the $Nr5a2^{Amhr2-/-}$ model, which had already been previously described and was used as the basis of our study, with the $Nr5a2^{Cyp19-/-}$ model, described herein for the first time, presenting an interesting and particular reproductive profile.

These two models are consistent in their lack of ovulation and the competence of the oocytes to be fertilized, but they differ regarding the formation of the luteal-like structures and their ability to undergo cumulus expansion. The studies were conducted in parallel, with both mutant models treated and analyzed in the same conditions, allowing for the comparisons between them. The role of Nr5a2 in cumulus expansion, explored in the Chapter 3, although substantially advanced herein, is not yet fully understood. It would be of interest to perform a next-generation transcriptome sequencing of the ovarian granulosa and cumulus cells to better clarify the regulation of Nr5a2 in cumulus expansion.

Together, our data provide new information on how Nr5a2 regulates peri- and post-ovulatory events in the mouse ovary. It complements the current array of basic research, and provides fundamental insight that may be useful towards an application for Nr5a2, for instance, on the rescue of female fertility or on the possibility of a contraceptive development[52]. To this end, it is important that different areas of research move forward together. The new discoveries on synthetic ligands regulating Nr5a2 benefit the investigations on its biological functions, and provide an opportunity for the treatment of infertility, cancer and metabolic disorders in which Nr5a2 might be involved[61].

The mouse constitutes an important animal model to study reproduction and other processes due to its anatomy, physiology and genetic presenting similarity to humans[11]. Using mouse in this kind of research has advantages like relatively short generation time, post-partum estrus and ability to manipulate its genome[50]. However, significant interspecies differences in gene regulation might exist when comparing mice data to human physiology[30]. Ideally, human ovarian cells should be investigated comparing women with ovulatory disruption with fertile women. Going even further, Nr5a2 is known to be expressed in ovarian cells of most animals as well, so it would be not only important in human fertility, but also in veterinary research.

In the case of human infertility, our mouse data raise a hope. We show, for the very first time, that the oocytes resulting from follicles lacking Nr5a2 in the somatic cells are fertilizable. Assisted reproductive technology (ART) includes fertility treatment for humans in which both female germ cell and male germ cell are manipulated *in vitro*. The resulting embryo is transferred to the woman's uterus for the progress of the pregnancy. The *in vitro* fertilization (IVF) and the intracytoplasmic sperm injection (ICSI) are widely used as ARTs. In IVF, the sperm and the egg are incubated together, and the sperm will penetrate

the egg by itself. In the ICSI, one single sperm is artificially introduced directly inside the oocyte.

If it is shown that the disruption of Nr5a2 in women granulosa cells is related to ovulatory disorders in humans, our mice data would suggest that the ART would be able to overcome the lack of ovulation and embryonic conception. It is important to mention that a pregnancy is dependent on a functional corpus luteum secreting progesterone, and the uterine factors are also essential. Our laboratory has recently shown that uterine functions are regulated by the expression of Nr5a2, mediating embryo implantation and decidualization[135]. Another recent study showed that the infertility caused by the depletion of Nr5a2 is reversible in the mouse[37]. Therefore, it would be of great value to apply and combine the available information to establish the relation between Nr5a2 and human infertility.

With the present study, we hope that the infertility statistics can change. Nr5a2 is a potential target for fertility dysfunctions and contraception. It is possible that, in the next decades, the studies on the fertility rates worldwide will show an improvement in female fertility, and this thesis will have contributed to the field as a fundamental portion of the puzzle.

Conclusion

In conclusion, our study permits an increase in understanding the role of Nr5a2 in female reproduction, with a focus on new information relative to ovarian peri- and post-ovulatory events. Our findings demonstrate that Nr5a2 regulates essential mechanisms of female fertility in granulosa cells during the process of follicular development, in a spatial and temporal manner. We have determined that the lack of functional Nr5a2 in ovarian granulosa cells of antral follicles results in development of non-functional luteal-like structures in the absence of ovulation. We elucidated the morphological and functional process of cumulus expansion regulated by Nr5a2 in preantral and antral follicles. Our data demonstrating the competence of the oocytes have shown that the disruption of Nr5a2 in somatic cells of the follicle does not affect the capacity of the germ cells to be fertilized. In summary, this study has provided new insight into the role of the nuclear receptor Nr5a2 in the ovarian regulation and allowed us to achieve our specific objectives. Moreover, new questions arise, such as: What would be the ovarian phenotype of female mice overexpressing Nr5a2 in granulosa cells? What is the relation between our mouse data and the human ovulatory dysfunctions? Is Nr5a2 involved in the regulation of female ovarian cancer or polycystic ovarian syndrome? This remains a fertile field for investigation of nuclear receptor regulation of ovarian functions.

References

1. Andrieu T, Pezzi V, Sirianni R *et al.* (2009) cAMP-dependent regulation of CYP19 gene in rabbit preovulatory granulosa cells and corpus luteum. *J Steroid Biochem Mol Biol* **116**, 110-117.

2. Annicotte JS, Chavey C, Servant N *et al.* (2005) The nuclear receptor liver receptor homolog-1 is an estrogen receptor target gene. *Oncogene* **24**, 8167-8175.

3. Annicotte JS, Fayard E, Swift GH *et al.* (2003) Pancreatic-duodenal homeobox 1 regulates expression of liver receptor homolog 1 during pancreas development. *Mol Cell Biol* **23**, 6713-6724.

4. Bain DL, Heneghan AF, Connaghan-Jones KD *et al.* (2007) Nuclear receptor structure: implications for function. *Annu Rev Physiol* **69**, 201-220.

5. Beato M & Klug J (2000) Steroid hormone receptors: an update. *Hum Reprod Update* **6**, 225-236.

6. Benod C, Carlsson J, Uthayaruban R *et al.* (2013) Structure-based Discovery of Antagonists of Nuclear Receptor LRH-1. *J Biol Chem* **288**, 19830-19844.

7. Benod C, Vinogradova MV, Jouravel N *et al.* (2011) Nuclear receptor liver receptor homologue 1 (LRH-1) regulates pancreatic cancer cell growth and proliferation. *Proc Natl Acad Sci U S A* **108**, 16927-16931.

8. Bertolin K, Bellefleur AM, Zhang C *et al.* (2010) Orphan nuclear receptor regulation of reproduction. *Anim Reprod* **7**, 146-153.

9. Boerboom D, Pilon N, Behdjani R *et al.* (2000) Expression and regulation of transcripts encoding two members of the NR5A nuclear receptor subfamily of orphan nuclear receptors, steroidogenic factor-1 and NR5A2, in equine ovarian cells during the ovulatory process. *Endocrinology* **141**, 4647-4656.

10. Botrugno OA, Fayard E, Annicotte JS *et al.* (2004) Synergy between LRH-1 and beta-catenin induces G1 cyclin-mediated cell proliferation. *Mol Cell* **15**, 499-509.

11. Brault V, Besson V, Magnol L *et al.* (2007) Cre/loxP-mediated chromosome engineering of the mouse genome. *Handb Exp Pharmacol*, 29-48.

12. Brendel C, Gelman L & Auwerx J (2002) Multiprotein bridging factor-1 (MBF-1) is a cofactor for nuclear receptors that regulate lipid metabolism. *Mol Endocrinol* **16**, 1367-1377.

13. Brosens JJ, Blanks AM & Lucas ES (2013) LRH-1: orphaned, adopted and needed for pregnancy. *Nat Med* **19**, 968-969.

14. Burendahl S, Treuter E & Nilsson L (2008) Molecular Dynamics Simulations of Human LRH-1: The Impact of Ligand Binding in a Constitutively Active Nuclear Receptor. *Biochemistry* **47**, 5205-5215.

15. Busby S, Nuhant P, Cameron M *et al.* (2010) Discovery of Inverse Agonists for the Liver Receptor Homologue-1 (LRH1; NR5A2). In *Probe Reports from the NIH Molecular Libraries Program*. Bethesda (MD).

16. Campbell LA, Faivre EJ, Show MD *et al.* (2008) Decreased recognition of SUMO-sensitive target genes following modification of SF-1 (NR5A1). *Mol Cell Biol* **28**, 7476-7486.

17. Carlberg C & Seuter S (2010) Dynamics of nuclear receptor target gene regulation. *Chromosoma* **119**, 479-484.

18. Chalkiadaki A & Talianidis I (2005) SUMO-dependent compartmentalization in promyelocytic leukemia protein nuclear bodies prevents the access of LRH-1 to chromatin. *Mol Cell Biol* **25**, 5095-5105.

19. Chand AL, Herridge KA, Thompson EW *et al.* (2010) The orphan nuclear receptor LRH-1 promotes breast cancer motility and invasion. *Endocr Relat Cancer* **17**, 965-975.

20. Chand AL, Wijayakumara DD, Knower KC *et al.* (2012) The orphan nuclear receptor LRH-1 and ERalpha activate GREB1 expression to induce breast cancer cell proliferation. *PLoS One* **7**, e31593.

21. Clyne CD, Kovacic A, Speed CJ *et al.* (2004) Regulation of aromatase expression by the nuclear receptor LRH-1 in adipose tissue. *Mol Cell Endocrinol* **215**, 39-44.

22. Clyne CD, Speed CJ, Zhou J *et al.* (2002) Liver receptor homologue-1 (LRH-1) regulates expression of aromatase in preadipocytes. *J Biol Chem* **277**, 20591-20597.

23. Committee NRN (1999) A unified nomenclature system for the nuclear receptor superfamily. *Cell* **97**, 161-163.

24. D'Errico I & Moschetta A (2008) Nuclear receptors, intestinal architecture and colon cancer: an intriguing link. *Cell Mol Life Sci* **65**, 1523-1543.

25. Duggavathi R, Volle DH, Mataki C *et al.* (2008) Liver receptor homolog 1 is essential for ovulation. *Genes & Development* **22**, 1871-1876.

26. Espey LL & Richards JS (2006) Ovulation. *Knobil and Neilsl's - Physiology of Reproduction* **1**, 425-474.

27. Falender AE, Lanz R, Malenfant D *et al.* (2003) Differential expression of steroidogenic factor-1 and FTF/LRH-1 in the rodent ovary. *Endocrinology* **144**, 3598-3610.

28. Fan H-Y & Richards JS (2010) Minireview: Physiological and Pathological Actions of RAS in the Ovary. *Mol Endocrinology* **24**, 286-298.

29. Fayad T, Levesque V, Sirois J *et al.* (2004) Gene expression profiling of differentially expressed genes in granulosa cells of bovine dominant follicles using suppression subtractive hybridization. *Biol Reprod* **70**, 523-533.

30. Fayard E, Auwerx J & Schoonjans K (2004) LRH-1: an orphan nuclear receptor involved in development, metabolism and steroidogenesis. *Trends Cell Biol* **14**, 250-260.

31. Fayard E, Schoonjans K, Annicotte JS *et al.* (2003) Liver receptor homolog 1 controls the expression of carboxyl ester lipase. *J Biol Chem* **278**, 35725-35731.

32. Feige JN & Auwerx J (2007) Transcriptional coregulators in the control of energy homeostasis. *Trends Cell Biol* **17**, 292-301.

33. Fernandez-Marcos PJ, Auwerx J & Schoonjans K (2011) Emerging actions of the nuclear receptor LRH-1 in the gut. *Biochim Biophys Acta* **1812**, 947-955.

34. Forman BM (2005) Are those phospholipids in your pocket? *Cell Metab* **1**, 153-155.

35. Fortin J, Kumar V, Zhou X *et al.* (2013) NR5A2 regulates Lhb and Fshb transcription in gonadotrope-like cells in vitro, but is dispensable for gonadotropin synthesis and fertility in vivo. *PLoS One* **8**, e59058.

36. Galarneau L, Pare JF, Allard D *et al.* (1996) The alpha1-fetoprotein locus is activated by a nuclear receptor of the Drosophila FTZ-F1 family. *Mol Cell Biol* **16**, 3853-3865.

37. Gerrits H, Parade MCBC, Koonen-Reemst AMCB *et al.* (2013) Reversible infertility in a liver receptor homologue-1 (LRH-1)-knockdown mouse model. *Reprod Fertil Dev*.

38. Giguere V (1999) Orphan nuclear receptors: from gene to function. *Endocr Rev* **20**, 689-725.

39. Gu P, Goodwin B, Chung AC *et al.* (2005) Orphan nuclear receptor LRH-1 is required to maintain Oct4 expression at the epiblast stage of embryonic development. *Mol Cell Biol* **25**, 3492-3505.

40. Guo G & Smith A (2010) A genome-wide screen in EpiSCs identifies Nr5a nuclear receptors as potent inducers of ground state pluripotency. *Development* **137**, 3185-3192.

41. Heng JC, Feng B, Han J *et al.* (2010) The nuclear receptor Nr5a2 can replace Oct4 in the reprogramming of murine somatic cells to pluripotent cells. *Cell Stem Cell* **6**, 167-174.

42. Heng JC, Orlov YL & Ng HH (2010) Transcription factors for the modulation of pluripotency and reprogramming. *Cold Spring Harb Symp Quant Biol* **75**, 237-244.

43. Heuvel JPV (2009) Nuclear Receptors: A Brief Overview. *Nuclear Receptor Resource*.

44. Higashiyama H, Kinoshita M & Asano S (2007) Expression profiling of liver receptor homologue 1 (LRH-1) in mouse tissues using tissue microarray. *J Mol Histol* **38**, 45-52.

45. Hilbert M & Lopez P (2011) The world's technological capacity to store, communicate, and compute information. *Science* **332**, 60-65.

46. Hinshelwood MM, Repa JJ, Shelton JM *et al.* (2003) Expression of LRH-1 and SF-1 in the mouse ovary: localization in different cell types correlates with differing function *Molecular and Cellular Endocrinology* **207**.

47. Hinshelwood MM, Shelton JM, Richardson JA *et al.* (2005) Temporal and spatial expression of liver receptor homologue-1 (LRH-1) during embryogenesis suggests a potential role in gonadal development. *Dev Dyn* **234**, 159-168.

48. Hsieh HT, Wang CH, Wu ML *et al.* (2009) PIASy inhibits LRH-1-dependent CYP11A1 expression by competing for SRC-1 binding. *Biochem J* **419**, 201-209.

49. Iyer AK & McCabe ER (2004) Molecular mechanisms of DAX1 action. *Mol Genet Metab* **83**, 60-73.

50. Jorgez CJ, Lin Y-N & Matzuk MM (2005) Genetic manipulations to study reproduction. *Molecular and Cellular Endocrinology* **234**, 127-135.

51. Kanayama T, Arito M, So K *et al.* (2007) Interaction between sterol regulatory element-binding proteins and liver receptor homolog-1 reciprocally suppresses their transcriptional activities. *J Biol Chem* **282**, 10290-10298.

52. Kawabe S, Yazawa T, Kanno M *et al.* (2013) A novel isoform of liver receptor homolog-1 is regulated by steroidogenic factor-1 and the specificity protein family in ovarian granulosa cells. *Endocrinology* **154**, 1648-1660.

53. Kelly VR, Xu B, Kuick R *et al.* (2010) Dax1 up-regulates Oct4 expression in mouse embryonic stem cells via LRH-1 and SRA. *Mol Endocrinol* **24**, 2281-2291.

54. Kir S, Zhang Y, Gerard RD *et al.* (2012) Nuclear receptors HNF4alpha and LRH-1 cooperate in regulating Cyp7a1 in vivo. *J Biol Chem* **287**, 41334-41341.

55. Kliewer SA, Lehmann JM & Willson TM (1999) Orphan nuclear receptors: shifting endocrinology into reverse. *Science* **284**, 757-760.

56. Krylova IN, Sablin EP, Moore J *et al.* (2005) Structural analyses reveal phosphatidyl inositols as ligands for the NR5 orphan receptors SF-1 and LRH-1. *Cell* **120**, 343-355.

57. Labelle-Dumais C, Jacob-Wagner M, Pare JF *et al.* (2006) Nuclear receptor NR5A2 is required for proper primitive streak morphogenesis. *Dev Dyn* **235**, 3359-3369.

58. Labelle-Dumais C, Pare JF, Belanger L *et al.* (2007) Impaired progesterone production in Nr5a2+/- mice leads to a reduction in female reproductive function. *Biol Reprod* **77**, 217-225.

59. Lai WA, Yeh YT, Lee MT *et al.* (2013) Ovarian granulosa cells utilize scavenger receptor SR-BI to evade cellular cholesterol homeostatic control for steroid synthesis. *J Lipid Res* **54**, 365-378.

60. Lala DS, Rice DA & Parker KL (1992) Steroidogenic factor I, a key regulator of steroidogenic enzyme expression, is the mouse homolog of fushi tarazu-factor I. *Mol Endocrinol* **6**, 1249-1258.

61. Lazarus KA, Wijayakumara D, Chand AL *et al.* (2012) Therapeutic potential of Liver Receptor Homolog-1 modulators. *J Steroid Biochem Mol Biol* **130**, 138-146.

62. Lécureuil C, Fontaine I, Crepieux P *et al.* (2002) Sertoli and Granulosa Cell-Specific Cre Recombinase Activity in Transgenic Mice. *Genesis* **33**, 114-118.

63. Lee JM, Lee YK, Mamrosh JL *et al.* (2011) A nuclear-receptor-dependent phosphatidylcholine pathway with antidiabetic effects. *Nature* **474**, 506-510.

64. Lee YK, Choi YH, Chua S *et al.* (2006) Phosphorylation of the hinge domain of the nuclear hormone receptor LRH-1 stimulates transactivation. *J Biol Chem* **281**, 7850-7855.

65. Lee YK & Moore DD (2002) Dual mechanisms for repression of the monomeric orphan receptor liver receptor homologous protein-1 by the orphan small heterodimer partner. *J Biol Chem* **277**, 2463-2467.

66. Lee YK, Schmidt DR, Cummins CL *et al.* (2008) Liver receptor homolog-1 regulates bile acid homeostasis but is not essential for feedback regulation of bile acid synthesis. *Mol Endocrinol* **22**, 1345-1356.

67. Li D & Abbruzzese JL (2010) New strategies in pancreatic cancer: emerging epidemiologic and therapeutic concepts. *Clin Cancer Res* **16**, 4313-4318.

68. Li M, Xie YH, Kong YY *et al.* (1998) Cloning and characterization of a novel human hepatocyte transcription factor, hB1F, which binds and activates enhancer II of hepatitis B virus. *J Biol Chem* **273**, 29022-29031.

69. Li Y, Choi M, Suino K *et al.* (2005) Structural and biochemical basis for selective repression of the orphan nuclear receptor liver receptor homolog 1 by small heterodimer partner. *Proc Natl Acad Sci U S A* **102**, 9505-9510.

70. Liu DL, Liu WZ, Li QL *et al.* (2003) Expression and functional analysis of liver receptor homologue 1 as a potential steroidogenic factor in rat ovary. *Biol Reprod* **69**, 508-517.

71. Luo X, Ikeda Y & Parker KL (1994) A cell-specific nuclear receptor is essential for adrenal and gonadal development and sexual differentiation. *Cell* **77**, 481-490.

72. Mascarenhas MN, Flaxman SR, Boerma T *et al.* (2012) National, regional, and global trends in infertility prevalence since 1990: a systematic analysis of 277 health surveys. *PLoS Med* **9**, e1001356.

73. Mataki C, Magnier BC, Houten SM *et al.* (2007) Compromised intestinal lipid absorption in mice with a liver-specific deficiency of liver receptor homolog 1. *Mol Cell Biol* **27**, 8330-8339.

74. Matzuk MM & Lamb DJ (2008) The biology of infertility: research advances and clinical challenges. *Nature Medicine* **14**, 1197-1213.

75. Mendelson CR, Jiang B, Shelton JM *et al.* (2005) Transcriptional regulation of aromatase in placenta and ovary. *J Steroid Biochem Mol Biol* **95**, 25-33.

76. Miao J, Choi SE, Seok SM *et al.* (2011) Ligand-dependent regulation of the activity of the orphan nuclear receptor, small heterodimer partner (SHP), in the repression of bile acid biosynthetic CYP7A1 and CYP8B1 genes. *Mol Endocrinol* **25**, 1159-1169.

77. Mooijaart SP, Brandt BW, Baldal EA *et al.* (2005) C. elegans DAF-12, Nuclear Hormone Receptors and human longevity and disease at old age. *Ageing Res Rev* **4**, 351-371.

78. Mueller M, Atanasov A, Cima I *et al.* (2007) Differential regulation of glucocorticoid synthesis in murine intestinal epithelial versus adrenocortical cell lines. *Endocrinology* **148**, 1445-1453.

79. Murphy BD (2000) Models of luteinization. *Biol Reprod* **63**, 2-11.

80. Musille PM, Pathak M, Lauer JL *et al.* (2013) Divergent sequence tunes ligand sensitivity in phospholipid-regulated hormone receptors. *J Biol Chem*.

81. Musille PM, Pathak MC, Lauer JL *et al.* (2012) Antidiabetic phospholipid-nuclear receptor complex reveals the mechanism for phospholipid-driven gene regulation. *Nat Struct Mol Biol* **19**, 532-537, S531-532.

82. NCBI (2013) Nr5a2. http://www.ncbi.nlm.nih.gov/gene/2494 **Online**.

83. Nitta M, Ku S, Brown C *et al.* (1999) CPF: an orphan nuclear receptor that regulates liver-specific expression of the human cholesterol 7alpha-hydroxylase gene. *Proc Natl Acad Sci U S A* **96**, 6660-6665.

84. Oakley O, Lin P-C, Bridges P *et al.* (2011) Animal Models for the Study of Polycystic Ovarian Syndrome. *Endocrinol Metab* **26**, 193-202.

85. Ohno M, Komakine J, Suzuki E *et al.* (2010) Repression of the promoter activity mediated by liver receptor homolog-1 through interaction with ku proteins. *Biol Pharm Bull* **33**, 784-791.

86. Olefsky JM (2001) Nuclear receptor minireview series. *J Biol Chem* **276**, 36863-36864.

87. Ortlund EA, Lee Y, Solomon IH *et al.* (2005) Modulation of human nuclear receptor LRH-1 activity by phospholipids and SHP. *Nat Struct Mol Biol* **12**, 357-363.

88. Pare JF, Malenfant D, Courtemanche C *et al.* (2004) The fetoprotein transcription factor (FTF) gene is essential to embryogenesis and cholesterol homeostasis and is regulated by a DR4 element. *J Biol Chem* **279**, 21206-21216.

89. Parker KL & Schimmer BP (1997) Steroidogenic factor 1: a key determinant of endocrine development and function. *Endocr Rev* **18**, 361-377.

90. Pedersen T & Peters H (1968) Proposal for a classification of oocytes and follicles in the mouse ovary. *J Reprod Fertil* **17**, 555-557.

91. Peng N, Kim JW, Rainey WE *et al.* (2003) The role of the orphan nuclear receptor, liver receptor homologue-1, in the regulation of human corpus luteum 3beta-hydroxysteroid dehydrogenase type II. *J Clin Endocrinol Metab* **88**, 6020-6028.

92. Petersen GM, Amundadottir L, Fuchs CS *et al.* (2010) A genome-wide association study identifies pancreatic cancer susceptibility loci on chromosomes 13q22.1, 1q32.1 and 5p15.33. *Nat Genet* **42**, 224-228.

93. Pezzi V, Sirianni R, Chimento A *et al.* (2004) Differential expression of steroidogenic factor-1/adrenal 4 binding protein and liver receptor homolog-1 (LRH-

1)/fetoprotein transcription factor in the rat testis: LRH-1 as a potential regulator of testicular aromatase expression. *Endocrinology* **145**, 2186-2196.

94. Privalsky ML (2003) Activation incarnate. *Dev Cell* **5**, 1-2.

95. Qin J, Gao DM, Jiang QF *et al.* (2004) Prospero-related homeobox (Prox1) is a corepressor of human liver receptor homolog-1 and suppresses the transcription of the cholesterol 7-alpha-hydroxylase gene. *Mol Endocrinol* **18**, 2424-2439.

96. Riancho JA, Liu Y, Sainz J *et al.* (2012) Nuclear receptor NR5A2 and bone: gene expression and association with bone mineral density. *Eur J Endocrinol* **166**, 69-75.

97. Richards JS, Russell DL, Ochsner S *et al.* (2002) Ovulation: new dimensions and new regulators of the inflammatory-like response. *Annu Rev Physiol* **64**, 69-92.

98. Sablin EP, Krylova IN, Fletterick RJ *et al.* (2003) Structural basis for ligand-independent activation of the orphan nuclear receptor LRH-1. *Mol Cell* **11**, 1575-1585.

99. Sablin EP, Woods A, Krylova IN *et al.* (2008) The structure of corepressor Dax-1 bound to its target nuclear receptor LRH-1. *Proc Natl Acad Sci U S A* **105**, 18390-18395.

100. Sadovsky Y & Crawford PA (1998) Developmental and physiologic roles of the nuclear receptor steroidogenic factor-1 in the reproductive system. *J Soc Gynecol Investig* **5**, 6-12.

101. Saevarsdottir D (2008) Two state model CB1 antagonists. *Available online:* http://commons.wikimedia.org/wiki *File:Two_state_model_CB1_antagonists.png*.

102. Safi R, Kovacic A, Gaillard S *et al.* (2005) Coactivation of liver receptor homologue-1 by peroxisome proliferator-activated receptor gamma coactivator-1alpha on

aromatase promoter II and its inhibition by activated retinoid X receptor suggest a novel target for breast-specific antiestrogen therapy. *Cancer Res* **65**, 11762-11770.

103. Saxena D, Safi R, Little-Ihrig L *et al.* (2004) Liver receptor homolog-1 stimulates the progesterone biosynthetic pathway during follicle-stimulating hormone-induced granulosa cell differentiation. *Endocrinology* **145**, 3821-3829.

104. Schoonjans K, Annicotte JS, Huby T *et al.* (2002) Liver receptor homolog 1 controls the expression of the scavenger receptor class B type I. *EMBO Rep* **3**, 1181-1187.

105. Schoonjans K, Dubuquoy L, Mebis J *et al.* (2005) Liver receptor homolog 1 contributes to intestinal tumor formation through effects on cell cycle and inflammation. *Proc Natl Acad Sci U S A* **102**, 2058-2062.

106. Sierens J, Jakody I, Poobalan Y *et al.* (2010) Localization and regulation of aromatase liver receptor homologue-1 in the developing rat testis. *Mol Cell Endocrinol* **323**, 307-313.

107. Sirianni R, Seely JB, Attia G *et al.* (2002) Liver receptor homologue-1 is expressed in human steroidogenic tissues and activates transcription of genes encoding steroidogenic enzymes. *J Endocrinol* **174**, R13-17.

108. Sladek FM (2010) What are nuclear receptor ligands? *Mol Cell Endocrinol*.

109. Steffensen KR, Holter E, Bavner A *et al.* (2004) Functional conservation of interactions between a homeodomain cofactor and a mammalian FTZ-F1 homologue. *EMBO Rep* **5**, 613-619.

110. Stocco C (2008) Aromatase expression in the ovary: hormonal and molecular regulation. *Steroids* **73**, 473-487.

111. Sun Q-Y, Liu K & Kikuchi K (2008) Oocyte-Specific Knockout: A Novel In Vivo Approach for Studying Gene Functions During Folliculogenesis, Oocyte Maturation, Fertilization, and Embryogenesis. *Biology of Reproduction* **79**, 1014-1020.

112. Suzuki T, Kasahara M, Yoshioka H *et al.* (2003) LXXLL-related motifs in Dax-1 have target specificity for the orphan nuclear receptors Ad4BP/SF-1 and LRH-1. *Mol Cell Biol* **23**, 238-249.

113. Taniguchi H, Komiyama J, Viger RS *et al.* (2009) The expression of the nuclear receptors NR5A1 and NR5A2 and transcription factor GATA6 correlates with steroidogenic gene expression in the bovine corpus luteum. *Mol Reprod Dev* **76**, 873-880.

114. Tsai MY, Lan KC, Huang KE *et al.* (2003) Significance of mRNA levels of connexin37, connexin43, and connexin45 in luteinized granulosa cells of controlled hyperstimulated follicles. *Fertil Steril* **80**, 1437-1443.

115. Tugwood JD, Issemann I & Green S (1991) Liver receptor homologues protein. *GenBank DNA database accession number M813985.*

116. Ueda H, Sonoda S, Brown JL *et al.* (1990) A sequence-specific DNA-binding protein that activates fushi tarazu segmentation gene expression. *Genes Dev* **4**, 624-635.

117. Ueda H, Sun GC, Murata T *et al.* (1992) A novel DNA-binding motif abuts the zinc finger domain of insect nuclear hormone receptor FTZ-F1 and mouse embryonal long terminal repeat-binding protein. *Mol Cell Biol* **12**, 5667-5672.

118. Venteclef N, Smith JC, Goodwin B *et al.* (2006) Liver receptor homolog 1 is a negative regulator of the hepatic acute-phase response. *Mol Cell Biol* **26**, 6799-6807.

119. Volle DH, Duggavathi R, Magnier BC *et al.* (2007) The small heterodimer partner is a gonadal gatekeeper of sexual maturation in male mice. *Genes Dev* **21**, 303-315.

120. von Figura G, Morris JPt, Wright CV *et al.* (2013) Nr5a2 maintains acinar cell differentiation and constrains oncogenic Kras-mediated pancreatic neoplastic initiation. *Gut*.

121. Wagner RT, Xu X, Yi F *et al.* (2010) Canonical Wnt/beta-catenin regulation of liver receptor homolog-1 mediates pluripotency gene expression. *Stem Cells* **28**, 1794-1804.

122. Wang ZN, Bassett M & Rainey WE (2001) Liver receptor homologue-1 is expressed in the adrenal and can regulate transcription of 11 beta-hydroxylase. *J Mol Endocrinol* **27**, 255-258.

123. Whitby RJ, Dixon S, Maloney PR *et al.* (2006) Identification of small molecule agonists of the orphan nuclear receptors liver receptor homolog-1 and steroidogenic factor-1. *J Med Chem* **49**, 6652-6655.

124. Whitby RJ, Stec J, Blind RD *et al.* (2011) Small molecule agonists of the orphan nuclear receptors steroidogenic factor-1 (SF-1, NR5A1) and liver receptor homologue-1 (LRH-1, NR5A2). *J Med Chem* **54**, 2266-2281.

125. WHO SG (1992) Recent advances in medically assisted conception. Report of a WHO Scientific Group. *World Health Organ Tech Rep Ser* **820**, 1-111.

126. Xu PL, Kong YY, Xie YH *et al.* (2003) Corepressor SMRT specifically represses the transcriptional activity of orphan nuclear receptor hB1F/hLRH-1. *Sheng Wu Hua Xue Yu Sheng Wu Wu Li Xue Bao (Shanghai)* **35**, 897-903.

127. Xu PL, Liu YQ, Shan SF *et al.* (2004) Molecular mechanism for the potentiation of the transcriptional activity of human liver receptor homolog 1 by steroid receptor coactivator-1. *Mol Endocrinol* **18**, 1887-1905.

128. Xu PL, Shan SF, Kong YY *et al.* (2003) Characterization of a strong repression domain in the hinge region of orphan nuclear receptor hB1F/hLRH-1. *Sheng Wu Hua Xue Yu Sheng Wu Wu Li Xue Bao (Shanghai)* **35**, 909-916.

129. Yang FM, Lin YC & Hu MC (2011) Identification of two functional nuclear localization signals mediating nuclear import of liver receptor homologue-1. *Cell Mol Life Sci* **68**, 1241-1253.

130. Yang FM, Pan CT, Tsai HM *et al.* (2009) Liver receptor homolog-1 localization in the nuclear body is regulated by sumoylation and cAMP signaling in rat granulosa cells. *FEBS J* **276**, 425-436.

131. Yazawa T, Inanoka Y, Mizutani T *et al.* (2009) Liver receptor homolog-1 regulates the transcription of steroidogenic enzymes and induces the differentiation of mesenchymal stem cells into steroidogenic cells. *Endocrinology* **150**, 3885-3893.

132. Yazawa T, Inaoka Y, Okada R *et al.* (2010) PPAR-gamma coactivator-1alpha regulates progesterone production in ovarian granulosa cells with SF-1 and LRH-1. *Mol Endocrinol* **24**, 485-496.

133. Yumoto F, Nguyen P, Sablin EP *et al.* (2012) Structural basis of coactivation of liver receptor homolog-1 by beta-catenin. *Proc Natl Acad Sci U S A* **109**, 143-148.

134. Zegers-Hochschild F, Adamson GD, de Mouzon J *et al.* (2009) The International Committee for Monitoring Assisted Reproductive Technology (ICMART) and the World

Health Organization (WHO) Revised Glossary on ART Terminology, 2009. *Hum Reprod* **24**, 2683-2687.

135. Zhang C, Large MJ, Duggavathi R *et al.* (2013) Liver receptor homolog-1 is essential for pregnancy. *Nat Med* **19**, 1061-1066.

136. Zhang CK, Lin W, Cai YN *et al.* (2001) Characterization of the genomic structure and tissue-specific promoter of the human nuclear receptor NR5A2 (hB1F) gene. *Gene* **273**, 239-249.

137. Zhang T, Zhou JH, Shi LW *et al.* (2008) Molecular dynamics simulation study for LRH-1: interaction with fragments of SHP and function of phospholipid ligand. *Proteins* **70**, 1527-1539.

138. Zhang Z, Burch PE, Cooney AJ *et al.* (2004) Genomic analysis of the nuclear receptor family: new insights into structure, regulation, and evolution from the rat genome. *Genome Res* **14**, 580-590.

139. Zhao GQ & Garbers DL (2002) Male germ cell specification and differentiation. *Dev Cell* **2**, 537-547.

140. Zheng W, Jimenez-Linan M, Rubin BS *et al.* (2007) Anterior pituitary gene expression with reproductive aging in the female rat. *Biol Reprod* **76**, 1091-1102.

141. Zhou J, Suzuki T, Kovacic A *et al.* (2005) Interactions between prostaglandin E(2), liver receptor homologue-1, and aromatase in breast cancer. *Cancer Res* **65**, 657-663.

142. Espey LL (1980) Ovulation as an inflammatory reaction - a hypothesis. *Biol Reprod* **22**, 73-106.

143. Richards JS (1994) Hormonal control of gene expression in the ovary. *Endocr Rev* **15**, 725-751.

144. Russell DL & Robker RL (2007) Molecular mechanisms of ovulation: coordination through the cumulus complex. *Human Reproduction Update* **13**, 289-312.

Chapter 5

5. Appendix

5.1. Reproductive tract changes during the mouse estrous cycle

Kalyne Bertolin[1] and Bruce D. Murphy[1,2]

Affiliations: [1]Animal Reproduction Research Centre (CRRA), University of Montreal, Saint-Hyacinthe, Quebec, Canada; [2]Corresponding author

Book chapter for "The Guide to Investigation of Mouse Pregnancy". ACADEMIC PRESS/ELSEVIER; Chapter 6: Part II: Basic Biology: Part A Estrus, Early Development, Implantation and Uterine Receptivity: IIA-1. Reproductive tract changes over the estrous cycle, December 2013 (IN PRESS).

Author contributions: My contribution involved designing the experiments; manipulation of animals and samples; preparation of the figures and writing of the text. BDM supervised the work and contributed to the writing task.

5.1.1. Summary

The laboratory mouse is an essential model for investigation of normal mammalian physiology, dysfunction and disease. Under conditions of long photoperiod, mice breed continuously throughout the year. In unbred mice, the estrous cycle is a continuum of approximately four days in length, characterized by hormonal variation and consequent morphological and physiological changes to the reproductive tract. Four stages of varying duration are recognized. Proestrus is the period during which pre- and peri-ovulatory development take place in the ovary, with consequent synthesis and secretion of estrogens. Estrus, the brief interval during which the female accepts the male and during which ovulation occurs, follows. Next is metestrus, the early luteal phase, followed by diestrus, during which progesterone is the dominant hormonal influence. Two cell types, polymorphonuclear leukocytes and squamous epithelial cells predominate in the exfoliative cytology of mouse vagina. Stages of the estrous cycle can be identified from the assemblage of these cells. In this chapter, the continuum of morphological changes in the reproductive tract and in vaginal cytology are documented to provide tools for reproductive management of a mouse colony.

Key words: estrous cycle, mouse, smears, vagina, ovaries, uterus

5.1.2. Introduction

The laboratory mouse (order *Rodentia*, family *Muridae*, genus *Mus*, species *musculus*) has a long history of use as a model for the investigation of reproductive events, for a number of reasons beyond its small size and inherent fecundity. Mice are polyestrual mammals, they spontaneously ovulate and the intervals between parturitions are short, requiring approximately 21 days. A further particularity in the mouse that render this species propitious for the studies in reproduction is the short length of its estrous cycle, which lasts only 4 to 5 days. The mouse estrous cycle is an iterative event manifested in changes in the anatomy, endocrinology, physiology and behavior, all coordinated to provide the maximum fecundity.

The synchrony of the hypothalamus-pituitary-gonadal axis is crucial for the rhythm of the cycle and for the success in reproduction. While the estrous cycle is continuous, discrete phases can be identified, proestrus, estrus, metestrus and diestrus. Specific hormones drive the changes that occur during each phase of the cycle and induce the transformations in the mouse anatomy. These variations render identification of individual phase possible by examination of the vaginal appearance and of exfoliated vaginal cells. The pioneer studies that revealed the elements of the mouse estrous cycle were published approximately 100 years ago, signaling the initial steps in a research journey that has allowed achievement of the current extensive understanding of animal reproduction.

The dynamic nature of this complex of cyclic physiological changes continues to intrigue researchers. Advancements, combining modern technology with traditional studies, have allowed the establishment of mouse strains that predictably develop cancers, obesity, neural dysfunction and other disorders. These models have been highly useful in

establishing the bases for human and animal disease. In addition, the mouse has been a robust model for transgenic investigation. Microinjection technology has been used to insert transgenes, and the development of homologous recombination in embryonic stem cells allowed for the production of chimeric mice. These methods permit the null mutation, overexpression and tissue and cell type targeted modifications of the mouse genome, providing powerful tools for the exploration of gene function in whole animal models. Immunodeficient mice, of which there are several strains, have served another important experimental purpose, as recipients of xenografts to explore development of cells and tissues, as recipients of embryos, and for development of pharmacological approaches to address disease states. Technology to exploit the mouse as an experimental model is evolving rapidly, with new approaches, such as incorporation of transgenes into spermatogonial stem cells[28], then transplanted to the testis, use of viral vectors to insert mutated sequences and use of specifically designed nucleases to transmit transgenes[33].

The enormous contribution that the mouse has made to understanding of mammalian biology required the establishment of accurate and reliable criteria for evaluating reproductive function. The purpose of this chapter is to illustrate the reproductive phenomena of the estrous cycle of the normal or wild type mouse as a guide, not only to successful propagation of mouse colonies, but also to investigation of the fascinating story of mammalian reproduction. Decades of mouse breeding in numerous laboratories and institutes have resulted in multiple strains of mice, with the consequence of some variation in reproductive events. In this chapter we will focus on a general view of the mouse estrous cycle, rather than focus on individual peculiarities or comparisons between different strains.

5.1.3. Female mouse reproductive tract anatomy

5.1.3.1. Macroanatomy

The laboratory mouse, as a murine rodent, displays the typical bilateral reproductive morphology that characterizes mammalian vertebrates. The ovaries are found in a subrenal fat pad and the bicornuate uterus (Figure 5.1, bottom panels) is confluent with the external vaginal opening (Figure 5.1, top panels). The ovarian blood supply originates from the ovarian arteries that branch from the descending aorta. The uterus is supplied by the uterine branch of the ovarian artery.

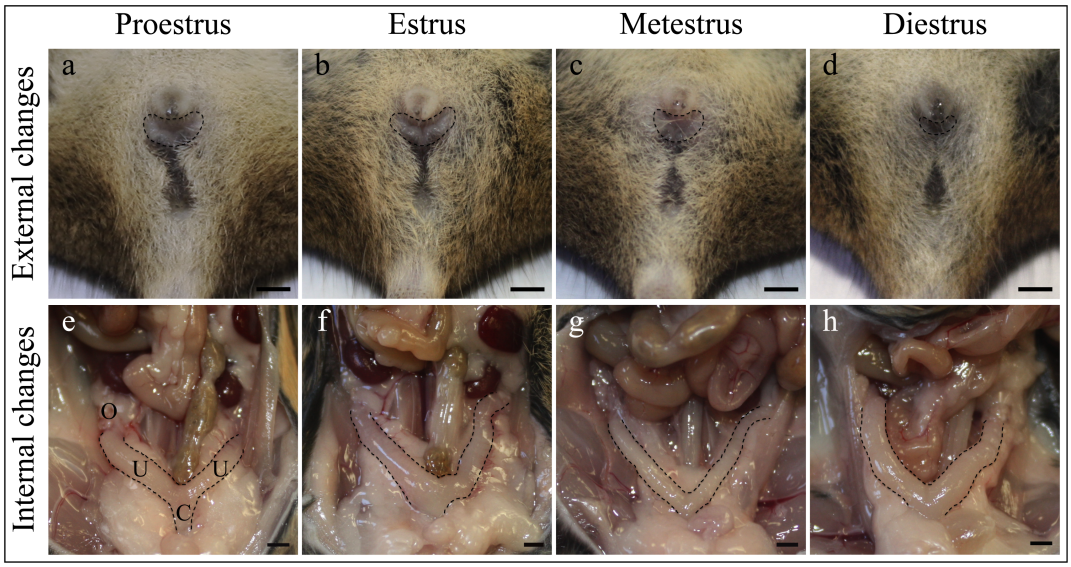

Figure 5.1 : The macroanatomic manifestations of the estrous cycle in a C57BL/6-129 mouse line, including external (top panels) and internal changes (bottom panels) in the reproductive tract. A-D) Changes in the vaginal opening along the cycle, underlining the vulva swelling with the lip demarcated by dotted lines. E-H) Internal reproductive tract in mice with the uterine horns outlined by a dotted line; letters identify the ovary (O); uterine horn (U); cervix (C). Scale bars calibrate to 2 mm.

The anterior end of the mouse oviduct forms a bursa that encapsulates the ovary, ensuring that the products of ovulation are directed toward the uterus. The oviduct itself is a coil of approximately 11 turns that, when uncoiled approximates 1.8 cm in length. It has three anatomic subdivisions, the infundibulum, a component of the bursa that receives the oocytes, the ampulla where fertilization takes place, and the isthmus that connects to the uterus via the utero-tubal junction (Figure 5.2, top panels).

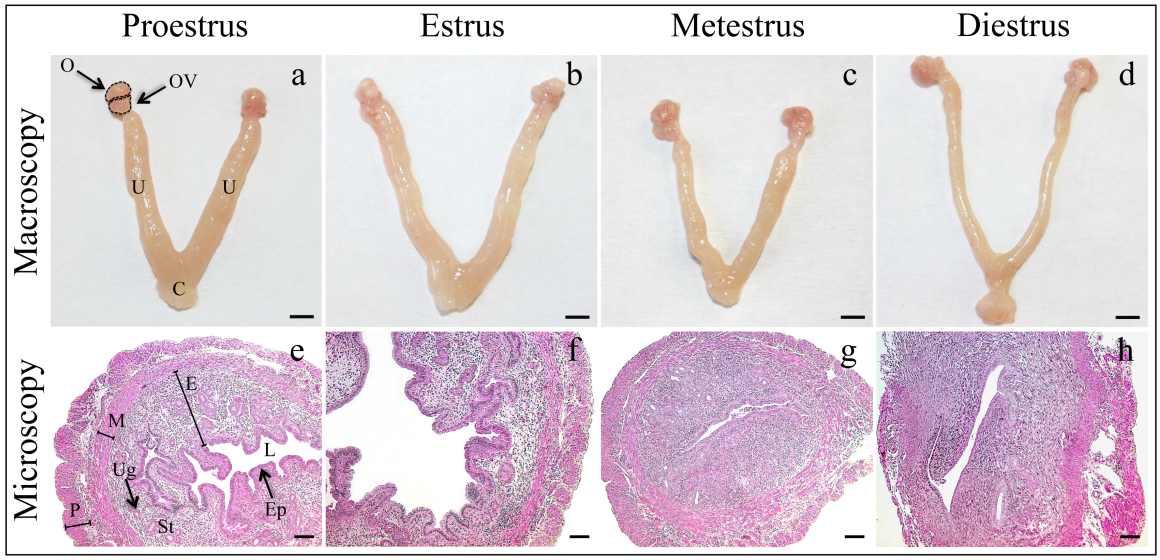

Figure 5.2 : The uterine macroscopy and microscopy during the estrous cycle. A-D) Dissected female internal reproductive tract, where O indicates the ovary, OV the oviduct, demarcated by dotted lines; U indicates the uterus and C the uterine cervix. Scale bars calibrate to 2 mm. E-H). Bright field microscopy images of hematoxylin-eosin stained sections of the uterus representing the histological changes in the uterine layers during the estrous cycle in the mouse. P indicates the perimetrium; M, myometrium; E, endometrium; L, lumen; Ep, endometrial epithelium; St, stromal compartment; Ug, uterine glands. Scale bars calibrate to 0.1 mm.

The oviduct and the uterine horns are both derived from the Müllerian ducts, and thus comprise a continuous tubular structure with mucosal, muscular and adventitial layers and

extending to the uterine cervix (Figure 5.2, bottom panels). All are sensitive to the local and systemic hormonal milieu, and undergo substantial changes during the adult mouse estrous cycle.

The cervix is the opening to the uterus, and it is continuous with the vagina, which maintains the trilaminar structure of the inner mucosa, smooth muscle layers and outer adventitia. In the adult mouse, the vaginal mucosa is lined by stratified squamous epithelium. As will be noted below, the epithelial and reticuloendothelial system cell morphology and composition undergo hormonal variations, reflecting the changes that occur during the estrous cycle. A single ventral and two dorsal lips characterize the vaginal opening and it is protected by the vulva, the female external genital organ. These regions likewise undergo recognizable morphological changes during the estrous cycle (Figure 5.1, top panels).

5.1.3.2. The ovary, development and microanatomy

The ovary of the mouse begins to develop at approximately day 9.5 post copulation (dpc). The somatic cells are derived from the embryonic mesonephros and the coelomic epithelium, and the primitive gonad begins to develop by dpc 10. The primordial germ cells that will give rise to the oocytes, differentiate at the base of the allantois about dpc 7.5 and migrate to the genital ridge at approximately 9.5 dpc[29]. Between 10.5 and 13.5 dpc, the mouse oocytes divide mitotically[25], and the consensus among scientists is that, this mitotic event supplies all of the oocytes that will populate the adult ovary. The oogonia, grouped in cysts, then begin to enter meiosis and proceed to the dictyate stage of the first meiotic

prophase. There, further meiotic progression is arrested until the oocyte and its follicular somatic component are recruited to the growing follicular pool.

Although follicle entry into the growing pool is a continuum, populations of follicles at different stages of the process have been defined based on morphological characteristics[17]. The primordial follicles appear 1 to 2 days after birth, when flat squamous pre-granulosa cells surround oocytes. Those with a single layer of cells that have transformed from squamous to cuboidal cells are seen first at postnatal day 3, and are designated primary follicles, while those with two or more layers but no antrum are known as secondary follicles. At day 7, primordial follicles are the most abundant follicular type, but primary and secondary follicles, having more than 1 layer of granulosa cells and an additional theca layer, are present in the medullar region. The first antral follicles in the mouse are present by day 13 following birth. By day 21, multiple layers of granulosa cells that contain scattered areas of interstitial fluid surround the oocyte[21]. Preovulatory follicles are identified by their defined cumulus oophorus, a multilayered investment of the oocyte with a subtype of the granulosa cells that is distinct from the mural population (Figure 5.3). First ovulations are seen in mice between 30 and 40 days of age.

The ovary of the adult mouse undergoing estrous cycles (Figure 5.3) is covered with epithelium of peritoneal origin. The point of entry and exit of the vasculature is the ovarian hilus, which defines the center or cortex of the ovary. The majority of the follicles is in the primordial state and located at the periphery of the medulla. Enumeration indicates that there are approximately 8000 of these present at birth in the C57BL/6 mouse, declining to about 2500 by day 7 after birth, mostly due to oocyte demise[13]. Once a follicle transits from the primordial population, it is committed to the growing pool to either ovulate (a small percentage) or become atretic (the majority). It has been estimated that 3-6 mouse follicles

enter the growing pool daily[3]. It requires approximately 16 days for the healthy follicles to reach the preovulatory stage[20]. Most atresia happens on follicles in the pre-antral and early antral state[10].

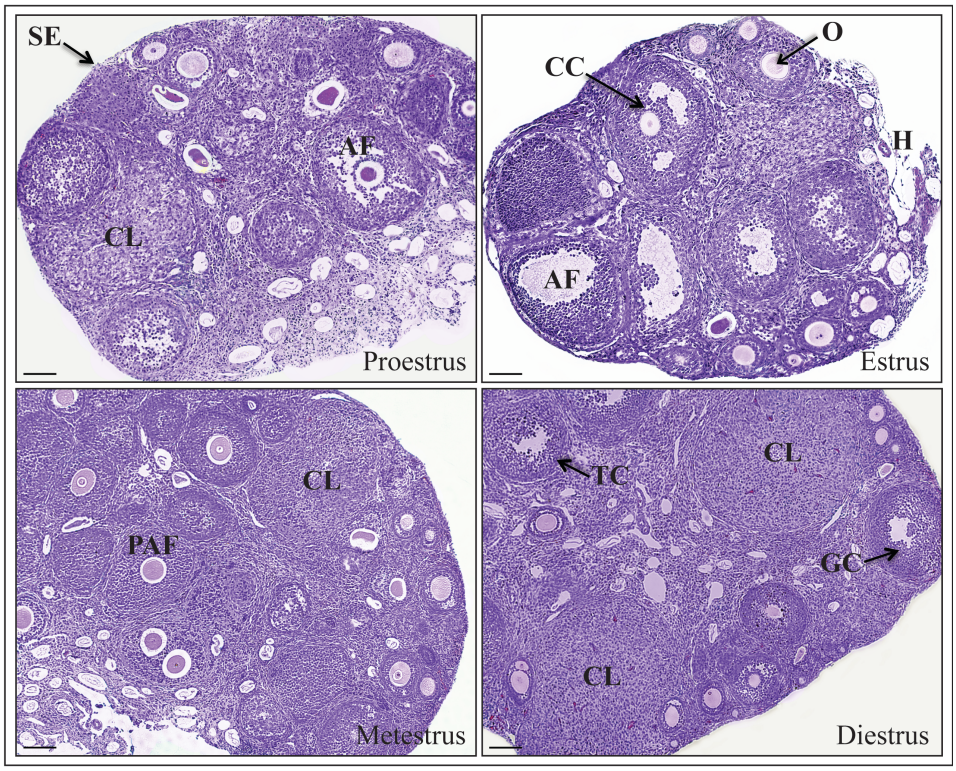

Figure 5.3 : Bright field microscopy images of hematoxylin-eosin stained sections of entire ovaries depicting the assemblage of structures present during the estrous cycle of the mouse. SE, surface epithelium; O, oocyte; CL, corpus luteum; AF, antral follicle; CC, cumulus cells; H, hilus; PAF, preantral follicle; TC, theca cells; GC, granulosa cells. Scale bars calibrate to 0.1 mm.

The web of interaction between the oocyte, granulosa cells, theca cells, pituitary and hypothalamus ultimately selects follicles for ovulation[23]. After ovulation, the follicle undergoes massive reorganization. The thecal vascular elements invade, bringing thecal cells to mix with the remodeling granulosa population to form the corpus luteum (CL) (Figure 5.3). If mating has not occurred, the CL undergoes functional regression, with

reduction in progesterone (P4) output that allows the next cycle to take place (see hormone variations, below).

5.1.3.3. Hormonal variations drive the estrous cycle

The hypothalamus-pituitary-gonadal axis regulates all the reproductive changes along the estrous cycle. Gonadotropin-releasing hormone (GnRH) from the hypothalamus reaches the anterior pituitary, stimulating the secretion of follicle-stimulating hormone (FSH) and luteinizing hormone (LH). Antral follicles are responsive to these two gonadotropic hormones when they reach the ovary. FSH acts primarily to promote follicular growth, granulosa cell proliferation, aromatization of androgens to estrogens and LH receptor expression. LH is also necessary for follicle growth, particularly at the late stages, and, as noted below, induces ovulation. Both gonadotropins promote the secretion of gonadal hormones, i.e., estrogen and progesterone, necessary for the proper execution of the follicle development program and responsible for maintaining the secondary sexual characteristics and reproductive cyclicity. The uterine and vaginal manifestations of the mouse estrous cycle are the product of the steroidal influences resulting from the cyclic changes in the ovary. The hormone profiles that accompany the ovarian cycle (Figure 5.4, a) have resulted from multiple studies from laboratories around the world during the last century.

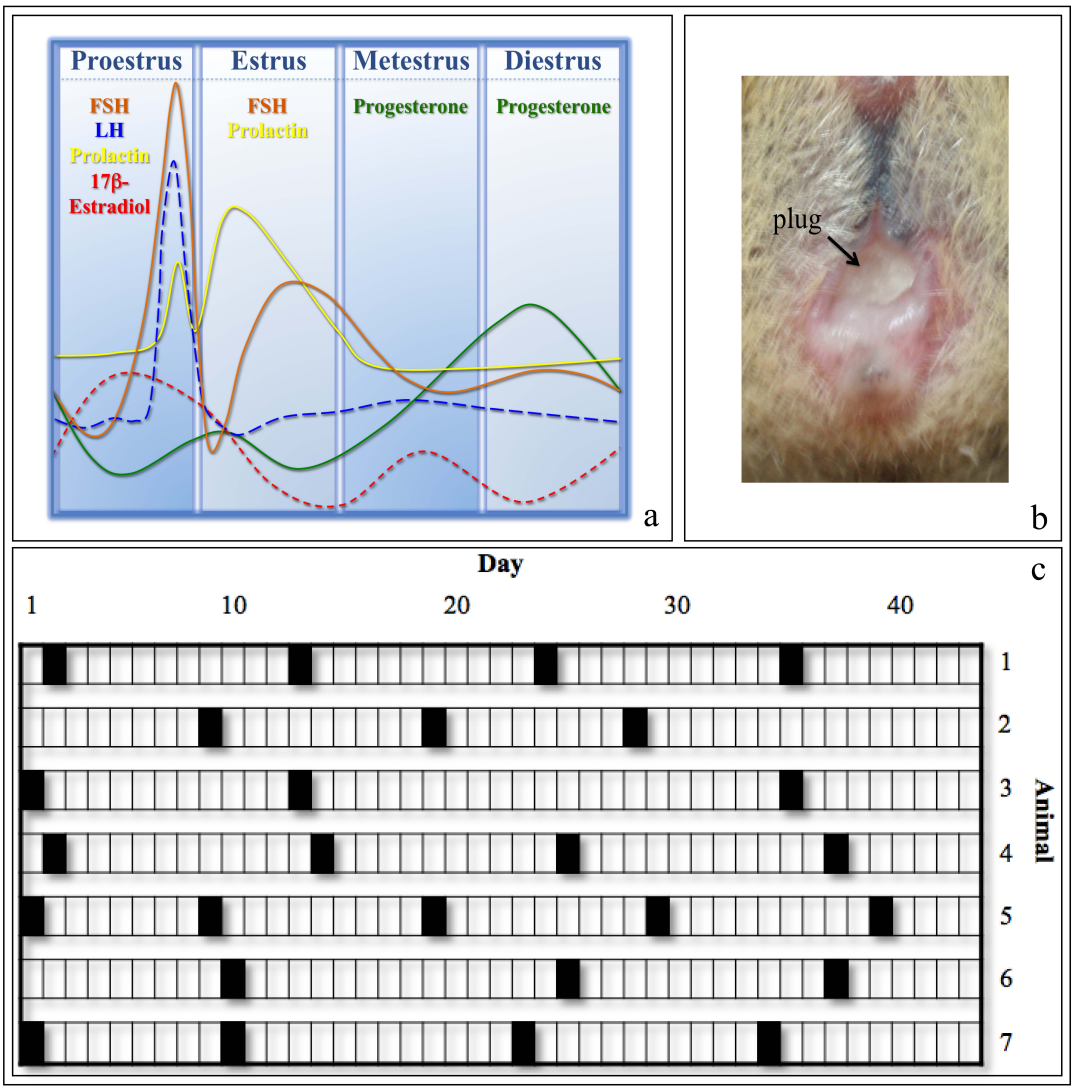

Figure 5.4 : Depiction of hormone profiles across the mouse estrous cycles and pseudopregnancy. A) Diagram of the serum hormonal profile for each different stage of the cycle. FSH in orange line; LH, blue; Prolactin, yellow; 17β Estradiol, red; Progesterone, green. Composite information from multiple publications, adapted from McLean et al, 2012[15]. B) Evidence of the male secretions forming the vaginal plug after copulation. C) Mating frequency of females housed with vasectomized males during 40 days of breeding trial; black squares mean copulation plugs, with approximate 10 day intervals between each plug, indicating pseudopregnancy induced by mating.

During proestrus, antral follicles grow exponentially under the influence of FSH, and we see the last stages of development of the cohort of preovulatory follicles. A large body of work across numerous species of mammals has shown that this stage of follicle

maturation, driven first by FSH, then by LH, results in a relatively large-scale conversion of thecal androgens to estrogens, mostly estradiol 17ß (E2). Proestrus is characterized by estradiol affecting the hypothalamus in a positive feedback manner, therefore when E2 increases, LH peaks, still during proestrus (Figure 5.4, a)[6].

Ovulation in the mouse follicle occurs approximately 12 to 14 hours after a surge of LH coinciding with the estrus phase, and coincident with the period during which the female will allow mating. Ovulation, due to the remodeling of the preovulatory ovarian follicles into corpora lutea, engenders the shift from the estrogen to progesterone as the principal secretory product. This takes place during metestrus and diestrus, the luteal phase of the mouse cycle. Beyond the positive feedback induction of the LH surge, the acute elevation of estrogens has multiple consequences. These include the generation of protein synthesis, uterine fluid accumulation, uterine elongation and cornification of the vaginal epithelium. Local concentrations of progesterone and estrogen, derived from circulation, alter the morphology of the endometrial component of the mouse uterus (Figure 5.2).

During metestrus and diestrus, progesterone inhibits the secretion of LH and consequently, prevents further ovulation. The functional demise of the corpus luteum toward the end of metestrus results in reduction in progesterone synthesis due to its conversion to the less potent progestogen, 20α-OH-progesterone. The decline in progesterone releases inhibition of LH secretion, allowing proestrus to ensue. Thus, in the unbred mouse the functional regression of the corpus luteum occurs during late diestrus.

Structurally, the CL in the unmated mouse persists for two to four cycles[4] after functional regression, and multiple generations of these structures can be present in the ovary at any time during the cycle. This renders in vivo studies of ovulation and early CL development difficult. The model of choice for exploration of this genre has been the

immature mouse, where follicle development is hormonally induced prior to the first ovulation. The protocol for hormonal synchronization in mice is based on the injection of equine chorionic gonadotropin (eCG), a hormone that mimics the FSH effect, followed by an injection of human chorionic gonadotropin (hCG), which has LH-like activity, 44 to 48 hours after eCG. Ovarian responsiveness to the hormonal superstimulation in the immature mouse takes place around 22 to 25 days of age. In this superstimulation model, all CL produced are products of the current ovulation.

Mating in the mouse is normally detected by the occurrence of vaginal plugs (Figure 5.4, b), formed by a mixture of the secretions of the vesicular and coagulating glands of the male, that usually fills the vagina from cervix to vulva[4]. Vaginal plugs are most likely to be seen in the morning after the copulation event, and it can persist from 16 to 48 hours. Mating induces the formation of a more persistent corpus luteum, that of pregnancy. The mechanism has been best studied in the rat[11] and comprises a neuroendocrine loop whereby mating induces a diurnal and a nocturnal surge of prolactin secretion from the pituitary, in a pattern that persists for 8 to 10 days[2]. Prolactin inhibits expression of 20α-hydroxysteroid dehydrogenase, thereby preventing conversion of progesterone to 20α-OH-progesterone[34]. Mating of the mouse to a vasectomized male results in persistence of a functional corpus luteum for approximately 10 days (Figure 5.4, c)[16]. The evolutionary utility of this system is evident, it abbreviates the return to estrus in the unbred mouse, increasing reproductive potential during the breeding season.

5.1.4. The mouse estrous cycle

5.1.4.1. General considerations

In some respects, repetitive estrous cycles in the mouse may be considered a condition induced by human intervention and captive breeding as *Mus musculus* is an efficient breeder in nature. The brief estrous cycle and postpartum estrus ensure that the female is in gestation at any given moment during the breeding season. Under natural conditions, the breeding season for this species includes summer and autumn[22] and photoperiod is the major environmental regulator. The strategy used in captivity to maintain mice breeding throughout the year in the laboratory colonies is based in the duration of the artificial light:dark cycle. Mice are under the light condition for 14 hours and under the dark for 10 hours per day, imitating the length of a summer day and night.

The estrous cycle in the laboratory mouse is most commonly of four days duration, but can be as long as six days, and can vary between strains of mice. The attempts to determine the length of the mouse estrous cycle required several years of investigation. Early work proposed that the cycle lasted approximately 20 days, substantiating the observations at the immediate post-partum estrus. Around the year 1888, using sterile mating, the interval between two copulations was considered the length of the cycle, leading the authors to place the length to 10 days. We now know that mating, even though sterile, results in the formation of a functional CL, as discussed above in the hormone variations section, inhibiting the occurrence of estrus for approximately 10 days. It was only in 1922 that the peak of frequency curve for length of cycle was discovered to be 4 to

5 days[1; 19]. This was possible because of the evaluation of vaginal cells to determine each phase of the cycle, avoiding the formation on the inducible CL by mating.

A fertile postpartum estrus results in simultaneous lactation and gestation, whereas the interval between parturition and ovulation is about 14 to 28 hours. Fertility at this postpartum mating is less efficient[4]. After this immediate postpartum period, no further estrus is observed until the end of the normal lactation period, which lasts about 19 to 21 days.

The length of each stage of the cycle may vary as well, but an average can be determined as: early proestrus, 11 hours; late proestrus, 21.4 hours; estrus, 20.7 hours; metestrus, 21.8 hours; and diestrus, 21.8 hours; for a total of 4.3 days[30]. The onset of estrus, determined by willingness to mate, usually occurs between 2200 and 0100 on the day of proestrus. Ovulation takes place between 2330 and 0430 and it is spontaneous, i.e., independent of the copulation. The interval between the onset of estrus and ovulation is variable, but it is estimated to be 2 to 3 hours[26]. There are a number of factors that can alter the length of the cycle, including the presence of a male, the number of females in the same group, the time of exposure to the light:dark system, and, of course, administration of exogenous hormones. Mice are sensitive to the olfactory-mediated stimuli, in the form of the pheromones released from both males and females. Olfactory stimuli originate from the presence of a male can induce estrus, accelerate the cycle, and regularize abnormal cycles. This effect can be mimicked by exposing female mice to urine from male mice, and this results in alteration of the expected pattern of estrous synchrony[14].

Mice are also responsive to neurotropic stimuli, including social stress associated with behavioral competition provoked by crowding which causes abnormal cycles found

under crowded conditions[31]. Crowding is known to alter some aspects of central nervous system activity and increase the synthesis and release of adrenocorticotropic hormone (ACTH), what may alter ovarian function[9], suppressing or inhibiting the estrous cycle. It is shown that housing large group of females (20 females/cage) resulted in prolonged vaginal diestrus, followed by evidence of ovulation at 10 to 12 day intervals, leading to the conclusion that housing female mice in large groups induces a luteotropic formation causing pseudopregnancy rather than anestrus[24].

The environment illumination also plays a role in the regulation of the estrous cycle. Continuous lighting prompts dramatic alterations in the cycle, comprising continuous vaginal cornification, cystic follicles in the ovary and the absence of ovulation, lengthening the cycle[7]. Reversing the daily rhythm of light and darkness reverses the time of estrus, ovulation and copulation.

The estrous cyclicity is also related to the age of the females. From puberty, which happens at 5 to 6 weeks of age, cycle frequency and length is initially low, due to prolonged cycles and late-starting cyclers. The peak of cycle frequency and length starts from 3 to 5 months of age, and it lasts until females are 7 to 10 months old. With aging, the frequency and the length of the cycle decline, and the age for the cessation of the cyclicity can be up to 16 months[18]. The average age for the onset of acyclicity starts from 11 months of age, and it is characterized by the persistent vaginal cornification, which is defined by an absence of CL, presence of poly-follicular ovaries that continue to secrete estrogens[12].

5.1.4.2. Changes in the reproductive tract

The estrous cycle is characterized by multiple remodeling events it the ovary in support of ovulation and gestation. As noted above, it has been divided into four stages of unequal length based on the events that occur in the ovary and their consequences on other reproductive tissues (Figure 5.1) and reproductive behavior. Figure 5.3 depicts the changes in ovarian landscape over the estrous cycle. In proestrus, the dominant structures are the antral follicles that are developing to the preovulatory state. Estrus is characterized by the final stages of development of the preovulatory follicles and ovulation. If the cycle is not interrupted by pregnancy, pseudopregnancy, or other phenomena, metestrus will begin. At metestrus, the new corpora lutea can be seen in the ovary. Diestrus, corresponding to the luteal phase, extends for two of a four day cycle during which prominent corpora lutea are present in the ovary (Figure 5.3).

The uterus also undergoes morphological variation across the estrous cycle in response to the steroidal environment engendered by the preovulatory and luteal events. The transformations seen in the uterus include histological changes in the luminal and glandular epithelium, in the stromal cells, in the secretory activity of the uterine glands and in the distention and shape of the uterine lumen (Figure 5.2). Total uterine thickness directly correlates with E2 levels, and inversely with P4. Luteal progesterone levels are correlated with uterine width, reduced luminal epithelial proliferation and decreased stromal apoptosis. The elevated estrogen levels of proestrus are associated to greater uterine width, more stromal cell proliferation, decreasing the glandular epithelial proliferation, and a reduced frequency of luminal, glandular and stromal apoptosis. E2 levels have been implicated in protection of glandular endometrial cells from apoptosis[32].

The uterus during proestrus and estrus is thick and edematous, and the distention appearance is due to the hyperfunction of the uterine glands, once the maximum secretory activity occurs at estrus, as the stromal proliferation is greatest associated with elevated level of E2 (Figure 5.2, a). At proestrus, a typical undulating endometrium with projections of endometrial tissue into the lumen is present (Figure 5.2, e); at estrus, the extracellular fluid throughout the endometrium is increased (Figure 5.2, b and f)[32]. Edema begins to diminish in late estrus, evidently declining during metestrus (Figure 5.2, c), and the stromal apoptosis is highest at this point, correlated with the relatively low levels of E2 and P4. During metestrus, a degenerative process takes place, and the epithelium loses its definitive organization, shows vacuolar degeneration, leukocytes appear in the basement membrane, and uterine glands show minimum activity (Figure 5.2, g). The turnover to a regenerative process determines the onset of diestrus[4]. At diestrus, uterus is thin and elongated (Figure 5.2, d), and the uterine wall is collapsed and anemic (Figure 5.2, h). During diestrus and proestrus, mitoses are frequent in the glands, becoming fewer in number as functional activity increases[1].

The hormonal milieu, especially predominately estrogen, will dictate the cell typology within the murine vaginal smears, reflecting changes in the vaginal epithelium (see estrous cycle determination, below). The cells found in the vaginal smears are basically leukocytes, cornified epithelial cells and nucleated epithelial cells. The changes in the vaginal epithelium comprise modifications in the number of layers in the epithelium, the amount of cornification and the changes from live to dead cells, the presence of surface mucus and the presence or absence of polymorphonuclear leukocytes. Proestrus and estrus are determined by the proliferation in the genital tract, culminating in ovulation, mating and

fertilization. Metestrus is characterized by degeneration in the reproductive tract, whereas diestrus is a period of quiescence or slow growth[4].

At proestrus, the vaginal epithelium consists of three layers, including the stratum germinativum, the stratum granulosum, and a layer composed of epithelial cells with nuclei showing signs of pyknosis[4]. In this stage, there is maximal opening of the vagina, accompanied by swollen labia and a moist external orifice, there are often wrinkles and striations along the dorsal and ventral edges (Figure 5.1, a)[5], and the fluid on its lumen is serous. During proestrus and early estrus, cells of the outer layer of the vagina are sloughed, producing the aspect of nucleated cell smear. Cells are sloughed from the cornified layer during late proestrus and throughout estrus[4]. In estrus, vulva may still be swollen, but the vagina appears less open, the tissues are less moist and less pink (Figure 5.1, b).

Metestrus is the stage when vulva has usually lost most of its swelling, the orifice of the vagina is tightly or partly closed and the lumen is less moist (Figure 5.1, c). The vaginal content changes from a pasty or viscous to a fluid consistency. It is characterized by the peeling off of the entire stratum, and the delamination process includes some of the superficial layers of the stratum germinativum. As diestrus ensues, the vulva becomes inconspicuous and the vaginal gap is tightly closed, containing a viscous and stringy fluid, with no tissue swelling (Figure 5.1, d)[6]. The vaginal epithelium in this stage contains only the stratum germinativum, which actively grows late in diestrus; by proestrus, the stratum granulosum has formed several cell layers below the surface, thereby completing the cycle[4].

5.1.4.3. Determining the estrous phase

Methods for determination of the stage of the estrous cycle are essential to mouse breeding programs, for determination of reproductive phenotypes and for investigation of reproductive landmarks such as puberty and age related depletion of the follicle reserve. The exterior aspect of the vagina has been successfully employed to approximate the stages of the cycle[8] (Figure 5.1, top panels). The openness of the vagina, the relative tumescence of the external genitalia and tissue coloration (in albino mice)[5] provide indicators of the stage of the ovarian cycle, as described above. Beyond the visual observation of the external genitalia, the changes in the mouse estrous cycle can be determined using methods such as electrical impedance and biochemical analysis of the urine[5].

As the ovarian and hormonal changes evoke major modification in the vaginal epithelium, the most frequently applied and reliable method for estrous cycle determination in mice is the evaluation of the vaginal cytology. The guinea pig was the species where cytology of exfoliated tissues in the vagina was first used to establish the estrous cycle, published nearly 100 years ago by Stockard and Papanicolaou[27]. Vaginal smears can be read with or without staining, but latter is somewhat more difficult, particularly to the inexperienced eye (for more details, see Monitoring mouse estrous cycle, the protocol).

The identification of the estrous stage is based on the proportion of two cell types observed in the vaginal smear, the epithelial cells derived from the stratified squamous epithelium that lines the vagina and polymorphonuclear leukocytes, primarily neutrophils[6]. Figure 5.5 depicts the cellular assemblages that characterize the temporal changes during the cycle.

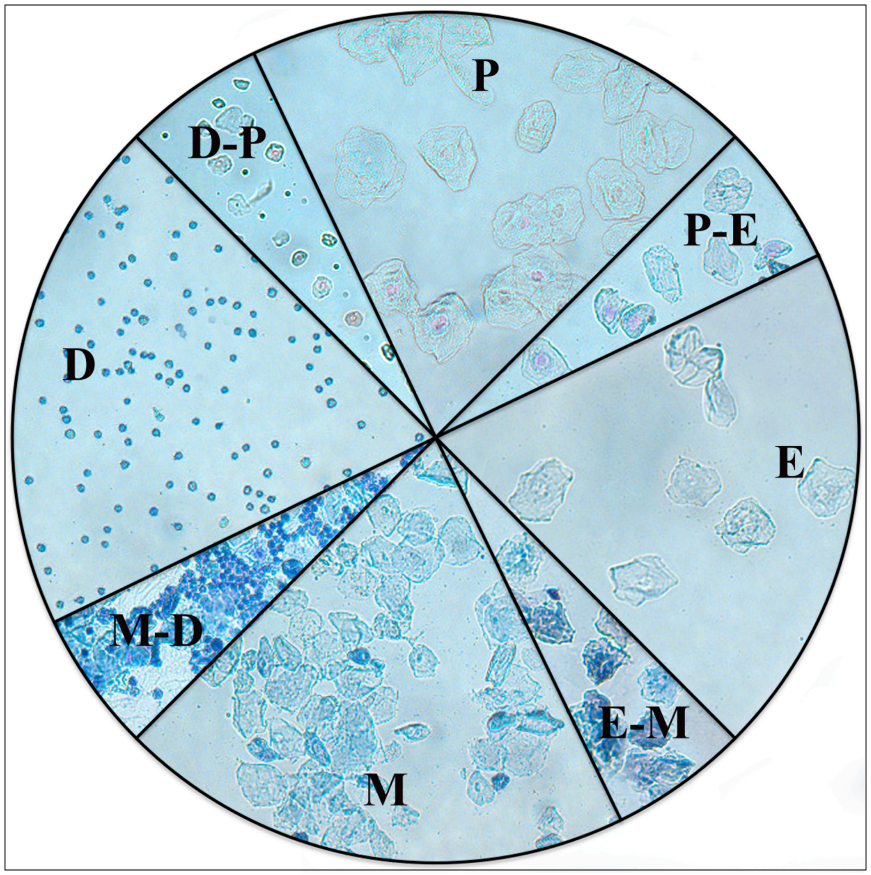

Figure 5.5 : Assemblages of cells exfoliated from the mouse vaginal epithelium across the estrous cycle of the laboratory mouse showing the cellular assemblages that define the days of the cycle and the transitions between stages of the cycle. P signifies proestrus; P-E, the transition between proestrus and estrus; E signifies estrus; E-M, the transition between estrus and metestrus; M, metestrus; M-D, the transition between metestrus and diestrus; and D, diestrus. Vaginal smears were collected by infusing and removing ≈10 µl of PBS 1X, smears were dried and stained with May-Grünwald Giemsa.

Proestrus is characterized by squamous epithelial cells with visible nuclei seen in clusters or individually; very few lymphocytes and polymorphonuclear cells are observed in this phase (Figure 5.5, P). Following proestrus, the estrus assemblage contains squamous epithelial cells gradually becoming more cornified (Figure 5.5, P-E), with no visible nuclei, granular cytoplasm and irregular shape (Figure 5.5, E). At the end of estrus, there is a mix of cell types including leukocytes and cornified epithelial cells aggregating into cluster formations (Figure 5.5, E-M). By metestrus, the exfoliated cell population is dominated by

leukocyte infiltration and cuboidal epithelial cells are present (Figure 5.5, M). As the cycle progresses, neutrophils are found in combination with the cuboidal like epithelial cells during the transition to diestrus (Figure 5.5, M-D). Diestrus consists predominately of leukocytes no longer in association with the epithelial cells, that are non-nucleated and in fusiform shape indicating cell death (Figure 5.5, D). During transition to proestrus, neutrophils decline and epithelial cells with obvious nuclei are the principal cell type found (Figure 5.5, D-P). Anestrus is characterized by non-cornified epithelial cells and by the absence of proestrus/estrus for a long period. It must be emphasized that, in the unbred mouse, the cycle is a continuum, thus transition phases have been included in the composite photomicrograph.

Acknowledgements

Kalyne Bertolin is recipient of the Quebec Merit Scholarship for Foreign Students from the Fonds de recherche du Québec – Nature et Technologie (FQRNT). The authors thank Amaëlys Di Salvo for aid with collection of the experimental materials and Vickie Roussel and Mira Dobias for technical assistance. Mouse studies in the lab of B. Murphy are supported by Canadian Institutes of Health Research Operating Grant 11018.

References

1. Allen E (1922) The oestrous cycle in the mouse. *The American Journal of Anatomy* **30**.

2. Barkley MS, Bradford GE & Geschwind, II (1978) The pattern of plasma prolactin concentration during the first half of mouse gestation. *Biol Reprod* **19**, 291-296.

3. Bristol-Gould SK, Kreeger PK, Selkirk CG *et al.* (2006) Fate of the initial follicle pool: empirical and mathematical evidence supporting its sufficiency for adult fertility. *Dev Biol* **298**, 149-154.

4. Bronson FH, Dagg CP & Snell GD (1966) *Reproduction*. New York: Dover Publications, Inc. .

5. Byers SL, Wiles MV, Dunn SL *et al.* (2012) Mouse estrous cycle identification tool and images. *PLoS One* **7**, e35538.

6. Caligioni CS (2009) Assessing reproductive status/stages in mice. *Curr Protoc Neurosci* **Appendix 4**, Appendix 4I.

7. Campbell CS, Ryan KD & Schwartz NB (1976) Estrous cycles in the mouse: relative influence of continuous light and the presence of a male. *Biol Reprod* **14**, 292-299.

8. Champlin AK, Dorr DL & Gates AH (1973) Determining the stage of the estrous cycle in the mouse by the appearance of the vagina. *Biol Reprod* **8**, 491-494.

9. Christian JJ (1964) Effect of Chronic Acth Treatment on Maturation of Intact Female Mice. *Endocrinology* **74**, 669-679.

10. Edwards RG, Fowler RE, Gore-Langton RE *et al.* (1977) Normal and abnormal follicular growth in mouse, rat and human ovaries. *J Reprod Fertil* **51**, 237-263.

11. Erskine MS (1995) Prolactin release after mating and genitosensory stimulation in females. *Endocr Rev* **16**, 508-528.

12. Felicio LS, Nelson JF & Finch CE (1984) Longitudinal studies of estrous cyclicity in aging C57BL/6J mice: II. Cessation of cyclicity and the duration of persistent vaginal cornification. *Biol Reprod* **31**, 446-453.

13. Kerr JB, Duckett R, Myers M *et al.* (2006) Quantification of healthy follicles in the neonatal and adult mouse ovary: evidence for maintenance of primordial follicle supply. *Reproduction* **132**, 95-109.

14. Marsden HM & Bronson FH (1964) Estrous Synchrony in Mice: Alteration by Exposure to Male Urine. *Science* **144**, 1469.

15. McLean AC, Valenzuela N, Fai S *et al.* (2012) Performing vaginal lavage, crystal violet staining, and vaginal cytological evaluation for mouse estrous cycle staging identification. *J Vis Exp*, e4389.

16. Mednick DL, Barkley MS & Geschwind, II (1980) Regulation of progesterone secretion by LH and prolactin during the first half of pregnancy in the mouse. *J Reprod Fertil* **60**, 201-207.

17. Myers M, Britt KL, Wreford NG *et al.* (2004) Methods for quantifying follicular numbers within the mouse ovary. *Reproduction* **127**, 569-580.

18. Nelson JF, Felicio LS, Randall PK *et al.* (1982) A longitudinal study of estrous cyclicity in aging C57BL/6J mice: I. Cycle frequency, length and vaginal cytology. *Biol Reprod* **27**, 327-339.

19. Parkes AS (1928) The length of the oestrus cycle in the unmated normal mouse: records of one thousand cycles. *Beit Memorial Research Fellow*.

20. Pedersen T (1970) Follicle kinetics in the ovary of the cyclic mouse. *Acta Endocrinol (Copenh)* **64**, 304-323.

21. Rajkovic A, Pangas SA & Matzuk MM (2006) Follicular Development: Mouse, Sheep, and Human Models. *Knobil and Neill's - Physiology of Reproduction* **1**, 383-423.

22. Raynaud A (1950) [State of development of the genital apparatus of field-mice (Apodemus sylvaticus L.) during different seasons of the year]. *C R Seances Soc Biol Fil* **144**, 938-940.

23. Richards JS (1994) Hormonal control of gene expression in the ovary. *Endocr Rev* **15**, 725-751.

24. Ryan KD & Schwartz NB (1977) Grouped female mice: demonstration of pseudopregnancy. *Biol Reprod* **17**, 578-583.

25. Sarraj MA & Drummond AE (2012) Mammalian foetal ovarian development: consequences for health and disease. *Reproduction* **143**, 151-163.

26. Snell GD, Fekete E, Hummel KP *et al.* The relation of mating, ovulation and the estrous smear in the house mouse to time of day. *The Anatomical Record* **76**.

27. Stockard CR & Papanicolaou G (1917) The existence of a typical oestrous cycle n in the guinea-pig with a study of its histological and physical changes. . *Am. J. Anat.* **22**.

28. Takehashi M, Kanatsu-Shinohara M & Shinohara T (2010) Generation of genetically modified animals using spermatogonial stem cells. *Dev Growth Differ* **52**, 303-310.

29. Tilmann C & Capel B (2002) Cellular and molecular pathways regulating mammalian sex determination. *Recent Prog Horm Res* **57**, 1-18.

30. Van Ebbenhorst Tengbergen WJ (1955) The morphology of the mouse anterior pituitary during the oestrous cycle. *Acta Endocrinol (Copenh)* **18**, 213-218.

31. Whitten MK (1957) Effect of exteroceptive factors on the oestrous cycle of mice. *Nature* **180**, 1436.

32. Wood GA, Fata JE, Watson KL *et al.* (2007) Circulating hormones and estrous stage predict cellular and stromal remodeling in murine uterus. *Reproduction* **133**, 1035-1044.

33. Yan Z, Sun X & Engelhardt JF (2009) Progress and prospects: techniques for site-directed mutagenesis in animal models. *Gene Ther* **16**, 581-588.

34. Zhong L, Parmer TG, Robertson MC *et al.* (1997) Prolactin-mediated inhibition of 20alpha-hydroxysteroid dehydrogenase gene expression and the tyrosine kinase system. *Biochem Biophys Res Commun* **235**, 587-592.

5.2. Monitoring mouse estrous cycles

Kalyne Bertolin[1] and Bruce D. Murphy[1,2]

[1]Animal Reproduction Research Centre (CRRA), University of Montreal, Saint-Hyacinthe, Quebec, Canada; [2]Corresponding author

Book chapter for "The Guide to Investigation of Mouse Pregnancy". ACADEMIC PRESS/ELSEVIER; Chapter 40: Part III: Protocols for Studies of the Placenta and Pregnancy in Mice: III-1. Monitoring estrous cycles, December 2013 (IN PRESS).

Author contributions: My contribution involved designing the experiments; manipulation of animals and samples; preparation of the figures and writing of the text. BDM supervised the work and contributed to the writing task.

5.2.1. Introduction

Managing a mouse colony requires careful observation at both macroscopic and microscopic levels to determine the phases of the estrous cycle. There are several situations that challenge the researcher, for instance, choosing the best females for a breeding program, to define the reproductive phenotype of a transgenic mouse line or to characterize events related to the different stages of the estrous cycle. The physiological changes that occur during the estrous cycle are manifest in changes in both the macro and microanatomy of the mouse reproductive system. An approximate determination of the estrous phase can be performed by visual observation of the external vagina (Figure 5.1 in section 5.1). This method is rapid, requires no special equipment, and permits numerous evaluations to be done without requiring sampling of the vaginal tissues. However, it can be inconclusive when the animals are in metestrus or diestrus, and it is hampered by the strain of mouse, i.e., it is more difficult in lines with darker pelage. This method can be employed as a preliminary evaluation but definitive evaluation requires confirmation by vaginal cytology assessment.

Vaginal smear analysis is the preferable technique for accurately determining the estrous phase in mice. This technique was first described in rats, based on the correlation between the layers of the characteristic desquamated vaginal epithelium and the hormonal profile for each stage of the estrous cycle[5]. In mice, evaluation of these exfoliated cells that can be obtained by scraping, swabbing or by vaginal washings, also serves as an indicator of the reproductive state. Recognition of the relative ratio of vaginal cells on a particular day is the imperative tool for successful determination of the estrous phase:

- Proestrus: the vaginal smear is characterized by the predominance of nucleated vaginal epithelial cells, seen in clusters or individually; very few leukocytes are present.
- Estrus: distinguished by the disappearance of leukocytes and the presence of cornified squamous epithelial cells, which are large, non-nucleated and irregular in shape. Early estrus may show some nucleated epithelial cells.
- Metestrus: there is a mix of cell types; an invasion of leukocytes occurs, and the non-nucleated epithelial cells are usually clustered; dying epithelial cells adopt a fusiform shape.
- Diestrus: leukocytes are predominant; non-nucleated epithelial cells are mostly fusiform; the vaginal contents in this phase consistently lack cornified cells.

To be able to determine whether the female is undergoing regular cycles, vaginal cytology patterns should be analysed over two weeks (at least three cycles). It is important to observe proestrus, indicating the beginning of a new cycle, followed by estrus. The persistence of non-cornified epithelial cells is an indication of anestrus. The invasiveness in collecting the smears should be taken into consideration, since it can alter the regular reproductive status. The first days of handling can cause stress to the animal and may cause a transient disruption in the estrous cycle. Frequent smearing can also artificially induce the cornification of the vaginal epithelium; result in pseudopregnancy followed by abnormally long cycles; or moreover, can elicit an inflammatory response that can mask the cytological assessment. The vaginal epithelial cell cycle is a continuum (Figure 5.5 in section 5.1); therefore smears taken at some times may not fit perfectly into the defined categories of estrous phases, as they represent a transition between two phases[1].

5.2.2. Protocol: Collecting the vaginal epithelial cells

Materials:

Post-pubertal female mice (approximately 40 or more days old)

Sterile plastic pipette (Figure 5.6, a)

Phosphate buffer saline (PBS 1X)

Light microscope with 10x objective

Glass slides

Identify the animal by number or other mark. Place the mouse so that its front paws grasp the top of the cage, with its posterior end towards you, and firmly restrain the tail and elevate the dorsum (Figure 5.6, b). Alternatively grasp the animal by the nape of the neck to immobilize it. A sterile plastic pipette is gently inserted at the vaginal opening (Figure 5.6, c) and used to flush the vagina gently 3 to 5 times with approximately 10 μl of PBS 1X at room temperature; care should be taken not to insert the dropper too deep and not to flush too much PBS at once. Place final flush containing vaginal fluid on a properly identified glass slide. Use a coverslip to spread the drop. Wash the droppers between mice. If the drop dries, it is possible to add more saline (<10μl) with another clean pipette tip to rehydrate.

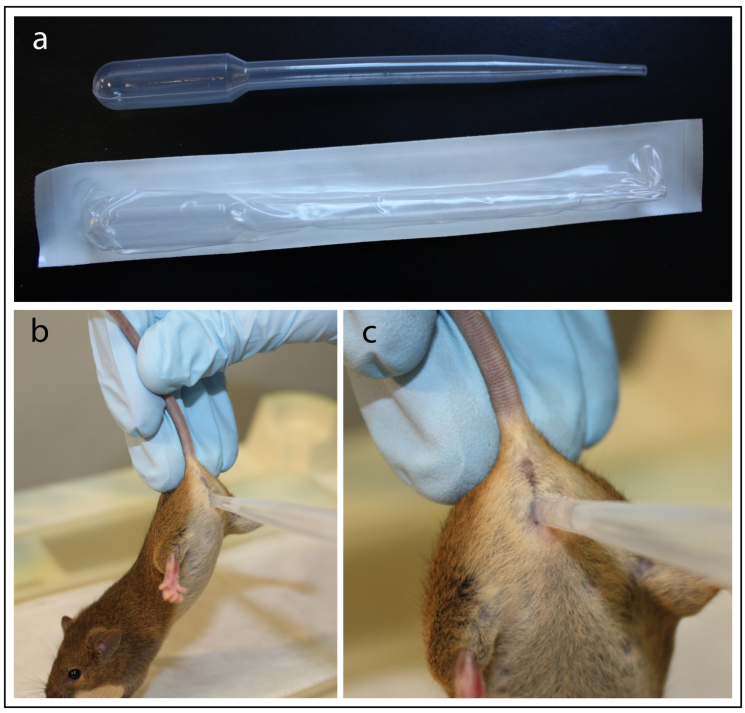

Figure 5.6 : Collection of vaginal smear in mice. A) Sterile plastic pipette recommended for collecting the cells. B) Restraint method. C) After the female mouse has been restrained, using the dominant hand, the tip of plastic pipette filled with PBS 1X is introduced in the vagina of the mouse and the liquid is flushed to collect the sample.

Observe vaginal smears at 10x and 40x magnification. Using the 40x objective lens, the characterization of the cell types is easier; however, using the 10x objective lens, it is easier to characterize the estrous cycle phase based on the proportion of cell types present. Unstained slides of vaginal cells can be examined under the microscope[3]. This technique is called “wet smear” [2]. Although the estrous cycle phase can be determined without staining the slides (Figure 5.7, right panels), the advantages of staining are better perception of the nucleus in the proestrus phase, more accurate identification of transition phases, and better pictures for publication. For routine and frequent evaluations we support the use of the “wet smear”.

Once the cells are collected, there are several staining techniques described in the literature for evaluation of these cells under the microscope. The classical Papanicolaou staining has been frequently used, allowing for discriminating the maturity of the nucleated epithelial cells. It is likewise useful to differentiate transition phases between proestrus and estrus. As an alternative, staining the vaginal smears can be simply achieved with methylene blue[6] and some researchers also have recommended the use of the Cresyl violet staining[4]. In this chapter, we have addressed the reliability of the "wet smear" by comparing it with an alternative technique known as the May-Grünwald Giemsa protocol for staining vaginal smears (Figure 5.7). The May-Grünwald contains an acid dye, eosin, and a basic dye, the methylene blue; Giemsa solution is a mixture of methylene blue, eosin, and azure B. The epithelial cells are stained in pale beige, while their nuclei and leukocytes will be stained as violet-blue.

5.2.3. Protocol: Staining vaginal smears with May-Grünwald Giemsa stain

For stained slides, it is recommended to use a gelatin coated slide. It can be homemade following the protocol:

- Prepare a 1% gelatin solution. Dissolve gelatin powder for 10 minutes in a 37^{o}C water bath
- Place slides on a flat surface
- Put 1 or 2 drops of the 1% gelatin solution on the top of each slide
- Spread the gelatin with a gloved finger
- Dry slides on a flat surface and store them at 4^{o}C

After collecting the vaginal cells according to the above protocol onto a gelatin-coated slide, the smears are air dried for 30 to 40 minutes (or for a briefer interval at 37^{o}C). Place the slides into a 100% methanol solution at -20^{o}C for 5 minutes. Quickly air-dry the slides at room temperature. Cover the slides with 1:10 May-Grünwald* solution for 3 minutes. Cover the slides with 1:5 Giemsa** staining solution for 5 minutes. Wash the slides in running tap water. Dry the slides at 37^{o}C for 40 minutes. Observe vaginal smears at 10x (Figure 5.7, left panels) and 40x magnifications.

* 9ml 100% methanol + 1ml May-Grünwald 0.25% (in 100% methanol)

** Stock solution Giemsa 0.6%: 66 ml glycerine + 1g Giemsa, dissolve it at 45^{o}C for 30 minutes or longer if necessary; add 66 ml 100% methanol. Working solution Giemsa: 38ml distilled water + 7 ml stock solution Giemsa 0.6% + 5ml 100% methanol. Staining solution Giemsa: 8 ml 100% methanol + 2 ml working solution Giemsa

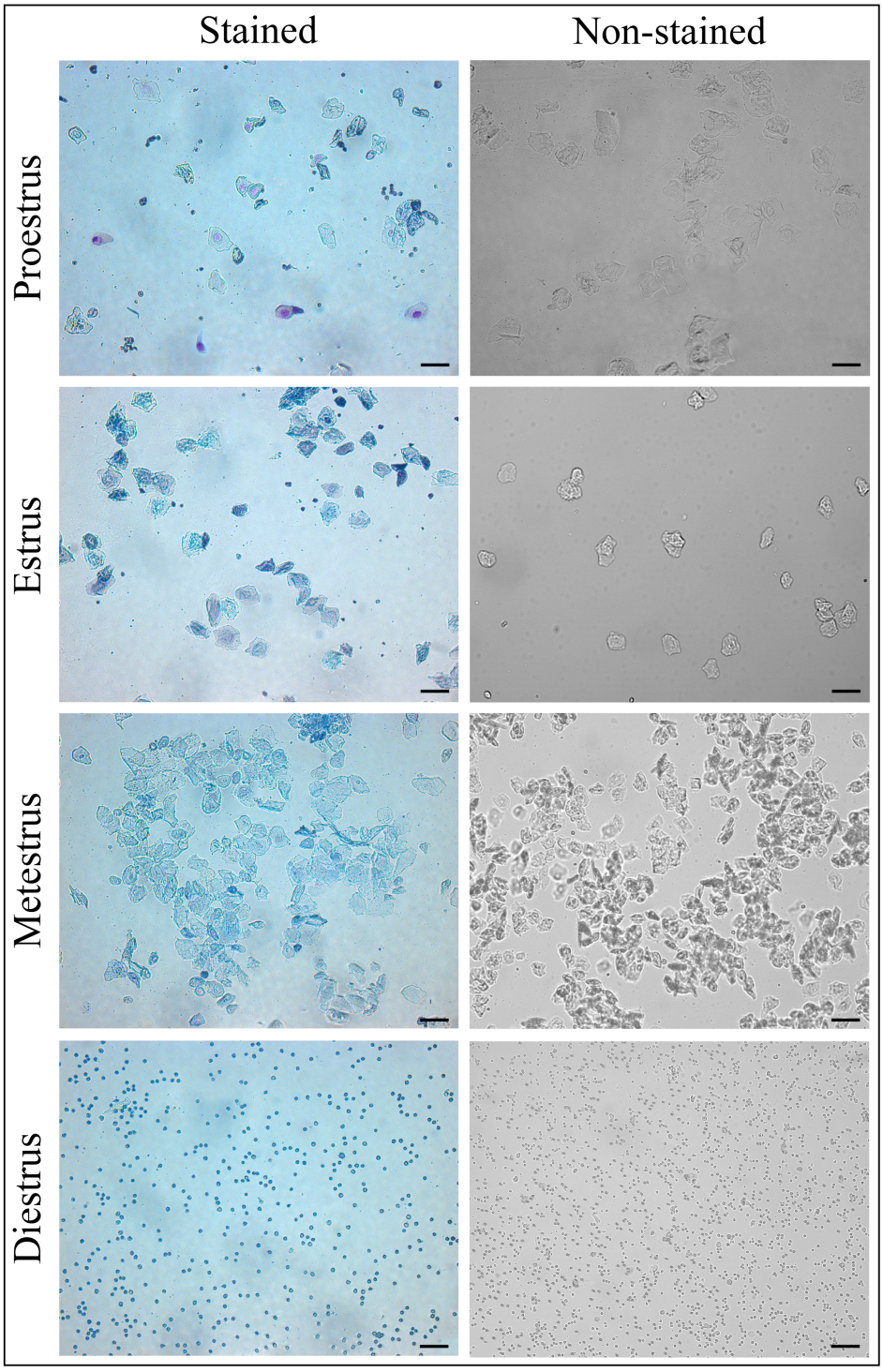

Figure 5.7 : Comparison of stained versus unstained vaginal smears from the mouse estrous cycle. Slides on the left panel were air-dried and stained with May-Grünwald Giemsa, while those on the right were photographed unstained. Scale bars calibrate to 0.1 mm (magnification 100x).

References

1. Byers SL, Wiles MV, Dunn SL *et al.* (2012) Mouse estrous cycle identification tool and images. *PLoS One* **7**, e35538.

2. Caligioni CS (2009) Assessing reproductive status/stages in mice. *Curr Protoc Neurosci* **Appendix 4**, Appendix 4I.

3. Marcondes FK, Bianchi FJ & Tanno AP (2002) Determination of the estrous cycle phases of rats: some helpful considerations. *Braz J Biol* **62**, 609-614.

4. McLean AC, Valenzuela N, Fai S *et al.* (2012) Performing vaginal lavage, crystal violet staining, and vaginal cytological evaluation for mouse estrous cycle staging identification. *J Vis Exp*, e4389.

5. Montes GS & Luque EH (1988) Effects of ovarian steroids on vaginal smears in the rat. *Acta Anat (Basel)* **133**, 192-199.

6. Yener T, Turkkani Tunc A, Aslan H *et al.* (2007) Determination of oestrous cycle of the rats by direct examination: how reliable? *Anat Histol Embryol* **36**, 75-77.